Manipulation of Seed Carbon Flow from Cellulose to Lipid and Protein Biosynthesis in *Arabidopsis* to Accelerate the Characterization of Protein-Related Genes in Canola

by

Kallum Cameron McDonald

A thesis submitted in partial fulfillment of the requirements for the degree of

Master of Science

in

Plant Science

Department of Agricultural, Food and Nutritional Science

University of Alberta

Abstract

Canola (*Brassica napus* L.) is the major oilseed crop in Canada. After oil extraction, the protein-rich seed meal (around 40% protein) serves as a nutritious feedstock for animals and the protein fraction has potential for human consumption. However, excess fiber in the seed meal (about 33%) can reduce the efficiency of digestion in animals. Therefore, it would be beneficial to partially reallocate seed carbon from cellulose, the major component of seed fibre, to storage protein biosynthesis without penalizing the seed oil content via engineering of multiple genes in these pathways. However, direct screening of different gene stacking combinations in canola is time and labor intensive. This work aimed to find promising gene combinations in the model plant *Arabidopsis thaliana* L. (henceforth *Arabidopsis*) to accelerate the genetic work needed to effectively manipulate seed carbon in canola.

The screening process requires lipid analysis of a large number of seed samples with direct transmethylation, followed by analysis with GC-FID. In Chapter 2, I optimized the lab protocol of direct transmethylation and the optimized method reduced the reaction time from overnight to no more than 2 hours, as well as replaced the expensive commercial methanolic HCl with self-prepared 2% H_2SO_4 in methanol.

A three-pronged strategy was used to find the best gene combinations: 1) seed-specific RNAi-down-regulation of *Arabidopsis CELLULOSE SYNTHASE 1* (*AtCESA1*) to partially reduce seed cellulose, 2) overexpression of *B. napus DIACYLGLYCEROL ACYLTRANSFERASE 1* (*BnDGAT1*), and its performance-enhanced variants, to restore the seed oil content, and 3) overexpression of several protein biosynthesis-related genes from *Arabidopsis* to determine whether seed carbon reallocation is effective for increasing seed protein content. Our previous work has successfully generated heterozygous *Arabidopsis* with *AtCESA1* down-regulation and overexpression of *BnDGAT1* and its performance-enhanced variants.

In this thesis project, we generated homozygous lines with *AtCESA1*-RNAi and *BnDGAT1*-OE and measured the seed cellulose, oil, and protein contents. Ideal lines with equal or increased oil, equal or increased protein, and reduced cellulose were chosen for further study. Subsequently, we overexpressed *Arabidopsis amino acid permease 1* (*AtAAP1)*, *alanine aminotransferase 1* (*AtALALAAT1)* and *asparagine synthase 1* (*AtASN1*) in those lines, respectively. Overexpression of *AtAAP1*, *AtALAAT1*, and *AtASN1* in the *AtCESA1*-RNAi*/ BnDGAT1*-OE background successfully increased the seed protein content beyond overexpression of protein-related genes alone (by up to +2.7%), as well as reduced the seed cellulose by an average of 21%. Importantly, the seed lipid contents were increased slightly in these lines relative to the empty vector (EV) controls, though this finding did not reach statistical significance for the lines with overexpression of *AtALAAT1* and *AtASN1*. There were several modest changes in the fatty acid composition, most notably a reduced proportion of 18:3 in all lines with *BnDGAT1*-OE.

The plant phenotype analysis found some evidence indicating increased seed yield, with a few small changes in 100 seed size, and seed weight in the carbon reallocated lines. No obvious or severe phenotypic abnormalities were reported during the growth of the transgenic lines, although some differences were detected in the seedling early growth assays, such as reduced hypocotyl length, root length, fresh seedling weight, and germination differences. Overall, the seed carbon reallocation strategy away from cellulose biosynthesis and towards lipid and protein biosynthesis is successful, with the *AtCESA1*-RNAi*/BnDGAT1*-OE/*AtAAP1*-OE stacking approach yielding the most positive seed composition outcomes overall.

Preface

Guanqun (Gavin) Chen conceptualized and designed the project. Gavin Chen, Kethmi Jayawardhane, Limin Wu and I designed the experiments described herein. The Plant Lipid Biotechnology lab provided existing research materials and data. I designed the protein-related gene overexpression vectors, performed all biomolecule/molecular analyses (except amino acids, performed by Lisa Nikolai), optimized the oil transmethylation protocol, grew five generations of plants, and collected plant morphology/development data. Most of the literature review section has been accepted for publication as a book chapter entitled "*Recent Advances in the Biosynthesis and Metabolic Engineering of Storage Lipids and Proteins in Seeds*", in *Functional Materials from Lipids & Proteins*, Bandara N and Ullah A (eds.), Royal Society of Chemistry (forthcoming). The experiments described in Chapter 2 were conceived by Kallum McDonald & Gavin Chen, the manuscript was edited by Yang Xu, and was submitted to the *Journal of the American Oil Chemists Society* (currently under review), and Chapter 3 will be submitted in the near future.

Acknowledgements

I want to extend my sincere gratitude to the many people who made my research possible. First, to Gavin Chen, my mentor who provided me encouragement and opportunities that added value to my graduate school experience, and for his financial support. Second, I appreciate the support from my supervisory committee member Stacy Singer, particularly regarding the editing of the book chapter. Thank you to Kethmi Jayawardhane and Limin Wu, who were instrumental in providing essential information, suggestions, and guidance across many experiments. I also am grateful for the lab technicians and support staff that made all my work possible (Bin Shan, Lisa Nikolai, Kelvin Lien, Kelley Dunfield, Shay Missiaen, Andrea Botero, Urmila Basu, Solomiya Kucharyshyn, Brock Mason) and my graduate colleagues (Qiong Xiao, Xiaoyu Wang, Mianmian Zhu, Siyu Wang, Juli Wang, Elias Rietzschel, Duncan Giebelhaus, Hannah Lantz) for providing a functional atmosphere for me to thrive in. Lastly, I want to thank all the scholarship providers that helped me afford my education and conference trips, particularly the Alberta Canola Producers Commission.

Table of Contents

List of Tables

List of Figures

Abbreviations

AA	amino acid
AAD	acyl-ACP desaturase
ACBP	acyl-CoA binding protein
ACCase	acetyl-coA carboxylase
ACP	acyl carrier protein
BADC	biotin attachment domain containing
BCCP	biotin carboxyl carrier protein
CESA	cellulose synthase
CPT	CDP-choline:diacylglycerol cholinephosphotransferase
CSC	cellulose synthase complex
DAG	*sn*-1,2-diacylglycerol
DGAT	diacylglycerol acyltransferase
ER	endoplasmic reticulum
EV	empty vector
FA	fatty acid
FAD	fatty acid desaturase
FAE	fatty acid elongase
FAME	fatty acid methyl ester
FAS	fatty acid synthase
FAT	acyl-ACP thioesterase
FAX	fatty acid export
GC-FID	gas chromatography with flame ionization detector

GC-MS	gas chromatography-mass spectrometry
GPAT	*sn*-glycerol-3-phosphate acyltransferase
G3P	*sn*-glycerol-3-phosphate
KAS	3-ketoacyl-ACP synthases
LACS	long-chain acyl-CoA synthetase
LEC	leafy cotyledon transcription factor
LPA	lysophosphatidic acid
LPAAT	lysophosphatidic acid acyltransferase
LPC	lysophosphatidylcholine
LPCAT	lysophosphatidyl:acyl-CoA acyltransferase
OB	oil body
gene-OE	gene overexpression
PA	phosphatidic acid
PAP	phosphatidic acid phosphatase
PC	phosphatidylcholine
PCR	polymerase chain reaction
PDAT	phospholipid:diacylglycerol acyltransferase
PDC	pyruvate dehydrogenase complex
PDCT	phosphatidylcholine:diacylglycerol cholinephosphotransferase
PL	phospholipase
PM	plasma membrane
PSV	protein storage vacuoles
RNAi	ribonucleic acid interference

SSP	seed storage protein
TAG	triacylglycerol
TF	transcription factor
VLCFA	very-long-chain fatty acid
WRI	WRINKLED

1 Chapter 1 Thesis Introduction and Literature Review

1.1 Introduction and Research Objectives

Vegetable oils (mainly triacylglycerols (TAGs)) are highly valued products globally, with uses in nutrition, biofuel, and beyond. Oilseed crops, such as canola (*Brassica napus* L.), produce substantial amounts of oil in their seeds to store energy. Global forces, such as population growth and climate change, have been driving increases in demand for vegetable oils, with a concomitant rise in research interest into enhancing plant oil production. Many studies have employed genetic engineering to improve seed oil contents and alter their fatty acid (FA) compositions (see section 1.1.1.4).

After seed oil extraction, the seed meal by-product, which consists primarily of protein and fiber, still possesses value as a feed component for livestock and aquaculture. Canola seed meal leftover from lipid extraction is often used for this purpose. The major components of black-seeded canola (the dominant cultivar in Canada) are oil, protein, and fiber (roughly 45%, 20%, and 10%, respectively) (Slominski & Campbell, 1990; Slominski et al., 2012; Anwar et al., 2015; Wanasundara et al., 2016; Canola Council of Canada, 2019). Although seed protein has valuable applications, the excess of fiber (especially cellulose, lignin, and cell wall-related anti-nutritive substances) in canola seed meal can inhibit digestion in some animals, thereby limiting the nutritional value of the meal (Bell, 1984; Annison & Choct, 1991; Slominski et al., 1994; Jiang & Deyholos, 2010; Wickramasuriya et al., 2015; Li et al., 2017B; Opazo-Navarrete et al., 2019; Lannuzel et al., 2022). Comparing and improving the digestibility of seed meal for animal diets, especially the effect of fiber on protein digestibility, is an active area of study (Zdunczyk et al., 2013; Anwar et al., 2015; Joehnke et al., 2018; Alhomodi et al., 2022; reviewed in Paula et al., 2019, and Lannuzel et al., 2022). It has also been shown that increased nutritional value can

be achieved in yellow-seeded canola cultivars with reduced fiber content or through dehulling of seeds from black-seeded canola cultivars which possess thick seed coat (Bell, 1984; Slominski et al., 1994; Slominski, 1997; Matthaus, 1998; Slominski et al., 2012). Furthermore, the desirable amino acid (AA) profile and high protein digestibility of canola meal suggests potential use of canola protein for human consumption (Anwar et al., 2015). Taken together, it is of interest to improve oil and protein content simultaneously (or increase protein content without penalizing oil content) and decrease cellulose content in oilseed crops such as canola.

Once fertilized by pollination, plant seeds undergo development by establishing a viable embryo as well as accumulating sufficient levels of various nutrients (especially a lipids, proteins, starch, and free sugars) to support the growth of the embryo upon germination (Allen & Young, 2013; Baud et al., 2008). Sugars produced by photosynthesis provide the carbon source for the biosynthesis of major biomolecules, including cell wall polysaccharides, starch, FAs for storage lipids, and AAs for storage proteins (Angeles-Núnéz & Tiessen, 2011; Baud et al., 2008). These storage substances typically accumulate within the cotyledons of the embryo, such as in canola and *Arabidopsis* (Murphy et al., 1989; Mansfield & Briarty, 1992), or within the endosperm, such as in corn, wheat, and rice (Lopes & Larkins, 1993). In canola and *Arabidopsis*, seed lipid and protein biosynthesis primarily occur in the mid to late stages of embryo growth and development, with lipid accumulation increasing and peaking somewhat earlier than protein (Baud et al., 2008; Murphy & Cummins, 1989). Seed carbon partitioning is important to the synthesis of storage compounds within seeds and varies greatly between plant species, depending on the genetics involved and the strength of carbon sinks, often leading to biosynthetic trade-offs between lipids, proteins, and carbohydrates. Carbon partitioning can be drastically impacted by the given genetics; for example, the seeds of *Arabidopsis lec2* mutants experienced precipitous

declines in protein and lipid contents, while sucrose and starch contents increased dramatically (Angeles-Núnéz & Tiessen, 2011). Relationships of carbon competition have been described between carbohydrate and lipid biosynthesis in both legumes (Song et al., 2017A) and *Arabidopsis* (Focks & Benning, 1998; Shi et al., 2012; Li et al., 2018B; Liu et al., 2022), as well as between seed lipid and protein biosynthesis (Katepa-Mupondwa et al., 2005; Kambhampati et al., 2020). These findings suggest that the allocation of carbon resources within seeds is not fixed, which raises the possibility of deliberately manipulating the flow of resources within crop seeds to obtain superior nutritional and economic value.

While in general there is a trade-off between oil and protein contents in seeds, including canola and yellow mustard (Grami et al., 1977; Katepa-Mupondwa et al., 2005) and soybean (Kambhampati et al., 2020), previous research has suggested that seed oil and protein contents may be increased simultaneously by partially reallocating metabolic resources away from seed fiber biosynthesis (Jiang & Deyholos, 2010; Slominski et al., 2012; Opazo-Navarrete et al., 2019; Jayawardhane et al., 2020). Thus, there is an opportunity for canola genetic engineering to contribute to research on adding value to seed meal by increasing the protein content (without reducing the oil content) and improving the digestibility of the meal by partially reducing the fiber content (Li et al., 2017B; Jayawardhane et al. 2020). Nevertheless, manipulation of seed carbon partitioning as a strategy for improving the nutritional and economic value of seeds by targeting fiber, lipid, and protein content simultaneously has not yet been attempted through genetic engineering. In addition, it would be reasonable to select target genes based on our knowledge of the relevant biosynthetic pathways and test their performance in the fast-growing model plant species, *Arabidopsis,* before employing the strategy to improve canola through biotechnology.

Plant storage lipid biosynthesis consists of two main biosynthetic pathways: assembly of carbon units into FAs and assembly of FAs into TAG (Fig. 1). Once FAs are synthesized in the plastids and exported, they are primarily channeled into TAG through the glycerol-3-phosphate (G3P) pathway, also known as the Kennedy Pathway. Diacylglycerol acyltransferase (DGAT) catalyzes the final and committed step in the Kennedy pathway, and has a well-documented and outsized role in seed oil biosynthesis. Overexpression (OE) of *DGAT1*, as well as improving DGAT enzymatic performance, is effective at increasing lipid accumulation (reviewed in Xu et al., 2018A and Chen et al., 2022).

Seed storage proteins (SSPs) serve as a form of nitrogen storage for germinating seedlings. AAs are the building blocks of proteins, and they must be channeled into developing seeds for SSP biosynthesis. A myriad of genes involved in AA synthesis, transport, and transcriptional regulation of SSP genes contribute to the level of protein accumulation in seeds (see section 1.1.2). Overexpression of several AA transport and biosynthesis-related genes has been demonstrated to increase SSP content (Rolletschek 2005; Lee 2020; Zhou 2009; see Table 1.2); in particular, *AtAAP1*, *AtALAAT1*, and *AtASN1* appear to have high potential for enhancing seed protein accumulation. In addition, *AtUmamiT18* has been shown to contribute to the flow of AAs into the seed during embryo development (Ladwig et al., 2012), though its potential for enhancing SSP accumulation through overexpression has not been studied.

Cellulose is a carbohydrate polymer and a major source of fiber in plant tissues as it comprises a large proportion of plant cell walls (Wilson et al., 2021). There are several known genes encoding the CESA complex which synthesizes cell wall cellulose, and previous research has implicated *AtCESA1* as a promising target for manipulating cellulose biosynthesis (Beeckman et al., 2002; Burn et al., 2002; Jayawardhane et al., 2020; see section 1.1.3). Seed-

specific ribonucleic acid interference (RNAi)-mediated down-regulation of *AtCESA1* in *Arabidopsis* has been shown to slightly reduce the seed cellulose content, without causing major phenotypic abnormalities. Partial down-regulation of seed cellulose led to a small increase in seed protein content, but the seed oil content declined slightly (Jayawardhane et al., 2020). Thus, down-regulation of *AtCESA1* appears to be a promising start for partially reducing the fiber content of oilseeds and improving their nutritive properties. In addition, since DGAT1 has an important role in TAG biosynthesis, its overexpression may offer a promising avenue for counter-acting the small negative effect of *AtCESA1* down-regulation on seed lipid accumulation.

Table 1.1 Recent genetic manipulations of seed storage protein content in plant seeds

Species	Gene	Expression	Target Pathway or Mechanism	Transformation Method	Phenotypic Outcome	Reference
Arabidopsis thaliana	*OsASN1*	ZmUBI promoter OE	AA Biosynthesis	A. tum	↑ SSPs	Lee et al., 2020
Arabidopsis thaliana	*SAT1*	OE (bundle sheath cell-specific)	AA Biosynthesis	A. tum	↑ SSPs	Xiang et al., 2018
Arabidopsis thaliana	*IbEXP1*	OE	Cell Wall Development	A. tum	↑ SSPs	Bae et al., 2014
Arabidopsis thaliana	*FAX1*	Seed-specific OE	FA Transport	A. tum	↑ SSP, ↑ oil	Tian et al., 2018
Arabidopsis thaliana	*FAX2*	Seed-specific OE	FA Transport	A. tum (CRISPR)	↑ SSP, ↑ oil	Tian et al., 2019
Arabidopsis thaliana	*GmLEC2a*	OE	Transcription	A. tum	↑ SSPs, ↑ oil	Manan et al., 2017
Arabidopsis thaliana	*TTG1*	Knockout mutant	Transcription	T-DNA insertion	↑ SSPs	Chen et al., 2015
Arabidopsis thaliana	*RGL3*	OE	Transcription	A. tum	↑ SSPs	Hu et al., 2021
Glycine max	*AAP6a*	OE (35S)	AA Transport	A. tum	↑ SSPs, ↑ NUE	Liu et al., 2020
Oryza sativa	*AAP6a*	OE (35S)	AA Transport	A. tum	↑ SSPs	Peng et al., 2014
Oryza sativa	*OsRAG2*	OE (ZmUBI1 promoter)	SSP Biosynthesis	A. tum	↑ SSPs	Zhou et al., 2017
Oryza sativa	*GZF1*	RNAi (seed-specific)	Transcription	A. tum	↑ SSPs	Chen et al., 2014
Oryza sativa	*NF-CY12*	OE (ZmUBI1 promoter)	Transcription	A. tum	↑ SSPs	Xiong et al., 2019
Pisum sativum	*PsAAP1(3a)*	OE	AA Transport	A. tum	↑ SSPs	Grant et al., 2021
Pisum sativum	*PsAAP1*	Phloem-specific OE	AA Transport	A. tum	↑ SSPs	Zhang et al., 2015A
Pisum sativum	*PsAAP1*	Phloem-specific OE	AA Transport	A. tum	↑ SSPs, ↑ NUE	Perchlik & Tegeder, 2017
Triticum aestivum	*TaAAP13*	Endosperm-specific OE	AA Transport	Particle bombardment	↑ SSPs	Wan et al., 2021
Triticum aestivum	*TuSPR*	RNAi	Transcription	Particle bombardment	↑ SSPs	Shen et al., 2021
Triticum aestivum	*ODORANT1*	RNAi	Transcription	Particle bombardment	↑ SSPs	Luo et al., 2021

The hypothesis of this project is that RNAi down-regulation of seed cellulose (*AtCESA1*-RNAi) biosynthesis will liberate carbon resources that can then be drawn into lipid biosynthesis through overexpression of selected genes in lipid and protein biosynthesis and gene down-regulation in cellulose synthesis. The overall research objective is to test the combination of *AtCESA1*-RNAi, overexpression of *BnDGAT1,* and overexpression of genes associated with SSP biosynthesis genes (*AtAAP1*, *AtALALAAT1*, *AtASN1*, *AtUmamiT18*) in *Arabidopsis* seeds, with the aim of finding the best combination for further investigation in canola and other oilseed crops. In addition, this project involves analyzing the lipids of a large number of *Arabidopsis* seed samples with direct methylation followed by quantification with GC-FID, but existing seed lipid analysis methods are time consuming. Therefore, it is necessary to generate a robust and faster seed lipid analysis method for the overall research objective.

The specific research objectives are:

(1) optimize the plant lipid analysis method, which will be used to analyze the *Arabidopsis* seeds generated in the following research objectives.

(2) generate homozygous lines with *AtCESA1*-RNAi and *BnDGAT1*-OE and choose the most promising lines.

(3) overexpress targeted protein biosynthesis-related genes (*AtAAP1*, *AtALALAAT1*, *AtASN1*, and *AtUmamiT18*) in these lines to test the functions of the gene combinations on seed cellulose, lipid, and protein content.

(4) generate homozygous lines with *AtCESA1*-RNAi/*BnDGAT1*-OE, and overexpress one of the protein biosynthesis-related genes to test the functions of the gene combinations on seed cellulose, lipid, and protein content.

1.2 Literature Review

This literature review section covers seed lipid biosynthesis (synthesis of FAs, TAG assembly, genetic engineering of plant lipids, plant lipid analysis methods), seed protein biosynthesis (seed storage proteins, regulation of storage protein synthesis, genetic engineering of seed protein), and cellulose biosynthesis (types of cellulose synthases and their effects on seed composition).

1.2.1 Seed Lipid Biosynthesis

1.2.1.1 *De novo* Fatty Acid Biosynthesis & Acyl Editing

The major biosynthetic processes involved in the accumulation of seed storage oil are FA synthesis and TAG assembly (depicted in Figure 1.1). Seed FAs are first synthesized in plastids, followed by transport to the endoplasmic reticulum (ER) for acyl editing and TAG synthesis (Ohlrogge et al., 1979; Thelen & Ohlrogge, 2002). Additionally, regulatory factors often play diverse and important roles in mediating storage lipid biosynthesis, especially transcription factors (TFs) (Kong et al., 2020A).

The *de novo* synthesis of FAs involves the consumption of the carbon substrate acetyl-coenzyme A (CoA), which is the building block of acyl chains. In order to supply the plastid with carbon substrates for FA synthesis, pyruvate transporters such as bile acid:sodium symporter family protein 2 (BASS2) facilitate the entry of pyruvate into the plastid (Lee et al., 2017). Once imported, FA synthesis begins through the conversion of pyruvate to acetyl-CoA by the pyruvate dehydrogenase complex (PDC) (Williams & Randall, 1979). Acetyl-CoA then acts as the substrate for acetyl-CoA carboxylase (ACCase) which catalyzes the conversion of acetyl-

CoA to malonyl-CoA (Konishi et al., 1996; Ke et al., 2000). This is considered the first step in FA synthesis because this reaction commits acetyl-CoA to acyl chain assembly (Thelen & Ohlrogge, 2002).

Subsequently, acyl-CoA molecules are joined to acyl carrier proteins (ACPs) for further extension (Baud et al., 2008). From this point, the acyl chain is assembled through a series of reactions catalyzed by ketoacyl synthases (KAS family members) in a process known as condensation, which elongate the ACP-bound acyl chain (Brown et al., 2006; Yang et al., 2016). KAS III catalyzes the first elongation reaction between malonyl-ACP and acetyl-CoA to produce a 4-carbon acyl-ACP, which is extended by 2-carbon subunits via KAS I catalysis until a 16:0-ACP is assembled (Baud et al., 2008; Dehesh et al., 2001). A cycle of condensation, reduction, dehydration and a second reduction take place to add 2-carbon increments. This 16:0-ACP can either be lysed by acyl-ACP thioesterase B (fatty acid thioesterase B, FATB), liberating 16:0 from the ACP, or catalyzed by KAS II to produce 18:0-ACP (Salas & Ohlrogge, 2002). The 18:0-ACP can either be cleaved by FATB to produce free 18:0 or the acyl chain can be converted to 18:1-ACP, which is catalyzed by stearoyl-CoA-desaturase (SAD) (Salas & Ohlrogge, 2002; Shanklin & Somerville, 1991). Alternatively, 16:0- and 18:0-ACP can undergo desaturation to 16:1- or 18:1-ACP by acyl-ACP desaturases (AADs) (Shanklin & Somerville, 1991; Browse & Somerville, 1991; Bryant et al., 2016). Acyl-ACP thioesterase A (fatty acid thioesterase A, FATA) can then hydrolyze the 18:1-ACP to yield free 18:1 (Salas & Ohlrogge, 2002). The thioesterase-mediated cleavage of acyl chains from ACPs is essential for providing free FAs that can then be shuttled and processed for downstream pathways, in particular TAG synthesis.

Fatty acid exporter (FAX) members, including FAX1 and FAX2, are FA transporters that provide an important contribution to the export of lipids from the plastid and positively impact seed oil accumulation (Li et al., 2015B; Li et al., 2020; Tian et al., 2018; Tian et al., 2019). The free FAs are then metabolically activated through linkage to CoA by long-chain acyl-CoA synthetases (LACSs) (Aznar-Moreno et al., 2018; Shockey et al., 2002). FAX and LACS members likely play important roles in acyl shuttling mechanisms through plastid membranes and enabling the accumulation of acyl-CoAs in the cytosol, which is a necessary precondition for acyl editing and TAG synthesis (Tian et al., 2019). Multiple FAX homologs have been reported in the model plant *Arabidopsis*, and their precise functions require further exploration. Studies of LACS homologs from a diversity of plant species have revealed that these enzymes are essential for acyl chain activation and acyl trafficking between organelles (e.g. from plastid to ER), and also play a role in seed oil accumulation and FA composition (Zheng et al., 2018; Wang et al., 2021; Jessen et al., 2015; Ding et al., 2020; Xu et al., 2018B). Higher plants generally possess several LACS homologs exhibiting certain levels of functional redundancy, as well as a diversity of effects on lipid metabolism, and their precise functions in seed oil accumulation and FA composition remain to be investigated further (Jessen et al., 2015; Zhao et al., 2019B; Zhao et al., 2021).

The synthesized acyl-CoAs persist in the cytosol and can be used in the biosynthesis of acyl lipids on the ER. Acyl-CoA binding proteins (ACBPs) bind to acyl-CoAs and enable the maintenance of an acyl-CoA pool, and thus play an intermediary role in lipid biosynthesis (Xiao & Chye, 2011; Guo et al., 2019B). The transportation of acyl-CoA to the ER for acyl editing and TAG assembly may be facilitated by acyl transporters (Guo et al., 2019B). ABCA9 has been identified as one such transporter and its activity contributes substantially to seed oil

accumulation, though other unknown ER-localized acyl-CoA importers may also contribute to the transport process Kim et al., 2013; Cai et al., 2021).

Acyl chains can be further modified (also known as acyl-editing) to increase their diversity, and subsequently the FA profile of the seed oil, with desaturation and elongation being the two main modification reactions (Stymne & Stobart, 1984). Desaturation occurs on phosphatidylcholine (PC), and the synthesis of 18:2-PC and 18:3-PC from 18:1-PC catalyzed by fatty acid desaturase 2 and 3 (FAD2 and FAD3), respectively, are two common reactions in plant seeds (Okuley et al., 1994; Arondel et al., 1992). The Land's cycle is comprised of de-acylation and re-acylation between lysophosphatidylcholine (LPC) and phosphatidylcholine (PC) and plays an important role in the exchange of acyl-chains between the PC pool and acyl-CoA pool, where lysophosphatidyl;acyl-CoA acyltransferase (LPCAT), phospholipase A and acyl-CoA synthase catalyze the reactions. Elongation catalyzed by fatty acid elongase (FAE) on the ER is the key step in producing very long chain FAs (VLCFA, with 20C or more), which includes a sequence of condensation, reduction, dehydration and a second reduction, much as with fatty acid synthase in the plastid (Rossak et al., 2001). However, the FA elongation reaction is different from *de novo* FA synthesis in several ways, such as the reaction positions (ER vs. plastid) and source of 2-carbon units (malonyl-CoA vs. malonyl-ACP). While desaturation and elongation are the main derivations of FAs, other modification reactions can also take place. These further enzymatic reactions may give rise to the synthesis of unusual FAs, such as ricinoleic acid through the hydroxylation of 18:1-PC (Moreau & Stumpf, 1981; van de Loo et al., 1995; Bates & Browse, 2012). In addition, it should be noted that although the desaturation and elongation of acyl-chains on the ER are pivotal for seed oil formation, desaturation also occurs in

the plastid catalyzed by FAD4 through FAD7, and the activity of these enzymes is important in lipid biosynthesis (Browse & Sumerville, 1991; Gutt et al., 2016).

1.2.1.2 TAG Biosynthesis & Storage

Acyl-CoA can serve as an acyl donor for three acyltransferase reactions producing TAG in the Kennedy pathway (Kennedy & Weiss, 1956; Weiss et al., 1960). Glycerol-3-phosphate acyltransferase (GPAT) catalyzes the first attachment of an acyl chain to the glycerol backbone, thereby converting glycerol-3-phosphate (G3P) to lysophosphatidic acid (LPA) and ultimately promoting oil accumulation (Jain et al., 2000; Singer et al., 2016; Bai et al., 2021; reviewed in Jayawardhane et al., 2018). The glycerol backbone in LPA is then acylated again, this time by lysophosphatidic acid acyltransferase (LPAAT), yielding phosphatidic acid (PA) (Lassner et al., 1995). The phosphate group is then cleaved from PA through the catalytic activity of phosphatidic acid phosphatase (PAP), which generates diacylglycerol (DAG) (Nakamura et al., 2009). Finally, the third and final acylation is catalyzed by diacylglycerol acyltransferase (DGAT), resulting in the production of TAG. As the enzyme catalyzing the last committed step in acyl-CoA dependent TAG biosynthesis, DGAT has been studied extensively for decades (reviewed in Xu et al., 2018 and Chen et al., 2022). An alternative TAG biosynthetic pathway involves the enzyme phospholipid:diacylglycerol acyltransferase (PDAT), which transfers an acyl group from PC to DAG to yield TAG (Xu et al., 2018; Banas et al., 2014; Stahl et al., 2004). The relative contribution of DGAT and PDAT to TAG formation may differ depending on the plant species (Zhang et al., 2009).

Other reactions also contribute to the Kennedy pathway for TAG biosynthesis. Since PC is a major substrate for acyl-editing, the entry and exit of FAs into PC and crosstalk between the

PC pool and DAG/TAG are important in determining FA composition. CDP-choline:DAG cholinephosphotransferase (CPT) and PC:DAG cholinephosphotransferase (PDCT) facilitate interconversion between DAG and PC (Slack et al., 1983; Slack et al., 1985; Lu et al., 2009). This interconversion allows DAG to be derived from the PC pool through the activity of PAP in combination with either phospholipase C (PLC) or phospholipase D (PLD) (Novotna et al., 2000; Lee et al., 2011). It is well-established that these dynamic reactions are important in the biosynthesis of seed oils with various FA profiles in different plant species.

TAGs accumulate in oil bodies (OBs) in the cytosol and serve as a major energy source for seedling growth (Yatsu & Jacks, 1972; Tzen, 2012; Gu et al., 2017). OBs are storage organelles for TAG, consisting of a single-layered phospholipid membrane, and are synthesized at the ER (Yatsu & Jacks, 1972; Tzen, 2012; Frey-Wyssling et al., 1963; Chen et al., 2019). Several oleosin proteins are found in abundance in OB membranes, contributing to their stability and facilitating the separation of OBs from the ER (Tzen 2012; Huang 1992; Jolivet et al., 2004; Huang et al., 2017) Oleosins are important for proper oil accumulation and the expression of *OLEOSIN* genes is promoted by several major transcription factors (Kim et al., 2014; Manan et al., 2017). Other OB membrane proteins, such as caleosin (CLO1) and steroleosin (HSD1), also contribute to OB stability and are important for long-term seed oil stability (Jolivet et al., 2004; reviewed in Tzen, 2012). Recent studies have revealed that OB biogenesis also involves other enzymes such as OB-associated protein (LDAP) LDAP-interacting protein (LDIP) and SEIPIN proteins in *Arabidopsis*, and the mechanisms underlying OB formation may involve different sets of OB-packaging proteins in different species (Pyc et al., 2021; Coulon et al., 2020; Greer et al., 2020; reviewed in Chapman et al., 2019). However, many *OLEOSIN* and other OB-related genes remain uncharacterized and further research is warranted (Zhang et al., 2019A).

1.2.1.3 Regulation of Lipid Biosynthesis

During seed development and the accumulation of seed oil, the expression of lipid biosynthesis genes is subjected to regulation by a variety of mechanisms (Figure 1.2). Because of its involvement in the crucial step in FA synthesis, ACCase is an important target for regulation. The biotin carboxyl carrier protein (BCCP) subunit of ACCase is a known target for biotin attachment domain containing (BADC) proteins, which are negative regulators of ACCase activity (Liu et al., 2019A; Salie et al., 2016). ACCase activity can also be regulated by carboxyl transferase interactor (CTI) 1, CTI2, and CTI3, which are plastid envelope proteins that dock ACCase at the plastid membrane, reducing its activity (Nikovics et al., 2020). The flow of carbon into FA synthesis is thereby reduced through the inhibition of ACCase mediated by CTIs. However, knockout of these *CTI* genes in *Arabidopsis* did not affect the quantity of seed oil (Nikovics et al., 2020), which may imply that other unidentified regulatory factors are involved and warrants further research.

Regulating the expression of lipid-related genes is necessary to coordinate the development of the seed as well as the synthesis and sequestration of TAG for storage. TFs have manifold influential roles in mediating lipid biosynthesis in seeds. Since the discovery of the *WRINKLED1* (*WRI1*) TF, which is one of the most important regulatory factors in lipid biosynthesis, there has been extensive study of the roles and interactions of TFs in the regulation of lipid biosynthesis regulation (Focks & Benning, 1998; Kong et al., 2020A). WRI1 is known to promote the expression of more than twenty lipid biosynthesis-related genes, including *BCCP2* (which encodes a subunit of ACCase), *ACP1*, and *KASI* (Liu et al., 2019; Maeo et al., 2009). Loss-of-function *wri1* mutants consequently accumulate up to 80% less seed oil, illustrating the

substantial importance of WRI in storage lipid biosynthesis (Focks & Benning 1998). The diverse interactions and regulatory targets involving WRI1 have been recently reviewed (Kong et al., 2019).

WRI1 was recently found to promote the expression of negative regulators of FA synthesis, such as *BADC1/2/3*. WRI1 binds directly to *BADC* promoters and drives their expression, providing a fine-tuning mechanism of FA synthesis that allows cells to achieve lipid homeostasis by promoting *BADC* expression and inhibiting ACCase activity (Liu et al., 2019). While the recruitment of RNA polymerase to lipid biosynthesis genes is necessary for the WRI1-mediated promotion of transcription, the relationship between RNA polymerase and WRI1 was unknown until the recent discovery of the Mediator complex subunit 15 (MED15). MED15 was shown to act in concert with WRI1 to deliver RNA polymerase to the promoters of genes involved in lipid biosynthesis pathways and to positively contribute to seed oil accumulation (Kim et al., 2016B).

Several pre- and post-transcriptional regulatory factors have been identified that influence WRI1 itself, including LEC1, LEC2, FUS3, 14-3-3, BPMs, and KIN10/SnRK1, leading to downstream effects on the expression of oil biosynthesis genes (Kong et al., 2020A). TFs such as MYB89 and TCP4 have also been shown to directly repress *WRI1* expression, leading to reduced expression of oil biosynthesis genes and consequently seed oil accumulation (Kong et al., 2020B; Li et al., 2017A). There are also post-translational regulatory mechanisms for WRI1. For example, 14-3-3 proteins are regulatory proteins capable of binding to and stabilizing phosphorylated WRI1, thus reducing WRI1 degradation, promoting the expression of lipid biosynthesis genes, and enhancing seed oil synthesis (Kong & Ma, 2018; Ma et al., 2016). The TF DRBEL, from the DREB family, was also recently identified as a direct positive regulator of

major lipid TFs such as *WRI1, ABI3, and ABI5*, illustrating the complexity of interactions between transcriptional regulators that modulate lipid biosynthesis (Zhang et al., 2016C).

Several other TFs contribute to the regulation of lipid biosynthesis gene expression and seed oil accumulation. For example, many MYB-class TFs have also been found to play roles in lipid biosynthesis; in particular, MYB96 strongly impacts seed oil accumulation by driving the expression of *DGAT1* and *PDAT1*, which are the main enzymes involved in *de novo* and derived TAG synthesis, respectively (Lee et al., 2015). On the other hand, MYB5 functions as part of a transcription activation complex that stimulates the expression of *GL2*, which encodes a known repressor of seed oil synthesis (Cheng et al., 2021). MYB5 is negatively regulated by MYB Interacting Factor 1 (MIF1), which binds to and targets MYB5 for degradation, thereby reducing the GL2-mediated repression of oil synthesis. Similarly, MYB73 promotes oil biosynthesis by decreasing the expression of oil-reducing *GL2* (Liu et al., 2014). Some MYB TFs also have specific impacts on FA composition, such as MYB115 and MYB118, which stimulate the synthesis of unsaturated FAs in the seed by promoting the transcription of two acyl desaturation genes, *AAD2* and *AAD3* (Troncoso-Ponce et al., 2016).

Several TFs from the TZF family have been shown to strongly promote the expression of lipid-related genes and promote oil synthesis. ZF392 forms a regulatory mechanism with two other TFs, ZF351 and NF-YA, to promote oil accumulation by driving the expression of key genes involved in FA synthesis (*BCCP2*, *KASIII*), TAG synthesis (*DGAT1*), TAG storage (*OLEO1*), and transcriptional regulation of lipid genes (*WRI1*) (Lu et al., 2021). However, further research is needed to characterize the roles of other TZF family members in modulating oil biosynthesis.

AIL7, a TF in the AIL/PLT subfamily, appears to have a broad influence on seed oil content and FA composition through the transcriptional regulation of a multitude of genes involved in lipid biosynthesis, including FA synthesis (*KASI, ACCase, ACP*), acyl-CoA activation (*LACS9*), TAG synthesis (*LPAAT, PDAT*), acyl editing (*FAD3, FAE1, KCS*), and OB formation (*OLEO1*) (Singer et al., 2021). Further characterization is needed to discern precisely how AIL7 modulates the expression of these downstream lipid biosynthesis genes. In addition, other AIL subfamily genes may also contribute to the regulation of lipid biosynthesis, as the up-regulation of *AIL5* and *AIL6* has been observed in *Arabidopsis* seedlings following the induced over-expression of *FUS3*, which encodes a TAG-enhancing TF (Zhang et al., 2016A).

Furthermore, several TFs have roles in repressing the expression of genes in oil biosynthesis pathways. For example, numerous TFs from the WRKY family, including WRKY2, WRKY6, and WRKY40, are known negative regulators of lipid biosynthesis that inhibit the transcription of lipid-promoting genes such as *WRI1* and *ABI5* (Song et al., 2020; Yeap et al., 2017). Similarly, the KIN10 kinase (also known as SnRK1) negatively regulates WRI1 and DGAT1 through phosphorylation, resulting in reduced expression of lipid biosynthesis genes and diminished TAG synthesis (Zhai et al., 2017; Caldo et al., 2018). The regulation of lipid biosynthesis can also occur at the epigenetic level. One such regulatory factor, GCN5, deactivates several lipid-related genes (particularly *FAD3*) through histone acetylation, thereby reducing desaturation of 18:2 to 18:3 and modifying the FA composition of the seed oil (Wang et al., 2016A).

The research described here illustrates the substantial progress that has been made in terms of characterizing the major TFs and regulatory mechanisms involved in seed lipid biosynthesis. However, the regulation of lipid biosynthesis by TFs is complex and requires a

substantial amount of further exploration. For example, a recent transcriptomic study in canola has identified a vast network of TFs that are putatively involved in seed oil accumulation that have yet to be properly characterized and situated within transcriptional regulation networks of lipid biosynthesis (Rajavel et al., 2021).

1.2.1.4 Highlights in Seed Oil Engineering

Much of the research on seed oil engineering is focused on increasing seed oil accumulation or altering the properties of the seed oil by changing the FA composition. Since many studies have investigated the genetic engineering of seed oil biosynthesis, we have highlighted a limited selection of recent and promising examples in this chapter (also see Table 1.1). In addition, the genetic engineering of seed oil content and FA composition specifically through CRISPR/Cas9 has been recently reviewed elsewhere (Subedi et al., 2020).

Table 1.2 Recent genetic manipulations of oil content and fatty acid composition in plant seeds

Species	Gene	Expression	Target Pathway or Mechanism	Transformation Method	Phenotypic Outcome	Reference
A. thaliana, C. sativa	*ZmLEC1*	Seed-specific OE	Transcription	A. tum	↑ oil	Zhu et al., 2018
A. thaliana, Z. mays	*ZmSAD1*	Seed-specific OE	FA desaturation	A. tum, particle bombardment	↑ PUFAs	Du et al., 2016
Arabidopsis thaliana	*AAD2, AAD3, MYB115*	Seed-specific OE	FA desaturation	A. tum	↑ omega-7 FAs	Ettaki et al., 2018
Arabidopsis thaliana	*CnFATB3*	Seed-specific OE	FA desaturation	A. tum	↑ MCFAs & LCFAs	Yuan et al., 2017
Arabidopsis thaliana	*VfFAD2, VfDGAT2*	OE	FA desaturation, Kennedy	A. tum	↑ oil, 18:3, 20:3	Chen et al., 2015
Arabidopsis thaliana	*MCAMT*	Seed-specific OE	FA synthesis	A. tum	↑ oil	Jung et al., 2019
Arabidopsis thaliana	*SsDGAT2*	OE	Kennedy	A. tum	↑ 18:1, ↓ 18:3	Wang et al., 2016B
Arabidopsis thaliana	*AtDGAT1, RcFAH12, RcDGAT2*	OE & mutation	Kennedy	A. tum	↑ unusual Fas	van Erp et al., 2015
Arabidopsis thaliana	*Seipin1, RcFAH12*	Seed-specific OE	OBs, FA hydroxylation	A. tum	↑ HFAs	Lunn et al., 2018
Arabidopsis thaliana	*GmPLDy*	OE	PC Exchange	A. tum	↑ oil, ↑ LCFA	Bai et al., 2020
Arabidopsis thaliana	*AtPDAT*	OE	PC Exchange	A. tum	↑ oil	Banas et al., 2014
Arabidopsis thaliana	*BASS2*	Seed-specific OE	Pyruvate Transport	A. tum	↑ oil	Lee et al., 2017
Arabidopsis thaliana	*AIL7*	Seed-specific OE	Transcription	A. tum	↓ oil, ↓ LCFA, ↑ UFA	Singer et al., 2021
Arabidopsis thaliana	*SPATULA*	OE	Transcription	A. tum	↑ oil, ↓ SSP	Liu et al., 2017

Arabidopsis thaliana	*DGAT2*	Seed-specific OE	Kennedy	A. tum	↑ PUFA, ↓ 18:0	Jin et al., 2017
Arabidopsis thaliana	*GmLEC2a*	Seed-specific OE	Transcription	A. tum	↑ oil, ↑ SSP	Manan et al., 2017
Arabidopsis thaliana	*WRI1, DGAT1, SDP1*	Seed-specific OE	Transcription, Kennedy, Lipid turnover	A. tum	↑ oil, ↓ seed number	van Erp et al., 2014
Arabidopsis thaliana	*AtFAX1*	Seed-specific OE	Transport	A. tum	↑ oil, ↑ SSP, ↑ yield	Tian et al., 2018
Arachis hypogea	*AtLEC1*	Seed-specific OE	Transcription	A. tum	↑ oil, modified FA profile	Tang et al., 2018
B. napus, N. benthamiana	*BnGPDH, BnGPAT, DGAT, ScGPDH, ScLPAAT*	Seed-specific OE	Kennedy	A. tum	↑ oil	Liu et al., 2015
Brassica juncea	*AtDGAT1*	Seed-specific OE	Kennedy	A. tum	↑ oil, ↓ 18:1 & 18:2	Savadi et al., 2016
Brassica napus	*BnFAD2*	Gene edited allele	FA desaturation	CRISPR/Cas9, Ag tum	↑ 18:1, ↓ 18:2	Okuzaki et al., 2018
Brassica napus	*PgFADX, PgFAD2*	Seed-specific OE	FA desaturation	A. tum	Punicic acid synthesized	Xu et al., 2020
Brassica napus	*BnFATB2, BnSADs*	Seed-specific OE & miRNA	FA desaturation, FA synthesis	A. tum	↑ 16:0 & 18:0	Sun et al., 2014
Brassica napus	*SsDGAT1*	OE	Kennedy	A. tum	↑ oil	Peng et al., 2016
Brassica napus	*BnLACS2*	OE	Kennedy	A. tum	↑ oil, ↓ protein	Ding et al., 2020
Brassica napus	*GmDOF4, GmDOF11*	OE	Transcription, FA desaturation	A. tum	↑ 18:1, ↓ 18:2 & 18:3	Sun et al., 2018
Camelina sativa	*pPLAIIId*	Seed-specific OE	Acyl editing	A. tum	↑ oil, ↓ seed cellulose	Li et al., 2015A
Camelina sativa	*CpuFATB3, CvFATB1, CnLPAAT*	Seed-specific OE	FA desaturation, Kennedy	A. tum	↑ 10:0, 12:0, 14:0, 16:0	Kim et al., 2015
Camelina sativa	*LaKCS, AtKCR, AtHCD, AtECR,*	Seed-specific OE	FA synthesis	A. tum	↑ 24:1	Huai et al., 2015
Camelina sativa	*AtDGAT1, ScGPD1*	Seed-specific OE	Kennedy	A. tum	↑ oil & seed weight	Chhikara et al., 2018
Camelina sativa	*DGAT1A, DGAT1B, DGAT1C*	Seed-specific OE	Kennedy	A. tum	↑ oil and number of cells in seeds	Kim et al., 2016A
Camelina sativa	*AtWRI1*	Seed-specific OE	Transcription	A. tum	↑ oil & seed weight	An & Suh, 2015
Camelina sativa	*FAX1/ABCA9*	OE	Transport	A. tum	↑ oil & seed weight	Cai et al., 2021
Camelina sativa	*MYB96A, DGAT1C*	Seed-specific OE	Transcription, Kennedy	A. tum	↑ oil	Kim et al., 2019
Carthamus tinctorius	*FAD2.2, FATB*	Seed-specific RNAi	FA desaturation & synthesis	A. tum	↑ 18:1	Wood et al., 2018
Crambe abyssinica	*CaFAD2, CaFAE1*	Seed-specific RNAi	FA desaturation & elongation	A. tum	↑ 18:1, ↓ 22:1	Li et al., 2016
Glycine max	*SiDGAT1*	OE	Kennedy	A. tum	↑ oil, ↓ protein, ↓ sugars, changed FA profile	Wang et al., 2019
Glycine max	*GmDGAT1 variants*	Seed-specific OE	Kennedy	Recombination mediated cassette exchange	↑ oil, ↑ protein, ↓ carbohydrates	Roesler et al., 2016
Glycine max	*GmDGAT2A*	Seed-specific OE	Kennedy	A. tum	↑ oil, 18:2	Jing et al., 2021
Glycine max	*DGAT1A, DGAT1B*	Seed-specific OE	Kennedy	A. tum	↑ oil, ↓ protein	Zhao et al., 2019A
Glycine max	*ZF392*	OE	Transcription	A. tum	↑ oil	Lu et al., 2021
Gossypium hirsutum	*GhACCase (BCCP1, BC1, CTa2, CTb)*	Seed-specific OE	FA synthesis	A. tum	↑ oil	Cui et al., 2017
Gossypium hirsutum	*GhDGAT1*	Seed-specific OE	Kennedy	A. tum	↑ oil, ↓ protein, ↑ 16 :0, 18 :0, 18 :1	Wu et al., 2021
Gossypium hirsutum	*GhDOF1*	OE	Transcription	A. tum	↑ oil, ↓ seed protein	Su et al., 2017
Jatropha curcas	*DGAT1, DGAT2*	OE	Kennedy	A. tum	↑ oil, 18:2, ↓ protein, 16:0, 18:0, 18:1	Zhang et al., 2021
Lepidium campestre	*AtWRI1, AtHb2, BvHb2*	Seed-specific OE	Transcription, hemoglobins	A. tum	↑ oil	Ivarson et al., 2017
Nicotiana tabacum	*SiFAD7*	OE	FA desaturation	A. tum	↑ 18:3, ↓ 18:2	Bhunia et al., 2016
Oryza sativa	*ACBP2*	OE	Acyl Pool	A. tum	↑ oil & LCFAs	Guo et al., 2019A
Vernonia galamensis	*DGAT1A*	Seed-specific OE	Kennedy	Particle bombardment	↑ oil, ↓ carbohydrate	AL-Amery et al., 2019

Since *de novo* FA synthesis and acyl editing are essential components of seed oil content and FA profiles, numerous genes involved in these processes have been engineered in recent studies. For example, the transport of carbon substrates into the plastid in preparation for FA synthesis is an essential process but has lacked research attention. The plastid-localized transporter BASS2, which facilitates the import of pyruvate to supply the carbon substrate for FA synthesis, has been found to increase oil accumulation when overexpressed in *Arabidopsis* seeds (Lee et al., 2017). Several proteins involved in the FA synthesis pathway have also been identified as promising targets for seed oil engineering. The overexpression of genes encoding ACCase subunits leads to an increase in seed oil content, as does the down-regulation and/or knockout of several *BADC* genes (which encode ACCase repressors) (Salie et al., 2016; Cui et al., 2017; Keereetaweep et al., 2018). The engineering of FA synthesis can also be used to modify the types of FA that are synthesized. The overexpression of certain *FATB* members has been demonstrated to increase the proportions of short and medium chain FAs, while overexpression of *LACS*9 increased the abundance of long chain FAs at the expense of medium chain FAs (Wang et al., 2021; Yuan et al., 2017; Kim et al., 2015). The overexpression of *FAD2* or *SAD1* has been shown to increase levels of unsaturated FAs (Chen et al., 2015; Du et al., 2016).

Lipid transporters have also been the subjects of genetic engineering. For example, overexpression of *ABCA9* resulted in a substantial increase in seed TAG content (Kim et al., 2013). Notably, overexpression of either *FAX1* or *FAX2* greatly increased seed oil content while simultaneously increasing seed protein content, with no impact on the FA composition (Tian et al., 2018; Tian et al., 2019). The simultaneous overexpression of *FAX1*/*ABCA9* was shown to

substantially increase seed oil content, likely by enhancing the shuttling of lipids out of the plastid (FAX1) and into the ER (ABCA9) for TAG synthesis (Cai et al., 2021).

Much research has investigated enzymes in the Kennedy pathway for their potential in seed lipid engineering. For instance, the overexpression of LPAATs results in increased seed oil content and increased unsaturated FA levels, likely by elevating several lipid biosynthesis pathways (Chen et al., 2015; Liu et al., 2015). Furthermore, as the main enzyme responsible for synthesizing TAG in the final step of the Kennedy pathway, DGAT is an obvious and well-established candidate for genetic engineering of seed oil (Jako et al., 2001; Taylor et al., 2009; van Erp et al., 2014; Peng et al., 2016; Wang et al., 2019). Co-expression of DGAT with other genes has also been used to increase seed oil content. For example, the combination of seed-specific overexpression of yeast *GPD1* to increase availability of the G3P backbone substrate with overexpression of *DGAT1* to increase TAG synthesis led to increases in both seed oil content and seed yield (Chhikara et al., 2018). Some DGATs may also be promising for modifying the seed FA composition; for example, the overexpression of *SsDGAT2* increased the proportion of 18:1 at the expense of 18:3 (Wang et al., 2016B). DGAT continues to be a key target for increasing seed oil through augmenting TAG synthesis (reviewed in Xu et al., 2018A).

Studies have also aimed to improve seed oil content by targeting proteins involved in TAG storage organelles. OLEO1 is the major protein in the membranes of oil bodies and its overexpression in seeds increased the expression of several lipid biosynthesis-related genes, including *DGAT1*, leading to increased seed oil accumulation, despite reduced OB size (Zhang et al., 2019A; Lu et al., 2018). Overexpression of several oleosins from *Brassica napus* L. (*OLE1*, *OLE2*, and *OLE4)* increased the seed oil content, 18:2 content, and OB size (Chen et al., 2019). Altering the expression of *OLEOSIN* genes may increase the rate of budding of OBs from the ER

and results in smaller OBs, which may prove to be a limiting factor in using oleosins to engineer higher oil content (Song et al., 2017B). This occurrence may be related to the *SEIPIN* family, which localize to ER-OB junctions and are involved in determining OB size (Cai et al., 2015). For example, overexpression of *SEIPIN1* increases OB size and seed oil accumulation, while *SEIPIN1* down-regulation reduced OB size and oil content. Thus, there may be potential in combining overexpression of both seipins and oleosins to determine whether the number and size of OBs can be increased simultaneously to achieve an additive effect on seed oil accumulation.

TFs also hold an abundance of potential for seed oil engineering. WRI1 is a key target for genetic engineering because of its central regulatory role in oil biosynthesis (Ivarson et al., 2017; Ye et al., 2018). Overexpression of *WRI1* has been shown to increase the expression of *PDC* and *ACCase*, which are responsible for the initial channeling of carbon into FA synthesis, resulting in greater seed oil accumulation (An & Suh, 2015). Protecting post-translational WRI1 from degradation may also be a viable strategy to engineer seed oil, as demonstrated by the increased oil accumulation achieved by overexpression of a 14-3-3 protein (Ma et al., 2016).

The metabolic engineering of genes in other pathways may also affect lipid biosynthesis. For example, a gene with no obvious role in storage lipid biosynthesis, *chalcone synthase* (*CHS*), was recently found to influence seed oil pathways. Overexpression of *CHS* revealed the upregulation of several genes involved in seed maturation and FA synthesis, resulting in changes in the FA composition that increased the abundance of unsaturated FAs, especially 18:3, in the seed oil (Peng et al., 2021). This reveals a previously unknown effect by *CHS* on lipid biosynthesis, although further exploration is needed to clarify the mechanisms involved and determine the potential for *CHS* in seed oil engineering.

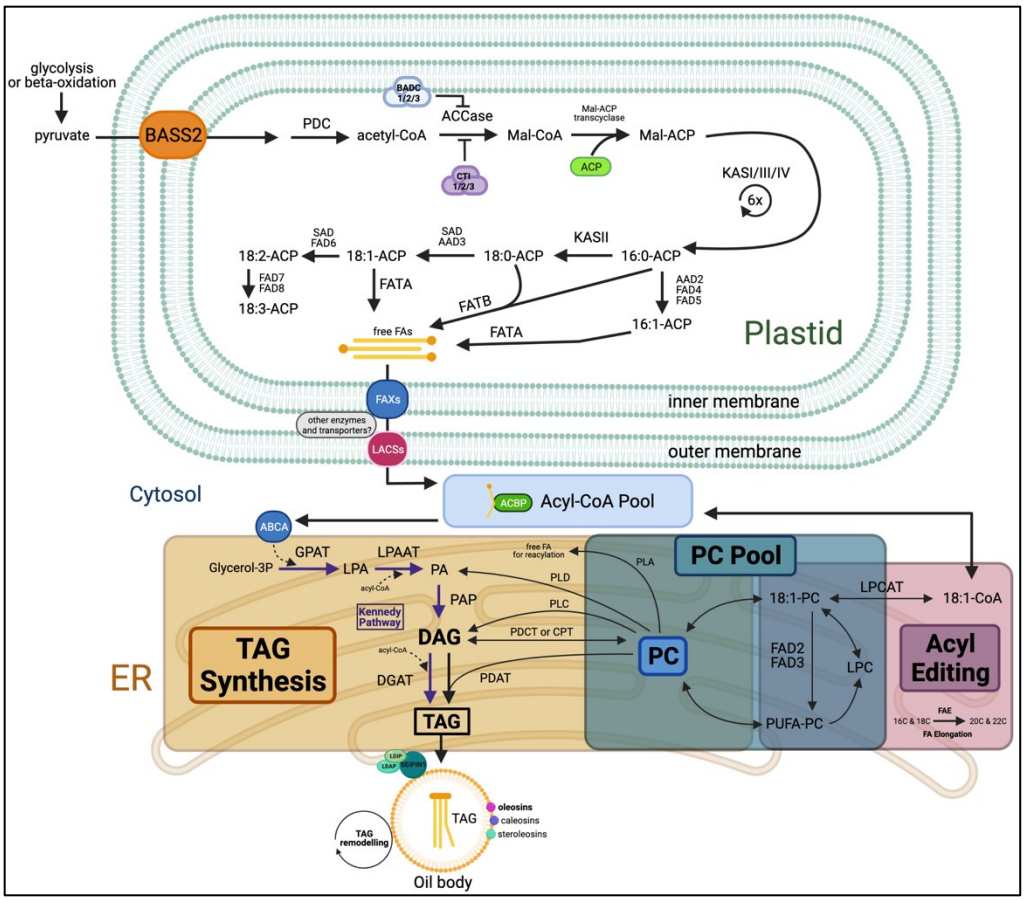

Figure 1.2.1 Overview of FA and TAG Biosynthesis Pathways in Plant Seeds
The fundamental proteins and chemicals involved in seed lipid biosynthesis, as well as recent discoveries and other key members with potential for seed oil engineering are included here. This figure is not a comprehensive rendering of all lipid biosynthesis enzymes and pathways. Made using Biorender.com. Abbreviations: BASS2, bile acid:sodium symporter family protein 2; PDC, pyruvate dehydrogenase complex; BADC (1/2/3), biotin/lipoyl attachment domain containing (1/2/3); CTI (1/2/3), carboxyltransferase interactor (1/2/3); ACCase, acetyl-CoA carboxylase; Mal, malonyl; ACP, acyl carrier protein; KAS, ketoacyl synthase; AAD (2/3), acyl-acyl carrier protein desaturase (2/3); FAD (4/5/6/7/8), fatty acid desaturase (4/5/6/7/8); FAT (A/B), fatty acid thioesterase (A/B); SAD, stearoyl-acyl carrier protein desaturase; FA, fatty acid; FAX, fatty acid exporter; LACS, long chain acyl-CoA synthetase; ACBP, acyl-CoA binding protein; ABCA, ATP-binding cassette A; GPAT, glycerol-3-phosphate acyltransferase; LPA, lysophosphatidic acid; LPAAT, lysophosphatidic acid acyltransferase; PA, phosphatidic acid; PAP, phosphatidic acid phosphatase; DAG, diacylglycerol; DGAT, diacylglycerol acyltransferase; TAG, triacylglycerol; LDAP, lipid dropletassociated protein; LDIP, LDAP interacting protein; PDAT, phospholipid:diacylglycerol acyltransferase; PDCT, phosphatidylcholine:diacylglycerol cholinephosphotransferase; CPT, CDP-choline:diacylglycerol cholinephosphotransferase; PL (A/B/C), phospholipase (A/B/C); PC, phosphatidylcholine; LPCAT, lysophosphatidylcholine acyltransferase; LPC, lysophosphatidylcholine; PUFA, polyunsaturated fatty acid; FAE, fatty acid elongase.

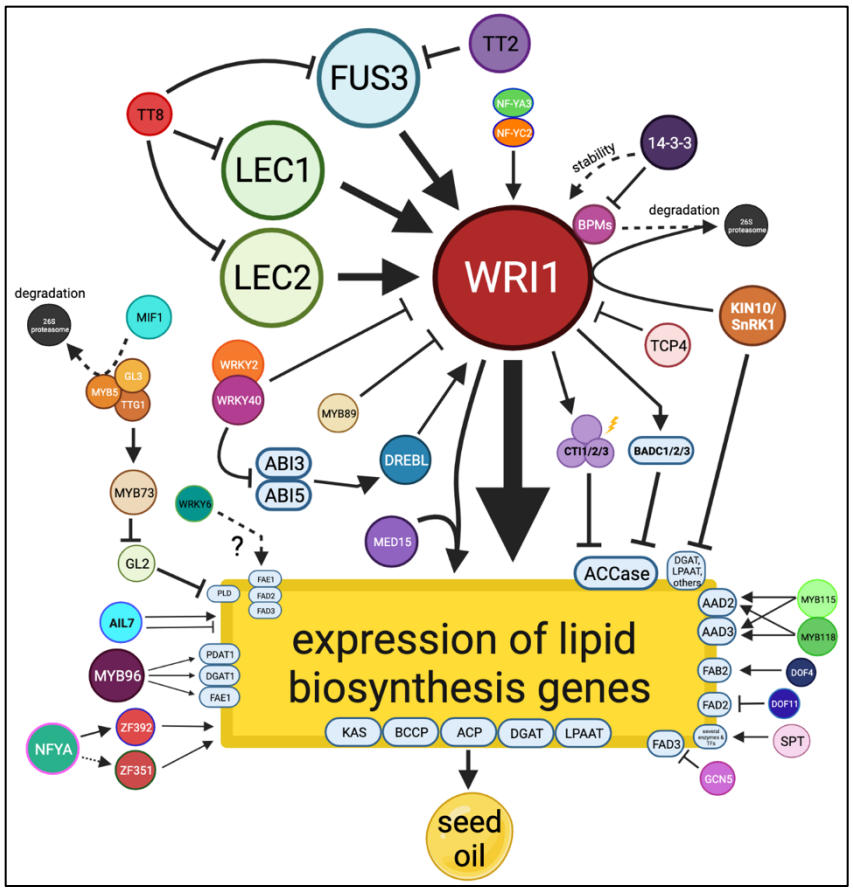

Figure 1.2.2 Overview of Lipid Biosynthesis Regulation in Plant Seeds
The fundamental regulatory and transcription factors involved in seed lipid biosynthesis, as well as recent discoveries and other key members with potential for seed oil engineering are included here. This figure is not a comprehensive rendering of all regulators and transcription factors in lipid biosynthesis. Made using Biorender.com. Abbreviations: TT (2/8), transparent testa (2/8); LEC (1/2), leafy cotyledon (1/2); FUS3, FUSCA3; NF-Y (A/A3/C2), nuclear factor of the Y box (A/A3/C2); BPM, BTB/POZMATH 1; SnRK1, sucrose non-fermenting-1-related kinase 1; TCP4, TCP family transcription factor 4; BADC (1/2/3), biotin/lipoyl attachment domain containing (1/2/3); CTI (1/2/3), carboxyltransferase interactor (1/2/3); DREBL, dehydration-responsive element-binding protein L; MED15, MEDIATOR 15; MYB (5/73/89/96/115/118), MYB-family domain protein (5/73/89/96/115/118); WRKY (2/6/40), WRKY-family transcription factor; ABI, abscisic acid insensitive; MIF1, mini zinc finger 1; TTG1, transparent testa glabra 1; GL (2/3), glabra (2/3); AIL7, aintegumenta-like 7; DOF (4/11), DNA binding with one finger (4/11); SPT, SPATULA; GCN5, general control nonderepressible 5; PLD, phospholipase D; FAE1, fatty acid elongase 1; FAD (2/3), fatty acid desaturase (2/3); PDAT, phospholipid;diacylglyerol acyltransferase; DGAT1, diacylglycerol acyltransferase 1; KAS, ketoacyl synthase; BCCP, biotin carboxyl carrier protein; LPAAT, lysophosphatidic acid acyltransferase; ACCase, acetyl-CoA carboxylase; AAD (2/3), acyl-acyl carrier protein desaturase (2/3); FAB2, fatty acid biosynthesis 2.

1.2.2 Seed Storage Protein Biosynthesis

SSPs allow for the long-term storage of nitrogen to supply seedling growth and accumulate during the late stages of seed development (Goldberg et al., 1994; Herman & Larkins, 1999). Upon germination, they are broken down into AAs that supply protein biosynthesis for seedling growth (Fujiwara et al., 2002; Thompson, 2018). SSPs also contribute to seed longevity by shielding the seed from oxidative damage, thereby slowing the pace of seed deterioration, and are important for proper germination (Nguyen et al., 2015; Kwak et al., 2019). The stability of SSPs themselves can be enhanced through sumoylation by SIZ1, which post-translationally modifies SSPs to improve their longevity (Kwak et al., 2019).

SSP biosynthesis, as distinct from AA biosynthesis, differs substantially from lipid biosynthesis in that it does not consist of sequential enzyme-catalyzed reactions with chemical intermediates. Rather, SSP genes that have been transcribed into mRNA are then translated by ER-localized ribosomes into proteins, followed by folding, processing, and transport (Herman & Larkins, 1999; Boston et al., 1996). After the transport and processing of SSPs, they accumulate within protein storage vacuoles (PSV) for storage (Chrispeels et al., 1991). As with most cellular functions, there is extensive transcriptional regulation of genes encoding SSPs, AA transporters, and other associated proteins (Fujiwara et al., 2002). This chapter does not cover the pathways of AA biosynthesis and instead focuses on factors that affect the accumulation of SSPs (especially TFs).

The two main storage protein classes in *Arabidopsis* and *B. napus* are 12S globulins (cruciferin, CRU) and 2S albumins (napins, NAP) (Fujiwara et al., 2002). Many other major SSPs exist and are often named after the species in which they are abundant, such as glycinin in *Glycine max* (soybean), and zeins in *Zea mays* (corn) (Fujiwara et al., 2002; Li et al., 2018A;

Xiong et al., 2019). SSPs are typically multimeric assemblies of identical or related proteins; in *Arabidopsis*, napins are encoded by a five-member gene family (*At2S1-At2S5*) while cruciferins are encoded by four genes (*AtCRA1/CRU1*, *AtCRA2*, *AtCRB/CRU2*, and *AtCRC/CRU3*). In legumes such as faba bean (*Vicia faba* L.) and pea (*Pisum sativum* L.), the main SSPs are vicilins and legumins (Thompson et al., 2018; Warsame et al., 2018).

Several studies have demonstrated that SSP composition has remarkable plasticity because knocking out one or more SSP-encoding genes typically results in negligible or small impacts on the overall SSP content (Lyzenga et al., 2019; Rolletschek et al., 2020). Instead of reducing overall SSP content, the knockout or down-regulation of genes encoding SSPs, including even the most important SSPs, leads to large compensatory shifts in the abundance of other SSPs (Schmidt et al., 2011; Kawakatsu et al., 2010; Zhang et al., 2015A; Zheng et al., 2019). The redistributions in SSP composition reported in these studies are typically accompanied by changes in the AA and FA profiles as well. These studies demonstrate the impressive plasticity of maturing seeds with knockdowns or knockouts of major SSPs to adjust their proteomes and provide insights for engineering seed proteins.

1.2.2.1 Regulation of Seed Storage Protein Biosynthesis

The expression of SSP-encoding genes is regulated by many TFs (Figure 1.2.3), but a select set of TFs play an outsized role in seed maturation, development, and accumulation of storage compounds (Thompson, 2018; Baumlein et al., 1994; Fatihi et al., 2016). These include master TFs such as ABI3, ABI5, FUS3, LEC1, and LEC2, which are essential for SSP accumulation (Fujiwara et al., 2002; Baumlein et al., 1994; Reidt et al., 2000). The expression of many SSP genes is directly promoted by these master TFs (Thompson, 2018; Ezcurra et al.,

1999; Kroj et al., 2003; Lara et al., 2003; Monke et al., 2004; Braybrook et al., 2006; Sun et al., 2017). There is also regulatory interaction between these master TFs, with LEC1 able to directly promote the expression of *FUS3* and *ABI3*, which has a positive effect on expression of SSP genes as well as overall seed protein content (Kagaya et al., 2005). The transcription-promoting action of ABI3 can be enhanced through synergistic interaction with the regulatory protein RGL3, thereby augmenting SSP gene expression and seed protein accumulation (Hu et al., 2021). FUS3 can contribute to seed protein content through indirect means, such as by repressing the expression of *TTG1*, a repressor of genes encoding napin, thereby supporting seed protein accumulation (Chen et al., 2015). There is partial functional redundancy between these key TFs, making it challenging to precisely define the extent of their roles and targets.

In addition to the key TFs discussed above, many other TFs are also known to affect SSP gene expression and seed protein content (Gacek et al., 2018). MYC2, MYC3, and MYC4 are negative regulators of cruciferin synthesis but positively regulate napin synthesis, with a net negative effect on seed protein content (Gao et al., 2016). Another negative regulator, GZF1 directly represses expression of the SSP gene *GluB-1* and attenuates seed protein content (Chen et al., 2014). A pair of TFs, RISBZ1 and RPBF, have been shown to function in tandem to synergistically promote SSP accumulation, specifically globulins and prolamins (Yamamoto et al., 2006; Kawakatsu et al., 2009). NF-YC12 directly promotes expression of *GS1;3*, which is involved in AA synthesis and subsequently increases seed protein content (Xiong et al., 2019). Some TFs have broad, negative effects on SSP gene expression, such as the MYB-family TF ORDORANT1 and the NAC-family member TuSPR, both of which attenuate seed protein levels. Other NAC TFs such as NAC019, NAC20, NAC26, NAC128, and NAC130 have been

shown to foster SSP accumulation by promoting the expression of several SSP-encoding genes (Luo et al., 2021; Shen et al., 2021; Wang et al., 2020; Zhang et al., 2019B; Gao et al., 2021).

The expression of zein-encoding genes is regulated by several major TFs including O2, PBF, OHP1, and OHP2, all of which positively influence the zein content in seed (Yang et al., 2016; Zhang et al., 2015B). Both bZIP22 and MADS47 can interact with other major zein-promoting TFs such as PBF1, OHP1, and OHP2 to stimulate SSP gene expression and biosynthesis (Li et al., 2018A; Qiao et al., 2016). ABI9 was found to be a positive regulator of seed protein accumulation by promoting the expression of several SSP-related TFs, including O2, PBF1, NAC128, NAC130, O11, and VP1 (Zheng et al., 2019; Yang et al., 2021). The transcriptional regulation of zeins in corn has been recently described in a detailed review (Li & Song, 2020).

1.2.2.2 Amino Acid Transporters & Seed Storage Protein Accumulation

SSP biosynthesis requires an adequate supply of AA substrates and is therefore dependent on the translocation of these molecules through the phloem to developing seeds (Fujiwara et al., 2002; Frommer et al., 1993; Yang et al., 2020). AA transport proteins are involved in the movement of AAs through the plant body and supply them to the seeds for SSP synthesis (Yang et al., 2020). Amino acid permeases (AAPs) are important long-distance transporters of AAs throughout the plant, including root-to-shoot and source-to-sink transport as well as between tissues and between organelles. *AAP1* and *AAP8* are known to be highly expressed in seeds and their function is essential for providing AAs during seed development for SSP accumulation (Gacek et al., 2018; Miranda et al., 2001; Sanders et al., 2009; Weigelt et al., 2008; Grant et al., 2021). However, loss of AAP8 function does not eliminate source-to-sink AA

transport and seed protein does not decrease, implying compensatory function by yet-unidentified transporters (Yang et al., 2020; Santiago & Tegeder, 2016). Several AA transporters such as OMT, AAP2, AAP6, and CAT6 are all known to provide important contributions in AA transport to developing seeds and increasing seed protein content (Gacek et al., 2018; Yang et al., 2020; Grant et al., 2021; Riebeseel et al., 2009; Schmidt et al., 2007; Peng et al., 2014; Liu et al., 2020). Another class of AA transporters called, UmamiTs, are known to play important roles in supplying AAs to developing seeds (Muller et al., 2015). Several of these transporters, such as UmamiT18, have been shown to be important in supplying AAs to developing embryos and that single knockout mutants for these genes produce substantially smaller seeds with reduced AA content (Ladwig et al., 2012; Muller et al., 2015). However, loss of function of some transporters (e.g., UmamiT24 and UmamiT25) does not reduce AA content or seed protein content upon maturity, suggesting some level of redundancy within the UmamiT transporter family (Besnard et al., 2018). Although the importance of these UmamiT members in AA transport and seed development has been partially explored, the potential for using them in engineering to increase SSP content has not yet been explored.

1.2.2.3 Highlights in Seed Storage Protein Engineering

Much of the research on SSP biosynthesis pathways is focused on the regulation of SSP gene expression (summarized in Table 1.2). Transcriptional regulators are obvious targets for seed protein engineering; for example, overexpression of major TFs such as *LEC2*, *ABI19*, and *FUS3* have been shown to increase SSP gene expression and seed protein content while knockdown of the expression of *ORDORANT1* and *SPR* (SSP-repressing TFs) enhanced seed protein accumulation (Manan et al., 2017; Sun et al., 2017; Luo et al., 1863; Shen et al., 2021;

Yang et al., 2021). The transport and synthesis of AAs have also been explored for increasing seed protein content through genetic interventions. For example, the overexpression of the AA-synthesizing genes (e.g., *ASN1*) or AA transporters (e.g., *AAP1*, *AAP6*, *AAT*) improved nitrogen use efficiency and led to concomitant increases in seed protein content (Peng et al., 2014; Liu et al., 2020; Lee et al., 2020; Perchlik & Tegeder, 2017; Zhou et al., 2009). These studies demonstrate that the synthesis and movement of AAs is a promising area for enhancing seed protein levels. A unique approach to enhance SSP content is through overexpression of *RAG2*, an amylase/trypsin inhibitor, which caused an increase in SSP accumulation, although the mechanisms involved are unclear (Zhou et al., 2017).

As mentioned previously, the overexpression of the lipid transporters *FAX1* and *FAX2* greatly increases seed oil content while simultaneously increasing seed protein content (Tian et al., 2018; Tian et al., 2019). This is an unusual outcome given that seed oil and protein accumulation are typically negatively correlated due to the competition of their biosynthesis pathways for resources, indicating that FAX transporters may be promising targets for simultaneously engineering increased storage oil and protein content in seeds (Kanai et al., 2016 & references therein).

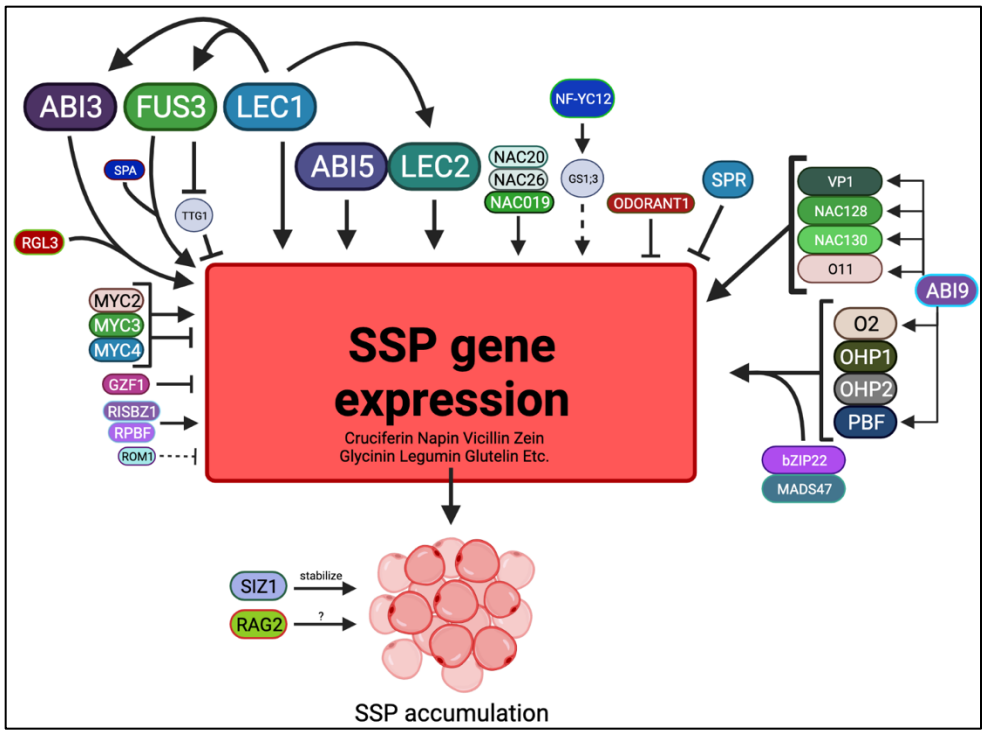

Figure 1.2.3 Overview of Storage Protein Biosynthesis Regulation in Plant Seeds
The fundamental regulatory and transcription factors involved in seed protein biosynthesis, as well as recent discoveries and other key members with potential for seed protein engineering are included here. This figure is not a comprehensive rendering of all regulators and transcription factors in seed protein biosynthesis. Made using Biorender.com. Abbreviations: ABI (3/5/9), abscisic acid insensitive (3/5/9); FUS3, FUSCA3; LEC (1/2), leafy cotyledon (1/2); NAC (19/20/26/128/130), NAC-family transcription factor (19/20/26/128/130); NY-FC12, nuclear factor of the Y box C12; GS1;3, glutamine synthase 1;3; SPR, storage protein repressor; VP1, viviparous 1; O (2/11), opaque (2/11); OHP (1/2), O2 heterodimerizing protein (1/2); bZIP22, basic leucine zipper transcription factor 22; PBF, prolamin-box binding factor; MADS47, MADS-box transcription factor 47; MYC (2/3/4), MYC-family basic helix-loop-helix transcription factor (2/3/4); GZF1, GDNF inducible zinc finger protein 1; RISBZ1, rice seed b-Zipper 1; RPBF, rice prolamin-box binding factor; ROM1, regulator of MAT1; SIZ1, E3 SUMO ligase SIZ1; RAG2, rice albumin gene 2; RGL3, RGA-like protein 3; SPA, storage protein activator; TTG1, transparent testa glabra 1.

1.2.3 Seed Cellulose Biosynthesis

Cellulose is a major structural polymer comprising the body of plants and is synthesized by large multimeric complexes anchored in the plasma membrane (PM) (Polko et al., 2018; Wilson et al., 2021; Fig. 1.2.4). These cellulose-synthesizing structures are referred to as

cellulose synthase complexes (CSCs) and are comprised of cellulose synthase (CESA) subunits (Paredez et al., 2006; Desprez et al., 2007; Somerville, 2006; Wilson et al., 2021). Once synthesized in the ER and exported to the PM, the CSC is moved along microtubule tracks. CSC then synthesize cell walls by depositing cellulose microfibrils. Cellulose synthase interacting 1 (CSI1) was the first protein identified that does not belong to the CESA family but directly interacts with CESA1, CESA3, and CESA6 (Gu et al., 2010). Interestingly, the CC members CC1 and CC2 are essential for supporting the connection between the CSC and microtubules while experiencing stresses such as salt, thereby supporting cell growth and elongation in spite of cell stress (Endler et al., 2016). Another key element for proper CSC function and trafficking is KORRIGAN (KOR), which directly interacts with the CSC and may serve as a point of regulation of cellulose biosynthesis (Vain et al., 2014; Zhang et al., 2016B). Likely, other unknown CSC-associated and CSC-regulation factors also contribute to the process, and their identification is an active area of study. Together, these proteins contribute to the tethering and movement of CSCs and are integral to proper cellulose biosynthesis and cell development.

In *Arabidopsis*, the CESA subunits are encoded by a family of ten genes (*AtCESA1-10*) and provide different contributions to cellulose synthesis depending on the developmental timing, tissue type, and whether primary or secondary wall is being synthesized (Persson et al., 2007; Somerville, 2006; Taylor et al., 2003). Among the ten *Arabidopsis* CESA members, AtCESA1/2/3/5/6/9 have been implicated in primary cell wall synthesis, while AtCESA4/7/8 are associated with secondary cell wall synthesis (Persson et al., 2007; Somerville, 2006; Taylor et al., 2003). There are various relationships of partial or complete redundancy amongst the various CESA members and although all ten *AtCESA* genes are expressed across *Arabidopsis* tissues, the level of expression varies by tissue and phase of development (Beeckman et al., 2002; Persson et

al., 2007; Desprez et al., 2007). Both *AtCESA1* and *AtCESA3* are likely to be non-redundant in cellulose biosynthesis because knock-out mutations for these genes resulted in severe phenotypic abnormalities (Beeckman et al., 2002; Persson et al., 2007). The interaction and functional overlap of AtCESA members is complex and there remain gaps in the understanding of these relationships, as well its involvement in the synthesis and structure of cell walls (Daras et al., 2021).

AtCESA1 has long been understood as an essential contributor to the proper assembly of the CSC, cellulose synthesis, and cell development within the embryo (Arioli et al., 1998). This is consistent with later work demonstrating that cell expansion is modulated by proper function and regulation of AtCESA1 (Chen et al., 2010). In the embryo, *AtCESA2*, *AtCESA3* and *AtCESA9* are co-expressed with *AtCESA1*, though *AtCESA1* is especially important in embryo cell wall development (Burn et al., 2002). Only these four *AtCESA* genes have significant expression levels in the developing embryos of *Arabidopsis*, indicating that they may be prime targets for modification of seed cellulose biosynthesis (Beeckman et al., 2002; Jayawardhane et al., 2020). Little is known about the regulation of AtCESA members, and thereby cellulose biosynthesis, although AtCESA1 is regulated by circadian and hormonal mechanisms, often via phosphorylation (Chen et al., 2010; Sanchez-Rodriguez et al. 2017; Speicher et al., 2018; Lehman & Sanguinet, 2019; Yuan et al., 2019). Recently, seed-specific down-regulation of *AtCESA1* in *Arabidopsis* through RNA interference (RNAi) has been shown to partially reduce the seed cellulose content without severe phenotypic abnormalities, whereas *AtCESA9*-RNAi down-regulation did not reduce the seed cellulose content (Jayawardhane et al., 2020). The *AtCESA1*-RNAi lines exhibited some compositional changes in the seeds, with protein and lipid contents increasing and decreasing slightly, respectively, and no effect on soluble glucose

content. This suggests that cellulose biosynthesis affects seed carbon partitioning and may have implications for modifying the protein and lipid content of seeds. However, some phenotypic effects may be associated with manipulation of seed cellulose biosynthesis. Mutation of *AtCESA1* and its subsequent impacts on seed cellulose content may affect the rate of germination (Zhang et al., 2022), along with slightly delayed germination, reduced seedling root length, and reduced hypocotyl length (Jayawardhane et al., 2020; Zhang et al., 2022). Besides these seedling phenotype abnormalities, no major growth and development abnormalities were reported in these studies. Although monitoring for some negative seedling phenotypes is warranted, taken together, the existing literature may suggest that *AtCESA1* is the most promising target within CSCs for reducing the seed fiber content in crops valued for their seed oil and protein, given the lack of redundancy for its function by other *AtCESA* members in *Arabidopsis* seeds.

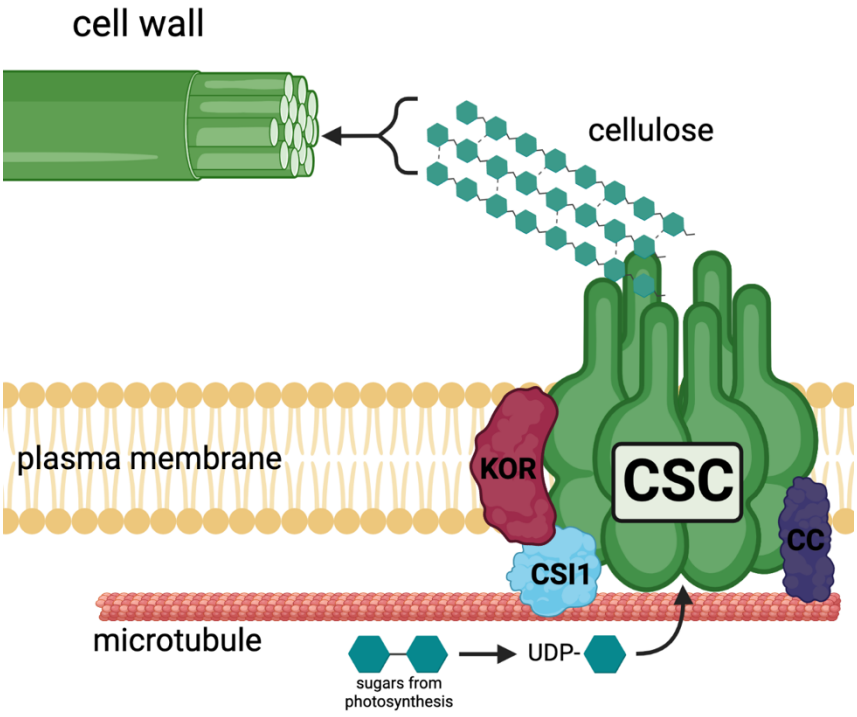

Figure 1.2.4 Scheme of Cellulose Biosynthesis by the Cellulose Synthase Complex

CSC, cellulose synthase complex; KOR, KORRIGAN; CSI1, cellulose synthase interacting 1; CC, companions of cellulose synthase; UDP, uridine diphosphate.

2 Chapter 2 Optimization of the Direct Transmethylation Procedure for Plant Lipid Analysis

2.1 Abstract

Measuring acyl lipid content and fatty acid composition is important in plant lipid research, and direct transmethylation followed by analysis with GC/FID has been broadly used in various studies. However, many existing protocols are time-consuming and labor-intensive, and the long reaction time under high temperature may artificially change fatty acid compositions of the samples. In this study, we optimized the direct transmethylation method for seed and leaf samples with a wide range of sizes, oil contents and fatty acid profiles, which can be completed in 2 hours. We also demonstrated that commercial disposable pipet tips, as well as polypropylene tubes under certain conditions, could be reliably used to replace glass tubes, Pasteur pipettes, and rubber bulbs to improve efficiency. Taken together, this optimized and generalized method could be used as a reliable and less time- and labor-intensive approach to analyze acyl lipid content and fatty acid profile of plant samples.

2.2 Introduction

Vegetable oils have diverse applications in food, feed, biofuel, and oleochemical industry. Accurate measurement of acyl lipid content and fatty acid (FA) composition is frequently carried out with GC-FID or GC-MS, which have been broadly used in plant lipid biology, oil crop breeding, food science and other studies (AL-Amery et al, 2019; Li et al, 2006; Ma et al, 2020; Xu et al, 2021). Prior to GC analysis, lipids can be extracted from plant seeds and other tissues using homogenization and large amounts of organic solvents, then converted to volatile derivatives such as fatty acid methyl esters (FAMEs). Some commonly used methods for oil extraction and derivatization, however, are time-consuming, labor-intensive, and produce

unnecessary organic chemical waste (Harrington & D'Arcy-Evans, 1985). Alternatively, direct transmethylation, which skips the tedious step of lipid extraction, has been used to prepare FAMEs from plant samples for GC analysis (Li et al, 2006; Ma et al, 2020).

For direct transmethylation, the extent of oil recovery from a sample is determined by the degree to which oil interacts with an acid catalyst and is converted to FAMEs (Ma et al, 2020). Several factors such as reaction temperature, time and catalysts could influence the rate of solvent penetration, transmethylation, and the rate of oil recovery from a sample. High temperature is generally used in the direct transmethylation process but the reaction time under high temperature should be considered. It should be long enough for all lipids in plant samples to be fully converted to FAMEs, but extended exposure of samples to high temperatures may artificially change their fatty acid composition (Kail et al, 2012; Ma et al, 2020). Acid catalysts such as hydrochloric acid (HCl) or sulfuric acid (H_2SO_4) are broadly used in direct transmethylation, and the choice of acid catalyst should also be considered in analysis. While methanolic hydrochloride is commonly used, its lab preparation by bubbling gaseous hydrogen chloride in methanol is a procedure with potential danger and the commercial product is expensive (Hardouin and Lemaitre, 2020). Methanol with 2.5-5% sulfuric acid (H_2SO_4) has been demonstrated as an effective alternative (Li et al, 2006; Ma et al, 2020).

Moreover, antioxidants such as butylated hydroxytoluene (BHT) may also be used to reduce oxidative damage during the transmethylation reaction (Ma et al., 2020), and physical breaking down of plant tissue can be used to facilitate transmethylation of lipids for analysis (Harrington & D'Arcy-Evans, 1985). However, although direct transmethylation provides a rapid approach for lipid analysis, its application is currently restricted to small seeds such as *Arabidopsis* (Li et al, 2006; Ma et al, 2020), likely because of the limited penetration of

methanolic acid into large and hard plant tissues (e.g., whole canola seeds). It would be interesting to optimize and generalize a rapid and reliable direct transmethylation protocol for a diverse set of seeds and other plant tissues. In addition, the convention in lipid analysis methods is to use glassware including glass tubes and borosilicate pipets rather than disposable plastics due to the risk of introducing plastic-derived contamination into the samples, especially with the use of DMSO and chloroform (Watson et al, 2009), potentially resulting in unwanted peaks in the GC chromatograms, which makes the lipid analysis process cumbersome and time-consuming. It would be interesting to test if disposable plastic tubes and tips can be used in direct methylation, especially when we do not use solvents such as DMSO or chloroform.

The aim of this study, therefore, is to establish a reliable and generalized direct transmethylation method for seeds and plant tissues with a large range of oil contents and fatty acid compositions by optimizing the reaction time, temperature, chemicals and consumables. Our results indicated that crushed plant samples from various species can be effectively transmethylated with 2% H_2SO_4 within two hours at 95^{o}C, and commercial disposable pipet tips, as well as polypropylene tubes under certain conditions, could be reliably used to replace glass tubes, Pasteur pipettes, and rubber bulbs in the optimized protocol to improve efficiency and reduce workload.

2.3 Materials & Methods

2.3.1 Plant Materials

Arabidopsis thaliana (accession Colombia-0) seed, flax (*Linum usitasissimum*) seed, Proso millet (*Panicum miliaceum*) seed, canola (*Brassica napus*) seed, poppy (*Papaver somniferum* var. “Double Red”) seed, Apple of Peru (*Nicandra physalodes*) seed, Hedge

Caragana (*Caragana arborescens*) seed, and alfalfa (*Medicago sativa*) shoot tissue were used in the current study. All mature seeds were air dried under room temperature for two weeks, while the alfalfa tissue samples were freeze dried and stored at -80°C until further analysis. For the plastic materials used for comparison with the conventional glassware, polypropylene P1000 pipet tips (T-1000-B 1 mL blue pipet tips, Axygen, USA) and 15 mL centrifuge tubes (Basix centrifuge tube, 15 mL, Fisher Scientific, USA) were used.

2.3.2 Direct Transmethylation

Intact *Arabidopsis* seeds were used in direct transmethylation because the thin seed coat of the tiny seeds will not affect lipid analysis (Li et al, 2006). All other plant samples were vigorously ground using a mortar and pestle for up to one minute until the material was crushed to evenly small pieces. For direct transmethylation, approximately 10-30 mg of each sample were added to a 15ml glass or plastic tube with screw cap with ~100 μg of triheptadecanoin (17:0 triacylglycerol) as the internal standard, 25 μL of 0.2% methanolic BHT as antioxidant, and 2 mL of methanolic acid [3M methanolic HCl (Sigma-Aldrich, USA), freshly prepared 5% H_2SO_4 in methanol, or freshly prepared 2% H_2SO_4 in methanol, respectively]. After the lids were securely tightened, the samples were gently mixed, briefly centrifuged and incubated at 80°C, 95°C, or 110°C for 45 minutes to 16 hours, respectively, in an oven (Fisherbrand Isotemp Oven, Fisher Scientific, USA). After the transmethylation reaction, the tubes were taken out of the oven and cool down to room temperature, and 2 mL 0.9% NaCl solution and 2 mL hexane were added to the tube, mixed and centrifuged (1000 rpm, 1 min) for the extraction of FAMEs. Finally, 1 mL of the upper phase (hexane with FAME) was transferred to a GC vial for analysis with GC/FID.

2.3.3 Traditional Lipid Extraction & Transmethylation

To compare the efficiency of direct transmethylation with transmethylation of extracted lipid from plant samples, lipids were extracted with the classical Hara-Radin method and then used in transmethylation (Hara & Radin, 1978). Briefly, the ground plant samples underwent lipase-inactivation using isopropanol at 80°C, followed by homogenization for 30 seconds in 7:2 (v/v) hexane/isopropanol. Each tube was vortexed and centrifuged with 2 mL of 3.3% aqueous Na_2SO_4 and the upper phase was carefully transferred to a new tube and dried under a nitrogen stream. The total lipid extracts were then transmethylated in 1.5 mL of 2% H_2SO_4 in methanol at 95°C for 1 hour, followed by FAME extraction with hexane as described above.

2.3.4 FAME Analysis with GC

The FAMEs were analyzed on GC-FID (7890A GC System, Agilent Technologies) equipped with a DB-23 capillary column (30 m × 250 μm × 0.25 μm, Agilent Technologies) in a 10:1 split mode as described in our previous study (Jayawardhane et al., 2020). The temperature program was as follows: 165 °C for 4 min, ramping from 165 to 180 °C in 5 min, then 180 to 230 °C in 5 min. Peaks were identified by comparing the retention times to a GLC 421-A standard series (Nu-Chek Prep, MN, USA). Lipid content was calculated upon the known content of internal standards. GC-MS (5977A MSD, Agilent Technologies) with the same column and temperature program was used for the double confirmation of FAME peaks and for analysis of the other peaks.

2.3.5 Statistical Analysis

All statistical analyses for Chapter 2 (Student's *t*-test, one-way ANOVA and Kruskal-Wallis) were conducted in RStudio (4.1.2), with incubation length (time) as the independent variable and total lipid content/FA content as the dependent variables. All figures were generated in Microsoft Excel (Version 16.54, 21101001).

2.4 Results of Lipid Extraction Optimization

2.4.1 Optimization of direct transmethylation for *Arabidopsis* seeds

We sought to optimize the transmethylation incubation length, temperature, and acid catalyst (methanolic HCl versus H_2SO_4) to determine the ideal conditions for plant lipid analysis. Low (80°C), medium (95°C), and high (110°C) temperatures were chosen within the range of those used in existing publications, and intact *Arabidopsis* seeds were used as the plant material in this optimization. Reaction temperatures (80°C and 95°C) and incubation lengths (1, 1.25, 1.5, 2, 3, 4 hours and overnight) were tested. With 3M methanolic HCl, total lipid content plateaus after 3-4 hours at 80°C (Fig. 2.4.1A) and after 1.5 to 2 hours at 95°C (Fig. 2.4.1B), respectively. The results suggested that increasing the incubation temperature increased the rate of lipid extraction, which was consistent with a recent study (Ma et al., 2020). The FA composition was not notably affected by the increase in reaction temperature from 80°C to 95°C (Table S1, S2). Moreover, there was no significant difference between the total lipid contents in the samples subjected to a single hexane extraction versus double hexane extraction (Fig. 2.4.1A), which is consistent with previous studies (Li et al, 2006; Ma et al, 2020). Single hexane extraction could substantially reduce sample handling time, especially when handling a large number of samples,

reduce the amount of hexane waste, and reduce the need for hexane evaporation to concentrate the sample.

Two common catalysts used in lipid transmethylation are methanolic acids such as HCl and H_2SO_4. Since the commercial 3M methanolic HCl is exceedingly costly, we chose to compare the efficacy of freshly prepared methanolic H_2SO_4 (2% and 5%, respectively) with 3M methanolic HCl for the transmethylation reaction at 95°C. The results indicated that transmethylation was complete within 2 hours and there were essentially no differences in the total lipid content and FA composition between the three acid catalysts (Fig. 2.4.1C, 2.1D; Table S3, S4).

Since increasing the transmethylation reaction temperature increases the rate of lipid conversion, an incubation temperature of 110°C was also tested on whole *Arabidopsis* seeds to compare with 80ºC and 95ºC. This incubation temperature saw the fastest rate of transmethylation reported for whole *Arabidopsis* seed, with complete lipid extraction after only 50 minutes (Fig. 2.4.1E) and comparable FA composition to the other methods (Table S1-S5) and a previous study (Jayawardhane et al, 2020). However, it should be noted that the FA composition was slightly affected by the 110°C reaction temperature over time; in the period between 50 to 120 minutes, there were small but statistically significant declines in the proportion of 18:2, and 18:3, while 20:1 increased (Table S5). These changes were potentially due to increased oxidation of the polyunsaturated FAs (18:2 and 18:3) at high temperature (110°C) over time. However, no degradation products or FA isomers were detected in GC-MS analysis comparing *Arabidopsis* seed lipids extracted using 95°C versus 110°C (data not shown), which may suggest that oxidation products are lost to the aqueous layer during FAME purification. Therefore, the 110°C transmethylation temperature enables the fastest extraction

and conversion of lipids from whole *Arabidopsis* seed (50 minutes), but longer incubation lengths beyond 50 minutes at 110°C should be avoided as they may lead to some lipid oxidation and slightly altered FA composition. Taken together, 2% methanolic H_2SO_4 demonstrates high efficacy for the transmethylation reaction of whole *Arabidopsis* seeds, with either 95°C or 110°C as suitable reaction temperatures. Because incubation lengths longer than 110°C may cause changes in FA composition, we selected 95°C in further studies.

2.4.2 Optimization of direct methylation for seed and leaf samples

With the chosen temperature and acid catalyst with *Arabidopsis* seeds, we further optimized the direct transmethylation method with several plant species with a wide range of lipid contents and FA compositions, including established oilseed crops (canola, flax), the forage crop alfalfa, as well as emerging and under-researched species (Apple of Peru, Caragana, poppy, sea buckthorn, and Proso millet). Based on the optimization of direct transmethylation for *Arabidopsis* seeds, the following conditions – 2% methanolic H_2SO_4, 95°C incubation temperature, and grinding of samples with mortar and pestle – were used to determine the optimal incubation length. As shown in Fig. 2.4.2, all reactions completed within 2 hours, whereby the optimal incubation lengths varied between species from 45 minutes to 2 hours. Minimal to no changes were detected for FAs in each species across incubation lengths (Tables S6-S13) and the values were generally comparable to those reported in previous studies (Ghazani et al, 2014; Liang et al, 2010; Ozbek & Ergonul, 2020; Pali & Mehta, 2014; Wijekoon et al, 2020), suggesting that 95°C was suitable for these plant samples with various FA compositions.

For species that showed no differences in total lipid content between time points, the lipid extraction likely went to completion before the earliest time point. These findings suggest that

the unique properties of each plant tissue being analyzed, such as the cell walls and seed coats, may play a significant role in determining the efficiency by which this analysis method extracts lipids from a given tissue. This suggests that protocol adjustments may be appropriate depending on the species being studied and that simply replicating methods used on other plant species may not always be suitable for complete lipid extraction. In addition, the results of Caragana (Fig. 2.4.2C) and Apple of Peru (Fig. 2.4.2F) indicate that the optimization approach described in this paper can work well in rapid and robust lipid analysis of new or under-studied species with diverse FA profiles.

2.4.3 Verification of optimized direct transmethylation by traditional methods

Although direct methylation has been used and published for many years, there is still value in comparing the results of the optimized method to a traditional lipid extraction method. To evaluate the efficacy of the optimized direct methylation method, the classical Hara-Radin method (Hara & Radin, 1978) was performed on canola, *Arabidopsis*, flax, Apple of Peru, and Proso millet seeds. As shown in Fig. 2.4.3, the total lipid contents were completely equivalent between the traditional method and the optimized direct methylation method, and only marginal differences were observed in the FA compositions (Table S14). Thus, the direct methylation method studied in this work is as effective as the well-established Hara-Radin method. Since total lipid analysis via the measurement of FAME with GC/FID has been proven to yield comparable determinations of total fat content to those achieved with conventional gravimetric methods such as Soxhlet and has been used in many studies (for a review, see Srigley and Mossoba, 2016), we did not further compare the method with gravimetric methods.

2.4.4 Comparison of the use of glass versus plastic wares in lipid analysis

Use of disposable laboratory plastic materials such as tubes would be more convenient and, in the case of pipet tips, improve accuracy and ease of handling samples, though plastic materials are generally avoided in lipid analysis protocols. Since the direct methylation and FAME extraction processes do not use DMSO or chloroform, we evaluated whether using plastic materials introduces contamination into samples for GC analysis. We compared glass tubes versus 15ml polypropylene tubes for direct transmethylation and hexane extraction. Although plastic tubes do result in some small contaminating peaks in GC-MS, they did not interfere with identification and quantification of the FAME peaks from *Arabidopsis* (Fig. 2.4.4). The use of polypropylene P1000 pipet tips for the hexane extraction did not introduce unwanted peaks in chromatograms from both GC-MS (Fig. 2.4.4) and GC-FID (data not shown). Thus, the use of plastic, rather than glass, tubes may be appropriate for GC analyses involving regular FAMEs (16:0 and longer FAs) from plant samples. The comparable results might be partially due to the improved quality of disposable laboratory plastic tubes and pipet, and the use of disposable plastic consumables could substantially reduce time and labor associated with lipid analysis with GC-FID.

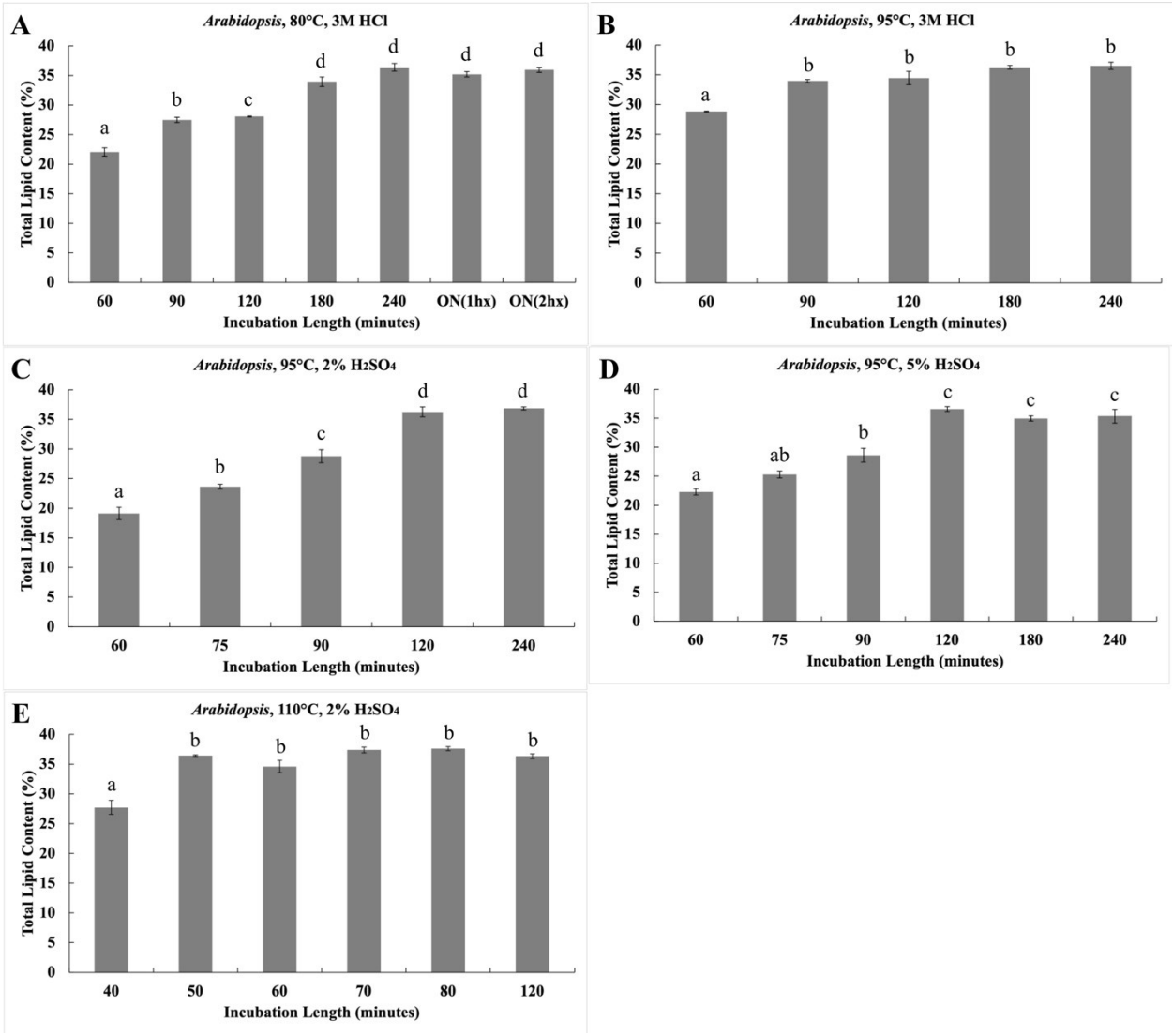

Figure 2.4.1 Effect of different direct transmethylation conditions on the lipid analysis of *Arabidopsis* seeds

Error bars represent standard errors of replicates (*n*=3-5). Letters represent significance categories and were calculated using one-way ANOVA and the Kruskal-Wallis test. ON, overnight; 1hx: single hexane extraction; 2hx, 2x hexane extraction.

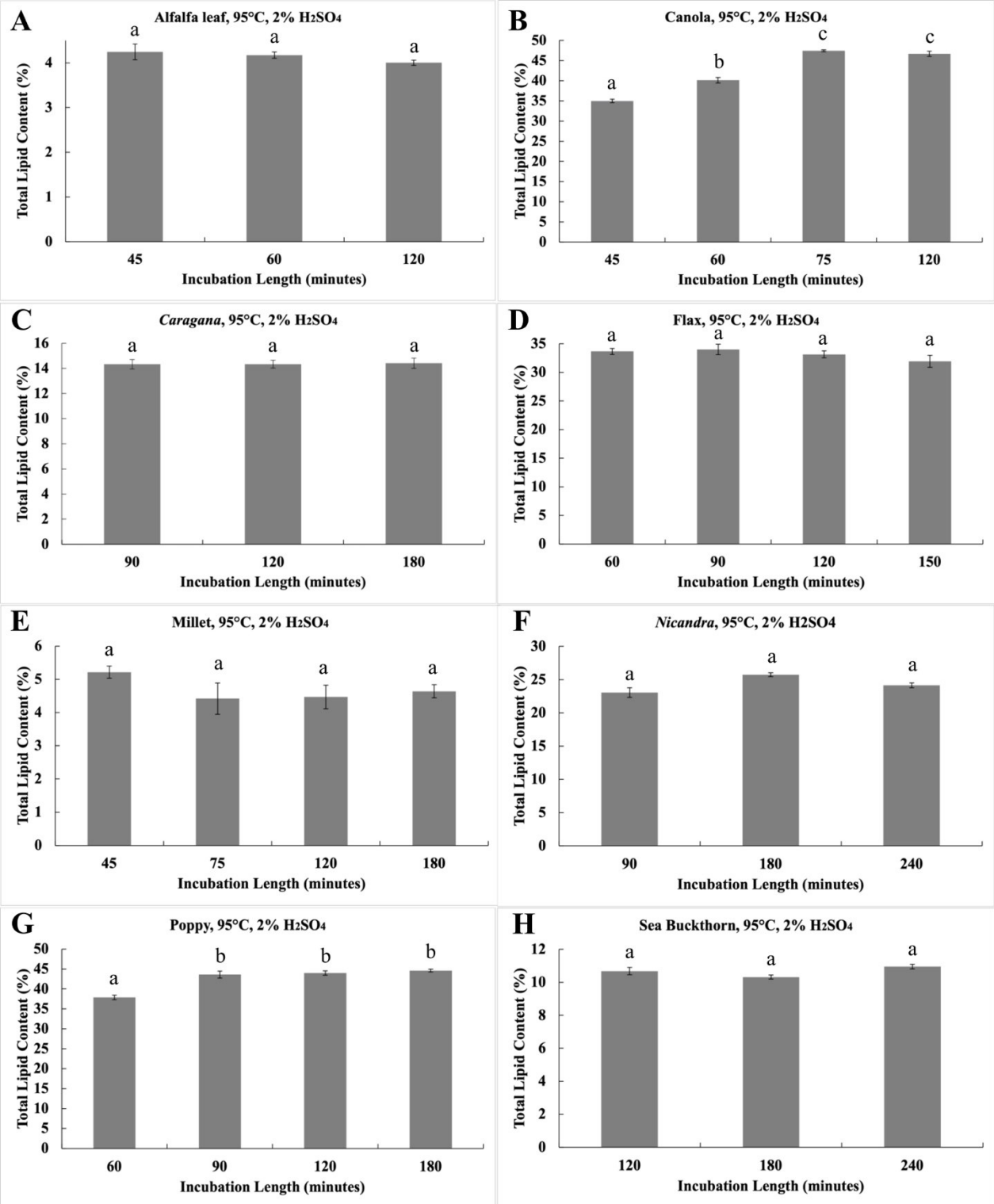

Figure 2.4.2 Lipid analysis of various plant species with direct transmethylation
Error bars represent standard errors of replicates (*n*=3-8). Letters represent significance categories and were calculated using one-way ANOVA and the Kruskal-Wallis test.

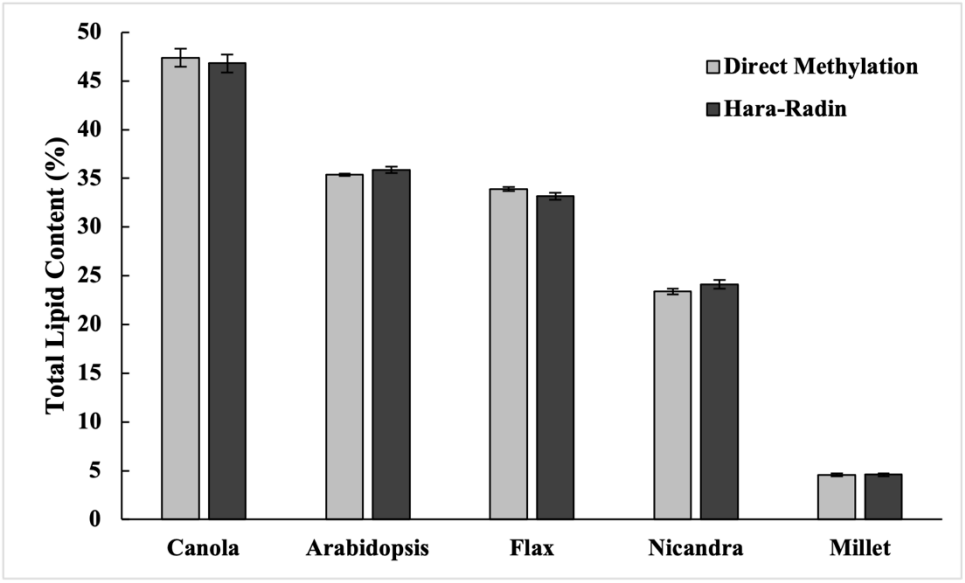

Figure 2.4.3 Comparison of the optimized direct methylation method to the classical Hara-Radin method
Error bars represent standard errors of replicates (n=3-5). No significant differences were found between the two methods using two-tailed Student's t-test.

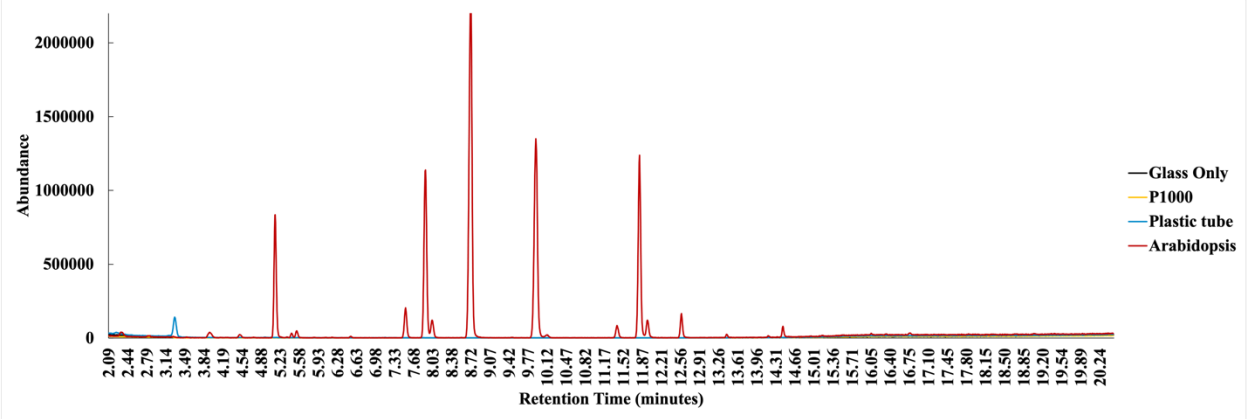

Figure 2.4.4 Evaluation of glass versus plastic consumable in lipid analysis using direct transmethylation
Representative GC-MS chromatograms were selected and overlayed for each treatment.

2.5 Conclusions

In summary, this study optimized the direct transmethylation method for rapid analysis of lipid content and FA composition from various plant samples. The combination of 2%

methanolic H_2SO_4, 95°C transmethylation incubation temperature, grinding of dry plant matter with a mortar and pestle, incubation lengths of at most 2 hours, and one round of hexane extraction illustrates improvements over several reported plant lipid analysis methods while continuing to deliver reliable and replicable data. We also provide evidence that current high quality commercial plastic wares, such as polypropylene tubes and pipet tips, are generally compatible with glassware in the process. These improvements to lipid analysis methods will allow researchers to save time, reduce the labor and effort required, and reduce chemical waste compared to many reported methods and contribute more consistency to plant lipid analysis methods going forward.

Supplemental Tables

Tables S1-S14 containing the FA data can be found at the end of the document.

3 Chapter 3 Manipulation of Carbon Flow in *Arabidopsis* seeds from Cellulose Synthesis Towards Storage Oil and Protein Synthesis

3.1 Abstract

Oil and protein are the two most important storage components in canola seeds, but the trade-off relationship of storage lipid and protein biosynthesis presents a challenging obstacle to simultaneously increasing both components. We are interested in redirecting carbon resources from cellulose (the major component of seed coats) towards protein and oil biosynthesis by manipulating multiple genes; however, directly testing different gene combinations in canola is difficult, time-consuming, and labour-intensive. In this work, we genetically engineered *Arabidopsis* to test several gene combinations for their ability to reallocate carbon, with the ultimate objective of finding the best approach for further evaluation in canola. Based on previous results, we partially reduced seed cellulose by seed-specific RNAi-down-regulation of *AtCESA1* and maintained or slightly increased oil content by overexpression of *BnDGAT1*, and its performance-enhanced variants, and obtained homozygous lines. Subsequently, several protein biosynthesis-related genes (*AtAAP1*, *AtALAAT1*, and *AtASN1*) were overexpressed in those lines, respectively. The combinations of *AtCESA1*-RNAi/*BnDGAT1*-OE/*AtAAP1*-OE and *AtCESA1*-RNAi/*BnDGAT1*-OE/*AtALAAT1*-OE were the most successful at restoring the seed lipid contents and increasing the protein content (up to 2.7%) while cellulose decreased, with only minor phenotypic changes during germination and early seedling growth. These findings illustrate the potential for carbon reallocation to enhance the nutritional and economic value of oilseed crops and these gene combinations could be further evaluated in canola.

3.2 Introduction

Plant-produced storage lipids represent a valuable commodity globally and have diverse applications for industrial, food, and biofuel purposes. Oilseed crops, such as canola, synthesize oil in their seeds as a form of energy storage. Demand for vegetable oils is expected to continue to increase, driven by factors like global population growth and climate change. In addition, plants are an increasingly appealing source for protein, such as for the emerging plant-based meat market. Accordingly, there is a growing research interest in enhancing storage molecule synthesis in plants.

Canola seed meal consists primarily of protein and fiber and is a valuable feed component for animals. Although canola seed protein is nutritionally desirable, the excess of fiber (primarily cellulose) in the meal can reduce the efficiency of digestion in animals, which limits overall nutritional value (Annison & Choct, 1991; Slominski et al., 1994; Jiang & Deyholos, 2010; Wickramasuriya et al., 2015; Opazo-Navarrete et al., 2019). Reduced meal fiber content has been linked to greater digestibility in yellow-seeded canola cultivars with lower seed fiber content or through dehulling black-seeded canola, which possess cellulose-rich seed coats (Bell, 1984; Slominski et al., 1994; Slominski, 1997; Matthaus, 1998; Slominski et al., 2012). Thus, it may prove valuable in oilseed crops to decrease seed cellulose content, thereby liberating resources that could be redirected to increase both oil and protein contents simultaneously or increase protein content without reducing the oil content.

Sugars derived from photosynthesis serve as the carbon source for the biosynthesis of major storage molecules, including starch, TAGs, and storage proteins (Angeles-Núnéz & Tiessen, 2011; Baud et al., 2008). In canola and *Arabidopsis*, these storage substances accumulate within the cotyledons of the embryo during mid to late embryo development

(Murphy et al., 1989; Murphy & Cummins, 1989; Mansfield & Briarty, 1992; Baud et al., 2008). Seed carbon partitioning affects the synthesis of storage substances and depends on genetic factors as well as strength of carbon sinks, often resulting in trade-offs between lipid, protein, and carbohydrate biosynthesis. This biosynthetic competition for carbon between carbohydrates, lipids, and protein has been described in many species (Focks & Benning, 1998; Shi et al., 2012; Li et al., 2018B; Liu et al., 2022; Katepa-Mupondwa et al., 2005; Kambhampati et al., 2020). Therefore, the deliberate manipulation of carbon flow within seeds would alter the composition of storage substances to enhance the nutritional and economic value of the seeds.

Although there is generally a trade-off between lipid and protein contents in plants such as canola and yellow mustard (Grami et al., 1977; Katepa-Mupondwa et al., 2005), previous work has proposed that seed lipid and protein contents could be increased simultaneously by reallocating carbon away from seed fiber biosynthesis (Jiang & Deyholos, 2010; Slominski et al., 2012; Opazo-Navarrete et al., 2019; Jayawardhane et al., 2020). Genetic engineering presents a means to attempt nutritional enhancement of seed meal by increasing the protein content, without reducing the lipid content, and partially reducing the seed fiber content (Li et al., 2017; Jayawardhane et al. 2020).

Plant storage lipid biosynthesis consists of two main biosynthetic pathways: assembly of carbon units into FAs and assembly of FAs into TAG (summarized in Fig. 1.2.1). Overexpression (OE) of *DGAT1*, which encodes the major synthesizing enzyme in the core TAG biosynthesis pathway, is effective at increasing lipid accumulation (reviewed in Xu et al., 2018A and Chen et al., 2022).

Many genes influence the synthesis of SSPs and contribute to the protein content of seeds (summarized in Fig. 1.2.2) Several genes have been shown to increase SSP accumulation

through overexpression (Rolletschek 2005; Lee 2020; Zhou 2009; see Table 1.2). For this work, we have selected *AtAAP1*, *AtALAAT1*, and *AtASN1* to evaluate their effects on SSP content in a carbon reallocated background. Another gene, *AtUmamiT18*, may have potential for enhancing SSP accumulation through overexpression but has not yet been studied.

Cellulose is a major source of fiber as it comprises a large proportion of plant cell walls and is synthesized by the CSC and previous work has suggested that *AtCESA1* is a promising target for altering cellulose synthesis (Beeckman et al., 2002; Burn et al., 2002; Jayawardhane et al., 2020; see section 1.1.3). The down-regulation of *AtCESA1* through seed-specific RNAi has been shown to slightly reduce the seed cellulose content, without causing major phenotypic abnormalities, along with slightly increased protein content, but slightly decreased lipid content (Jayawardhane et al., 2020). Thus, *AtCESA1* down-regulation may serve as a starting point for reducing seed fiber content and could be combined with overexpression of lipid and protein biosynthesis-related genes to improve the seed nutritional composition.

The hypothesis of this work is that down-regulation of seed cellulose (*AtCESA1*-RNAi) biosynthesis will reduce consumption of carbon resources, which can then be redirected into lipid and protein biosynthesis. We evaluated this hypothesis by combining *AtCESA1*-RNAi, overexpression of *BnDGAT1,* and overexpression of genes associated with SSP biosynthesis genes (*AtAAP1*, *AtALALAAT1*, and *AtASN1*) in *Arabidopsis* seeds.

The results indicated that seed cellulose content was successfully reduced (-21%) in *AtCESA1*-RNAi/*BnDGAT1*-OE homozygous seeds, in line with a previous study on *AtCESA1*-RNAi alone (Jayawardhane et al., 2020), and lipid content was restored back to wild-type levels. Overexpression of *AtAAP1*, *AtALALAAT1*, or *AtASN1* in *Arabidopsis* lines with seed carbon reallocation (*AtCESA1*-RNAi and *BnDGAT1*-OE) experienced larger increases in protein content

(+1.6%) than overexpression of *AtAAP1*, *AtALALAAT1*, or *AtASN1* alone in the Col-0 background.

The stacked genetic engineering approach described here appears to be an effective strategy for improving the nutritional properties of *Arabidopsis* seeds. The *AtCESA1*-RNAi/*BnDGAT1*-OE background may serve as a useful screening platform for characterizing candidate genes involved in seed protein biosynthesis, thereby accelerating the fundamental genetic research needed by crop breeders. The gene combinations identified in this work can be further tested in canola, which may contribute to the development of nutritionally enhanced canola seeds with increased protein and reduced fiber, and therefore benefit farmers, the animal feed market, and the plant-based protein industry.

3.3 Materials & Methods

3.3.1 Plant Growth Conditions

Arabidopsis ecotype Colombia-0 (Col-0) seeds were imbibed at 4ºC in the dark for 2-3 days prior to sowing on potting mix (Sunshine Mix 4, Sun Gro Horticulture, MA, US). Plants were grown from sowing onwards in a growth chamber at 22ºC with a photoperiod of 18h day/6h night and 250 µmol/m^2s light intensity. Plants were grown in 8x4 inserts and trays, with transparent plastic covers for the first week. Growth was supplemented with N:P:K 20:20:20 fertilizer (Plant Products Co., ON, Canada) weekly after appearance of the first true leaves.

3.3.2 Zygosity Screening on Antibiotic-Selective Plates

Seeds were subjected to surface sterilization using 70% ethanol and 30% bleach/Triton X-100 solution, followed by 2 days of imbibition and stratification at 4°C. Plants were grown for

2 weeks under fluorescent grow lights at 25°C on MS plates containing sucrose, MES buffer, and antibiotics: 25 ug/ml kanamycin and 50 ug/ml timentin (Murashige & Skoog, 1962; Nauerby et al., 1997). Non-segregant seedlings from heterozygous lines were characterized by growth retardation and chlorosis.

3.3.3 Seed Oil & Fatty Acid Quantification

Lipid content and FA composition of *Arabidopsis* seeds were determined, in triplicate, using GC-FID with the optimized method generated in chapter 2. Approximately 10 mg of seed was placed into Teflon screw-cap glass tubes with 100 µl of 1 mg/ml 17:0 heptadecanoin as the internal standard. The seed lipids were derivatized to FAMEs using 2% H_2SO_4 in methanol (prepared from 95-95% H_2SO_4, Fisher Chemical, MA, USA) at 95°C for 2 hours. Samples were subsequently cooled at 4°C for 5 minutes, followed by the addition of 1.7 ml of 0.9% aqueous NaCl. A single hexane extraction was performed to purify the FAMEs, which were then analyzed using a GC-FID (7890A GC System, Agilent Technologies, CA, USA) with a 10:1 split ratio and 1 µl injection volume. FAME separation was performed in a DB-23 capillary column (30 m × 250 µm × 0.25 µm, Agilent Technologies) using N_2 as the carrier gas. The temperature program was as follows: 165 °C for 4 minutes, ramping from 165 to 180 °C in 5 minutes, then 180 to 230 °C in 5 minutes. Peaks were identified by comparing the retention times to a GLC 421-A standard series (Nu-Chek Prep, MN, USA). GC-MS (5977A MSD, Agilent Technologies) was used to confirm the identity of the FAME peaks.

3.3.4 Crude Seed Protein Quantification

The crude seed protein content was determined, in triplicate, using the Dumas combustion method of nitrogen analysis (Sader et al., 2004; Watson & Galliher, 2001). The seed nitrogen content was estimated using 2-7 mg of dry seed sample and a FLASH 2000 Organic Elemental Analyzer (ThermoFisher, Missisauga, ON, Canada). The crude seed protein was then calculated using the standard conversion factor of 6.25 (Jones 1941), and tobacco (2.51% nitrogen) was used as the calibration standard (LECO, St. Joseph, MI, US).

3.3.5 Crystalline Cellulose Quantification

The crystalline cellulose content of seeds was measured by determining the acid insoluble glucose content using a modified Updegraff method with slight modifications (Updegraff, 1969; Griffiths et al. 2014). At least 20 mg of seed were ground in liquid nitrogen using a mortar and pestle, washed with 70% ethanol, and dried at 50°C overnight. The dry weights of the homogenized seeds were recorded and samples were treated with 2 ml of Updegraff reagent (consisting of 8:1:2 v/v/v acetic acid:nitric acid:water). Samples were then vortexed and incubated at 100°C for 1 hour, with brief vortexing after 20 minutes. The samples were then centrifuged at 13,000 rpm for 2 minutes and the resulting pellets were washed once with distilled water, then twice with acetone, and left to dry overnight at room temperature. Samples were then treated with 1 ml 72% H_2SO_4, vortexed, and incubated at room temperature for 90 minutes, followed by centrifugation at 13,000 rpm for 2 minutes. The samples were then used to create 10x dilution aliquots with water and measured using a colorimetric method (Foster et al. 2010). Briefly, 70 µl of diluted sample was combined with 140 µl of freshly prepared 2/mg/ml anthrone/72% H_2SO_4 in each well, all conducted in a 4°C room. The anthrone mixtures were

then incubated for 30 minutes at 80 °C and absorbance was recorded using a 620 nm wavelength in a spectrophotometer plate reader (Synergy H4 Hybrid reader, Biotek Instruments, Winooski, USA). A standard curve was prepared from a serial dilution of D-glucose, and the total cellulose-derived glucose contents were calculated per weight of dry seed mass.

3.3.6 Vector Design & Cloning of Protein Overexpression Genes

3.3.6.1 RNA Extraction & cDNA Synthesis

RNA was extracted from approximately 80 mg of siliques (harvested and stored at -80°C) using the RNeasy Plant Mini Kit following the protocol (Qiagen). A TURBO DNA-free kit (Invitrogen) was used to remove DNA from the RNA samples. RNA concentration was measured using a NanoDrop Spectrophotometer (Thermo Fisher Scientific). First-strand cDNA was synthesized from approximately 200 ng RNA with the SuperScript IV First-Strand cDNA Synthesis Reaction kit. The cDNA product was frozen at -20°C for later use.

3.3.6.2 Sequence Identification of Protein Biosynthesis-Related Genes

Protein biosynthesis-related genes that are expressed in *Arabidopsis* were identified using The *Arabidopsis* Information Resource (TAIR) (https://www.*Arabidopsis*.org). Four genes were selected for overexpression vector design: *amino acid permease 1* (*AtAAP1*), *alanine aminotransferase 1* (*AtALAAT1*), *asparagine synthase 1* (*AtASN1*), and *usually multiple acids move in and out transporter 18* (*AtUmamiT18*). The corresponding cDNA sequences were extracted and used in the design of overexpression vectors with homology-directed recombination in SnapGene (version 6.1.2) (Fig. S1).

3.3.6.3 Amplification of *AtAAP1*, *AtALAAT1*, & *AtASN1*

The cDNA sequences were purchased in synthesized plasmids (GeneArt). The promoter, dsRed, and kanamycin-resistance DNA sequences can be found in Table S15. Primers were designed to amplify the target genes from the synthesized plasmids (Table S16) using polymerase chain reaction (PCR). Overhangs were added to the flanking primers to enable homology-directed recombination with the pBinGlyRed and pBin35SRed vectors. Internal forward and reverse primers were also designed for eventual sequencing (Table S16). The following PCR components were combined on ice: 5 µl of 10x reaction buffer (without $MgCl_2$), 1 µl of 10 uM dNTP mix, 5 µl of 25 mM $MgCl_2$, 2.5 µl each of 10 uM forward and reverse primers, 1 µl of template plasmid, 0.5 µl of Taq enzyme, and 32.5 µl of nuclease-free water. Touch-down PCR was used to identify the optimal annealing temperatures for each primer pair. The thermocycler (Veriti, Applied Biosystems, MA, USA) program was as follows: initial denaturation 95°C for 5 minutes, then 35 cycles of 95°C denaturation for 30 seconds, 58-62°C annealing for 30 seconds, 72°C extension for 90 seconds, and a 72°C final extension for 7 minutes. Samples were stored at -20°C until further use.

3.3.6.4 Cloning of *AtAAP1*, *AtALAAT1*, *AtASN1,* and *AtUmamiT18* into pBinGlyRed and pBin35SRed plasmids.

The pBin plasmids were kindly provided by the laboratory of Dr. Ed Cahoon, University of Nebraska-Lincoln (Nguyen et al., 2015; Huai et al., 2015). Overexpression constructs were introduced into the plasmids via homology-directed recombination. The ClonExpress II One Step Cloning Kit (Vazyme Biotech Co.) was used for homology-directed recombination of the inserts into the vectors. The following reaction components were combined on ice: 4 µl of 5x CEII

buffer, 3 µl of linearized vector, ~1 µl amplicon (depending on the concentration; enough to supply around 50 ng of DNA), 1 µl of Exnase enzyme, and nuclease-free water to achieve a total reaction volume of 10 µl. The reaction tubes were then incubated in a 37°C thermocycler (Veriti Thermal Cycler, Applied Biosystems, MA, US) for 30 minutes. The recombination product was then combined with 100 µl of competent DH5α *E. coli* cells and incubated on ice for 30 minutes. The mixture was then heat-shocked in a 42°C water bath for exactly 45 seconds, then returned to ice for 2 minutes. The mixture was supplemented with 900 µl of liquid LB medium and placed in a shaker at 37°C for 1 hour. The transformed *E. coli* were then pelleted, resuspended in 100 µl liquid LB medium, and plated on 50 µg/ml kanamycin agar plates. The plates were then placed upside-down and incubated overnight at 37°C.

The seed-specific overexpression of the protein biosynthesis-related genes was driven by the Glycinin promoter, while the constitutive overexpression of *AtUmamiT18* was driven by the Cauliflower Mosaic Virus (CaMV) 35S promoter. The Glycinin promoter was chosen to avoid promoter silencing as the expression of the *AtCESA1*-RNAi and *BnDGAT1*-OE cassettes were driven seed-specific Napin and Phaseolin promoters.

3.3.6.5 Colony PCR and Sequence Verification

To confirm successful *E. coli* and *Agrobacterium* transformants, colony PCR was performed, and plasmid DNA was extracted for sequence verification. Briefly, a pipet tip was used to lightly touch a single colony and then dipped into 50 µl of water. The mixture was incubated at 99°C for 5 minutes in a thermocycler (Veriti Thermal Cycler, Applied Biosystems, MA, US) to lyse the cells and release the plasmids. The following reaction mix components were then combined: 2 µl of heat-lysed colony solution (plasmid template DNA), 1 µl each of 10 uM

forward and reverse primers, 10 µl of DreamTaq master mix (Thermo Fisher Scientific), and 6 µl of nuclease-free water. The thermocycler program was as follows: initial denaturation 95°C for 3 minutes, then 35 cycles of 95°C denaturation for 1 minute, 60°C annealing for 30 seconds, 72°C extension for 2 minutes, and a 72°C final extension for 2 minutes. The PCR products were then analyzed by agarose gel electrophoresis and amplicons were detected using a UV light. A minimum of two colonies were assessed for each construct. Plasmid DNA was extracted from positive colonies and sent for Sanger sequencing.

3.3.6.6 Preparing Competent *Agrobacterium tumefaciens* Cells through Electroporation

Electrocompetent cells were prepared using *Agrobacterium tumefaciens* (henceforth *Agrobacterium*; strain GV3103) (Jayawardhane et al., 2020). *Agrobacterium* were cultured overnight in 15 ml of liquid LB broth with 50 µg/ml kanamycin, 50 µg/ml rifampicin, and 30 µg/ml gentamycin with shaking at 225 rpm at 28°C. After culturing, 1 ml was combined with 50 ml of liquid LB with the same antibiotics for 2-3 hours, until an OD600 of around 0.5 was achieved. The cells were then pelleted, the pellet was washed with water, and aliquots were prepared in 50% glycerol for long-term storage at -80°C. Electroporation was then used to transform the *Agrobacterium* with the overexpression vectors (Kámán-Tóth et al., 2018). *Agrobacterium* aliquots (50 µl) were thawed on ice, then combined with 1-2 µl of overexpression vector (amounting to about 100 ng DNA). After adding 26 µl of the mixture into ice-cold Gene Pulser cuvettes (0.2cm diameter) (Bio-Rad), the cells were electroporated (*Agrobacterium* setting, 1.8V for 1 second) using a MicroPulser Electroporator (Bio-Rad). The electroporated cells were then incubated at 225 rpm and 28ºC for 3 hours in liquid LB medium with 50 µg/ml kanamycin, 50 µg/ml rifampicin, and 30 µg/ml gentamycin. The transformed *Agrobacterium*

cultures were then plated (100 µl) on LB agar plates containing 50 µg/ml kanamycin, 50 µg/ml rifampicin, and 30 µg/ml gentamycin at 28°C for 2 days. *Agrobacterium* transformants were confirmed by PCR, gel electrophoresis, and sequencing as described in section 3.3.6.5.

3.3.6.7 *Arabidopsis* Transformation

The overexpression vectors were introduced into homozygous T_3 *AtCESA1*-RNAi/*BnDGAT1*-OE *Arabidopsis* plants using the *Agrobacterium*-mediated floral dip transformation method (Clough and Bent, 1998) as follows. In brief, *Agrobacterium* containing the overexpression vectors were cultured in 500 ml of liquid LB medium (50 µg/ml kanamycin, 50 µg/ml rifampicin, 30 µg/ml gentamycin) and incubated (28°C, 225 rpm) overnight. The *Agrobacterium* cultures were pelleted by centrifugation (5000 rpm for 5 minutes). The pellets were re-suspended in 100 ml of 5% sucrose solution containing 0.05% (v/v) Silwet L77. *Arabidopsis* inflorescences (7 plants per 5" x 5" plastic pot, 5 pots per construct) carefully dipped into the solution for approximately 20-60 seconds (20 seconds for the first pot, time was gradually added for each pot until 60 seconds for the final pot for each construct). The dipped plants were covered with plastic covers and black garbage bags overnight to maintain high humidity and low light. After this, the plants were transferred to a growth chamber and grown as previously described. The T_1 seeds were harvested upon maturation and drying of the siliques.

Empty vectors with the dsRed fluorescence marker were transformed into wildtype Col-0 *Arabidopsis*, which served as the EV Control plants throughout the following analyses.

3.3.7 Selection of T_1 *AtAAP1*, *AtALAAT1*, *AtASN1,* and AtUmamiT18 Transformants using dsRed Marker

The floral-dipped T_0 plants were grown to maturity and the T_1 seeds were harvested once dry. The dsRed fluorescence marker was used to screen the seeds for successful transformants. To detect the fluorescence, a dark room was used to shine a green laser (595nm) on the seeds, contrasted against a white paper backdrop. When viewed through red glasses, successful transformants appeared as brightly glowing red seeds and were carefully isolated from the non-glowing, non-transformed seeds.

3.3.8 Seed Weight & Size Analysis

For seed weight analysis, approximately 100-200 seeds were spread on a white paper background and photographed. The seeds were then weighed on an analytic balance (MS104S NewClassic MS, Mettler Toledo, Switzerland). The images were then imported into ImageJ (Github.ImageJ.JS v0.5.5) and the Analyze Particles function was used to count the individual seeds.

For seed size analysis, approximately 50-100 seeds were spread on a white background and photographed using a mounted camera connected to a dissecting microscope (Leica MZ Microscope, Leica Microsystems, Germany). The images were then imported into ImageJ (Github.ImageJ.JS v0.5.5) and the Analyze Particles function was used to count the individual seeds. The 2-dimensional surface area (um^2) of the seeds was calculated using the pixel count for each seed.

3.3.9 Morphological & Histochemical Phenotype Assays

3.3.9.1 Seed Coat Permeability

Seed coat permeability was analyzed with the tetrazolium penetration assay as described in previous methods (Vishwanath et al., 2014), with slight modifications. Three independent T_3 *AtCESA1*-RNAi/*BnDGAT1*-OE/Protein Gene-OE and EV controls lines were imbibed in a 1% (w/v) aqueous solution of tetrazolium violet in the dark at 30°C (prepared from 2,3,5-triphenyl-tetrazolium chloride) (Sigma-Aldrich, MO, US). Three technical replicates were used per independent transgenic line and staining was evaluated at three points: 24, 43, and 48 hours.

3.3.9.2 Seed Germination Test

The germination rate was evaluated using a simplified version of existing standard methods (Zhong et al., 2016). Germination was evaluated by placing at least 30 surface-sterilized seeds on half-strength MS agar plates, in triplicate, and grown under fluorescent grow lights at 23°C for 7 days. Three independent T_3 *AtCESA1*-RNAi/*BnDGAT1*-OE/Protein Gene-OE and EV controls lines were evaluated, in triplicate. Germination was defined as emergence of the radicle through the seed coat. Seeds were imbibed and subjected to 2 days of cold stratification at 4°C in the dark.

3.3.9.3 Seedling Root Length

Seedling root growth was evaluated on agar plates (Corrales et al., 2014; Jayawardhane et al., 2020). Surface-sterilized seeds were carefully placed in a straight line on antibiotic-free, half-strength MS agar square plates (95 mm x 95 mm) and grown vertically under fluorescent grow lights at 23°C for 12 days. Seeds were imbibed and subjected to 2 days of cold stratification at

4°C in the dark. For each line, 3 biological replicates were assessed, with at least 10 seeds per plate, in triplicate.

3.3.9.4 Seedling Hypocotyl Length

The seeds and plates for the hypocotyl elongation assay were prepared in the same manner as the seedling root length assay. After cold stratification, the seeds were given 2 hours of exposure to fluorescent growth lights to synchronize germination. The plates were then covered in tin foil, covered by a black plastic bag, and stowed in a dark cabinet at room temperature for 6 days. Three independent T_3 *AtCESA1*-RNAi/*BnDGAT1*-OE/Protein Gene-OE and EV controls lines were evaluated, in triplicate.

3.3.9.5 Fresh Seedling Weight

Fresh seedling weight was evaluated by imbibing seeds for 2 days at 4°C, then transferred to potting soil (Sunshine Mix 4, Sun Gro Horticulture, MA, US) in 8x4 trays in a greenhouse with standard light and temperature conditions. Transparent plastic covers were placed over the trays and plants were grown for 12 days after germination. Seedlings were then carefully removed from the soil, washed, and fresh weights were recorded. Three independent lines each were evaluated, using 3 seedlings per line.

3.3.10 Amino Acid Quantification

Around 50 mg of seeds (pooled across several independent transgenic lines to ensure enough sample mass) were used for AA hydrolysis and HPLC analysis. The seeds were put into plastic 2 ml screw-cap tubes with 1.5 ml of aqueous 6M HCl (prepared from 36.5-38% HCl,

Fisher Chemical, MA, USA). After brief vortexing, the samples were incubated at 110°C for 24 hours. After about 30 minutes into the incubation, the lids were re-tightened, and the samples were briefly vortexed. The samples were then analyzed using an Agilent 120 HPLC System using a Supelcosil LC-18 column (150 mm x 4.6 mm, 3 μm diameter). Solvent A was 0.1 M Na acetate buffer and Solvent B was methanol. Gradient elution was used with a flow rate of 1.1 ml minute and the fluorescence detector used (excitation wavelength 340 nm, emission wavelength 450 nm). The standard used was Sigma Amino Acid Standard P/N AAS18-5ml, with γ-Aminobutyric Acid (BABA) as the internal standard and ellagic acid (EA) as the backup internal standard.

3.3.11 Statistical Analysis

The two-tailed Student's t-test was used for all comparisons of means between EV control and T_3 *AtCESA1*-RNAi/*BnDGAT1*-OE/Protein Gene-OE lines, with $P \leq 0.05$ as the significance threshold. In Chapter 3, all figures were generated and statistical analyses (one-way ANOVA and Tukey test) were performed in Microsoft Excel (Version 16.54, 21101001).

3.4 Results

The *Arabidopsis* lines with seed-specific or constitutive overexpression of *AtUmamiT18* have been excluded from the Results and Discussion sections as they require additional study and functional characterization, with potential for publication as an independent study in the future.

3.4.1 Seed Oil Quantification of T_2 *AtCESA1*-RNAi/*BnDGAT1*-OE lines

Preliminary seed lipid content data, generated previously in our lab, was used to select several T_2 *AtCESA1*-RNAi/*BnDGAT1*-OE lines from the DAS 17, 19, and 20 lineages with potentially increased lipid content (unpublished). The DAS 17 lineage overexpressed wildtype *BnDGAT1*, while DAS 19 and 20 overexpressed performance enhanced *BnDGAT1* variants previously identified in yeast (variants S112R and L441P, respectively) (Chen et al., 2017). These heterozygous lines were re-analyzed to identify increases in lipid content using GC-FID. As shown in Fig. 3.4.1, eight out of ten lines had significantly higher seed lipid content (36.1-37.3%) while the remaining 2 lines were comparable to the EV controls (about 34.9%). There were no clear differences in contribution to seed lipid content between the native *BnDGAT1* and the two performance enhanced variants. The lines with significantly increased lipid content were selected and grown to the T_3 generation.

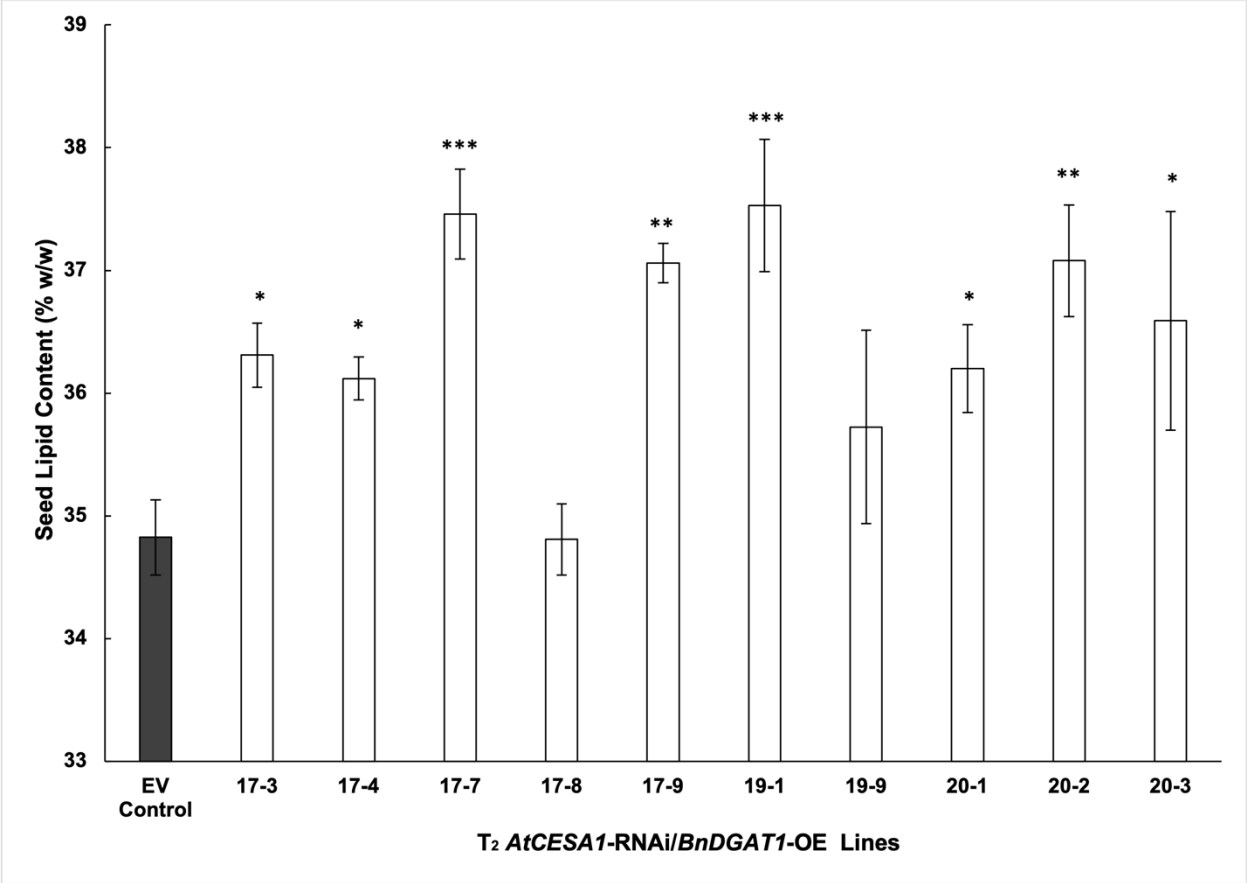

Figure 3.4.1 Seed lipid content of heterozygous T₂ *AtCESA1*-RNAi/*BnDGAT1*-OE lines
Averages are shown for 8 independent EV control and 10 experimental lines. Line names starting with 17, 19, and 20 refer to the WT, S112R, and L441P *BnDGAT1* variants, respectively. Three technical replicates were carried out for each line and bars denote standard error. Significant differences are designated by asterisks ($P \leq 0.05$ = *, $P \leq 0.01$ = **, $P \leq 0.001$= ***).

In addition to the seed lipid content, the FA composition was also evaluated in the T_2 *AtCESA1*-RNAi/*BnDGAT1*-OE lines. Statistically significant but minor changes were detected in the proportions of most FAs between the EV control and T_2 *AtCESA1*-RNAi/*BnDGAT1*-OE lines, as well as between the *BnDGAT1* variants (Table 3.4.1). The greatest changes were in the major *Arabidopsis* FAs, with increased C18:1Δ^{9cis} and C18:1Δ^{11cis} (combined as 18:1) in both S112R- and L441P-*BnDGAT1*-OE (0.90% and 0.84%, respectively), increased C18:2$\Delta^{9cis,12cis}$ (18:2) in all experimental lines (from 0.98% to 1.32%), decreased C18:3$\Delta^{9cis,12cis,15cis}$ (18:3) in all transgenic lines (from 1.73% to 3.90%), and increased C20:1Δ^{11cis} in all experimental lines

(from 0.97% to 1.13%). Regarding the saturated FAs, both C16:0 (16:0) and C18:0 (18:0) very slightly increased (0.14-0.49% and 0.17-0.61%, respectively) in all transgenic lines, while C20:0 (20:0) decreased slightly (0.12-0.16%). Small changes were also observed in the remaining minor FAs. The most substantial shift in seed FA composition was the decline in 18:3, especially in lines overexpressing the *BnDGAT1* variants.

Table 3.4.1 Seed fatty acid composition of T_2 *AtCESA1*-RNAi/*BnDGAT1*-OE lines

Fatty acid	EV Control	*AtCESA1*-RNAi/WT-*BnDGAT1*-OE (DAS 17)	*AtCESA1*-RNAi/S112R-*BnDGAT1*-OE (DAS 19)	*AtCESA1*-RNAi/L441P-*BnDGAT1*-OE (DAS 20)
C16:0	7.44 (±0.18)	7.58 (±0.19)↑*	7.93 (±0.11)↑***	7.69 (±0.25)↑**
C16:1	0.26 (±0.01)	0.28 (±0.02)↑**	0.28 (±0.00)↑***	0.28 (±0.02)↑*
C18:0	3.27 (±0.09)	3.44 (±0.15) ↑***	3.88 (±0.03)↑***	3.73 (±0.27)↑***
C18:1	16.50 (±0.60)	16.72 (±0.71)	17.41 (±0.08)↑***	17.34 (±0.45)↑***
C18:2	28.24 (±0.52)	29.22 (±0.43)↑***	30.52 (±0.26)↑***	29.56 (±1.05)↑**
C18:3	17.76 (±0.29)	16.03 (±0.47)↓***	13.86 (±0.16)↓***	14.97 (±1.89)↓**
C20:0	2.37 (±0.08)	2.21 (±0.12)↓***	2.22 (±0.02)↓***	2.25 (±0.16)↓*
C20:1	20.48 (±1.61)	21.58 (±0.82)↑***	21.61 (±0.23)↑***	21.45 (±0.87)↑**
C20:2	1.77 (±0.04)	1.44 (±0.15)↓***	1.15 (±0.02)↓***	1.34 (±0.26)↓***
C22:1	1.91 (±0.07)	1.50 (±0.38)↓***	1.13 (±0.03)↓***	1.39 (±0.35)↓**

Average percentages (%) are shown for EV control, DAS 17, DAS 19, and DAS 20 lines with 8, 5, 2, and 3 independent biological replicates each, respectively. Three technical replicates were carried out for each line and significant differences are designated by asterisks ($P \leq 0.05$ = *, $P \leq 0.01$ = **, $P \leq 0.001$= ***). The direction of the difference (increase or decrease) is indicated with arrows (↑ or ↓). (±SD).

3.4.2 Seed Lipid Analysis of T_3 *AtCESA1*-RNAi/*BnDGAT1*-OE lines

Using kanamycin screening a total of 45 homozygous T_3 *AtCESA1*-RNAi/*BnDGAT1*-OE lines were identified from 163 lines, and their seed oil content and fatty acid composition were analyzed with GC-FID. On average, the T_3 *AtCESA1*-RNAi/*BnDGAT1*-OE lines had comparable seed lipid content (35.72%) relative to the EV controls (34.98%) (Fig. 3.4.2). Among the

transgenic lines, there were 8 lines each with significant increases (2-3.1%) and decreases (2-5%) in lipid content. In general, the seed lipid content of the lines from the DAS 19 lineage (overexpressing the S112R variant of *BnDGAT1*) were slightly lower (34.10%) than the EV controls, while lines from the DAS 20 lineage (overexpressing the L441P variant of *BnDGAT1*) were relatively higher (36.49%).

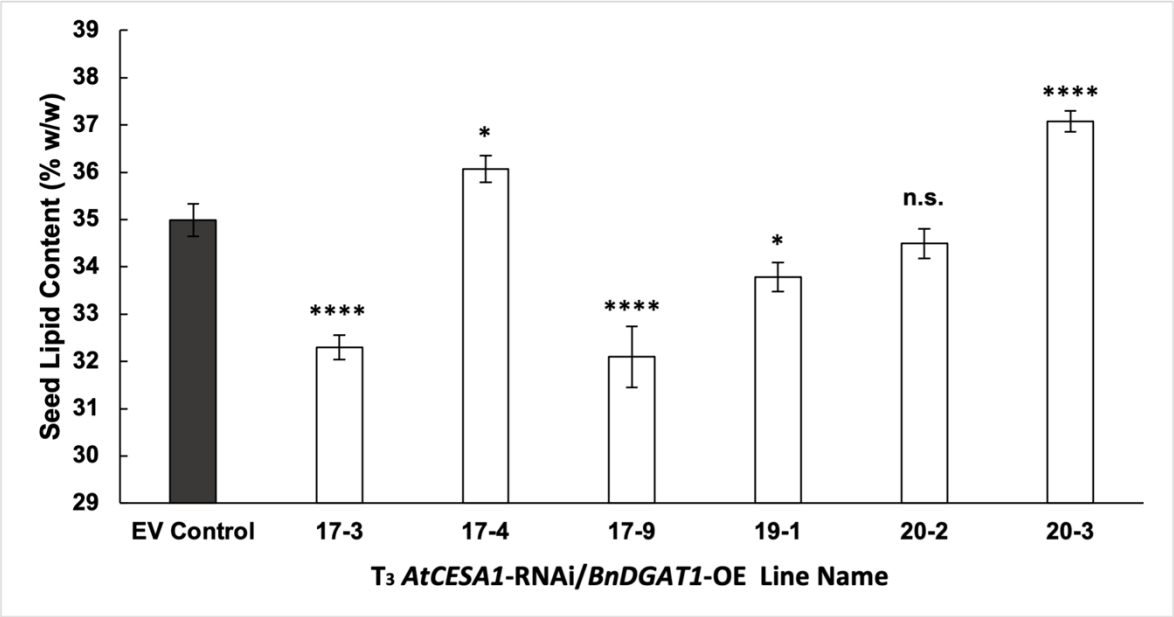

Figure 3.4.2 Seed lipid content of homozygous T3 *AtCESA1*-RNAi/*BnDGAT1*-OE lines
Averages are shown for 17 independent EV control and 5, 9, 5, 4, 4, and 9 *AtCESA1*-RNAi/*BnDGAT1*-OE biological replicates, respectively. Line names starting with 17, 19, and 20 refer to the WT, S112R, and L441P *BnDGAT1* variants, respectively. Three technical replicates were carried out for each biological replicate and bars denote standard error. Significant differences are designated by asterisks (n.s. = not significant, $P \leq 0.05$ = *, $P \leq 0.0001$= ****).

The effects of the *BnDGAT1* variants on seed lipid accumulation were compared. Overexpression of the *BnDGAT1*-S112R variant did not increase lipid content beyond the WT *BnDGAT1* (Fig. 3.4.3). In contrast, the *BnDGAT1*-L441P-OE exerted a small but significant increase in seed lipid content (about 2%) beyond the WT *BnDGAT1*. Further experiments excluded the S112R variant but analysis of the L441P variant continued.

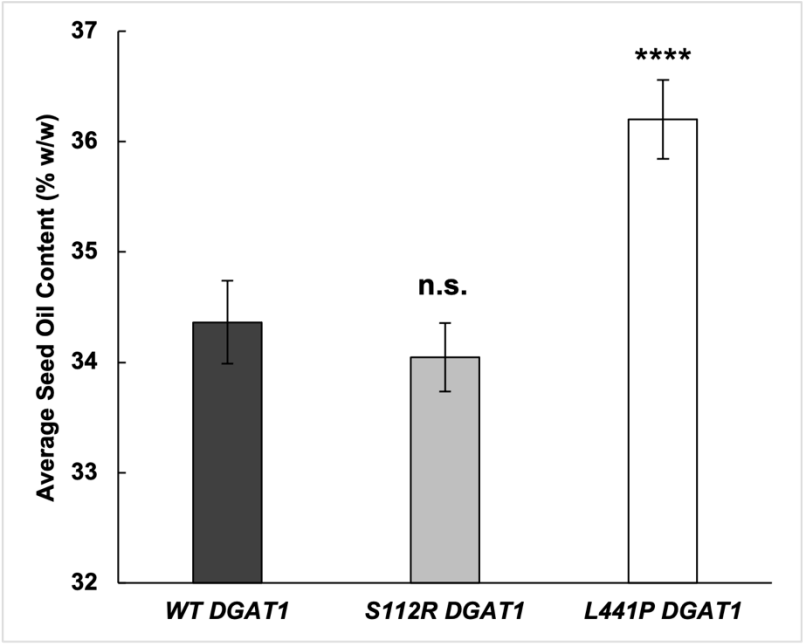

Figure 3.4.3 Seed lipid content in T_3 *AtCESA1*-RNAi lines with overexpression of wildtype & enhanced variants of *BnDGAT1*
Averages are shown for independent control and two BnDGAT1 variant lines, with 17, 4, and 14 biological replicates each, respectively. Three technical replicates were carried out for each line and bars denote standard error. Significant differences are designated by asterisks (n.s. = not significant, $P \leq 0.0001$= ****).

Statistically significant but minor changes were detected in the proportions of most FAs between the EV control T_3 *AtCESA1*-RNAi/*BnDGAT1*-OE lines, as well as between the *BnDGAT1* variants. Since S112R *BnDGAT1* variant did not result in higher oil content, their fatty acid compositions were not analyzed in detail. The greatest changes were in the major *Arabidopsis* FAs, with increased 18:2 (0.98-1.32%), decreased 18:3 (1.73-2.79%), and increased 20:1 (0.97-1.10%) in all *BnDGAT1*-OE lines (Table 3.4.2). Very slight increases were also noted in 16:0 and 18:0 in the transgenic lines, as well as small changes in the minor FAs.

Table 3.4.2 Seed fatty acid composition of T3 *AtCESA1*-RNAi/*BnDGAT1*-OE lines

Fatty acid	EV Control	*AtCESA1*-RNAi/WT-*BnDGAT1*-OE	*AtCESA1*-RNAi/L441P-*BnDGAT1*-OE
C16:0	7.44 (±0.18)	7.58 (±0.19)↑*	7.69 (±0.25)↑**
C16:1	0.26 (±0.01)	0.28 (±0.02)↑**	0.28 (±0.02)↑ *
C18:0	3.27 (±0.09)	3.44 (±0.15)↑***	3.73 (±0.27)↑***
C18:1	16.50 (±0.60)	16.72 (±0.71)	17.34 (±0.45)↑***
C18:2	28.24 (±0.52)	29.22 (±0.43)↑***	29.56 (±1.05)↑**
C18:3	17.76 (±0.29)	16.03 (±0.47)↓***	14.97 (±1.89)↓**
C20:0	2.37 (±0.08)	2.21 (±0.12)↓***	2.25 (±0.16)↓*
C20:1	20.48 (±0.26)	21.58 (±0.82)↑***	21.45 (±0.87)↑**
C20:2	1.77 (±0.04)	1.44 (±0.15)↓***	1.34 (±0.26)↓***
C22:1	1.91 (±0.07)	1.50 (±0.38)↓***	1.39 (±0.35)↓**

Average percentages (%) are shown for EV control, T3 *AtCESA1*-RNAi/WT-*BnDGAT1*-OE, and T3 *AtCESA1*-RNAi/L441P-*BnDGAT1*-OE lines with 8, 5, and 3 independent biological replicates each, respectively. Three technical replicates were carried out for each line and significant differences are designated by asterisks ($P \leq 0.05$ = *, $P \leq 0.01$ = **, $P \leq 0.001$= ***). The direction of the difference (increase or decrease) is indicated with arrows (↑ or ↓).

The lines with equal or increased oil were used for analysis of CSP with EV as the control. Several lines exhibited significantly higher CSP (1.1-5.5%) while only a few lines had slightly lower CSP (0.7-1.8%) (Fig. 3.4.4). Overall, the average percent CSP of the T3 *AtCESA1*-RNAi/*BnDGAT1*-OE lines was nearly significantly higher than the EV controls.

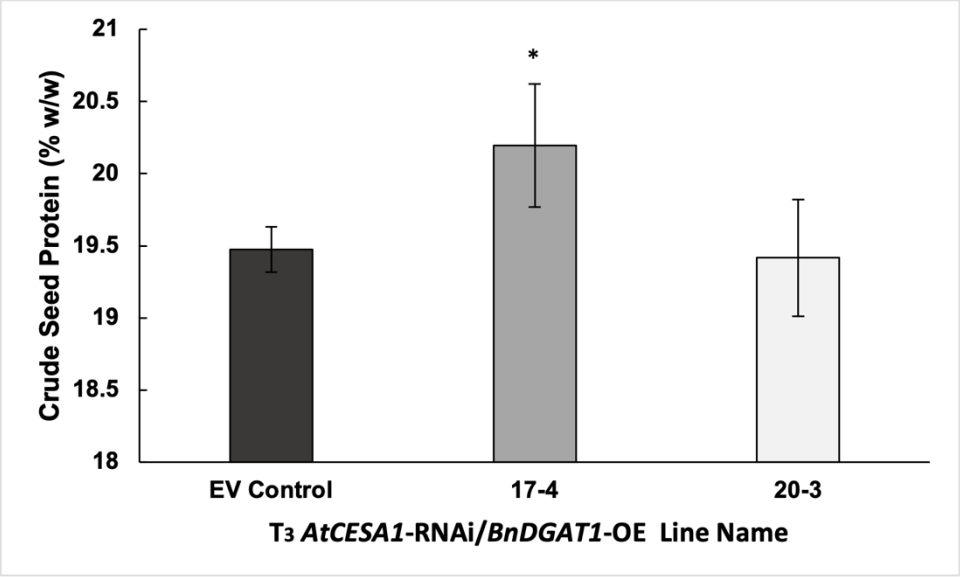

Figure 3.4.4 Crude seed protein content of homozygous T3 *AtCESA1*-RNAi/*BnDGAT1*-OE lines
Averages are shown for 9 EV control and 25 experimental lines. Line names starting with 17, 19, and 20 refer to the WT, S112R, and L441P *BnDGAT1* variants, respectively. Three technical replicates were carried out for each line and bars denote standard error. Significant differences are designated by asterisks ($P \leq 0.05$ = *).

3.4.3 Crystalline Cellulose Quantification of T3 *AtCESA1*-RNAi/*BnDGAT1*-OE lines

A selection of lines with equal or increased seed lipid and protein content were then advanced for relative changes in cellulose-derived acid-insoluble glucose analysis. The eight lines analyzed had significantly lower seed cellulose content (10-30%) than the EV controls (Fig. 3.4.5) and were advanced for further analysis.

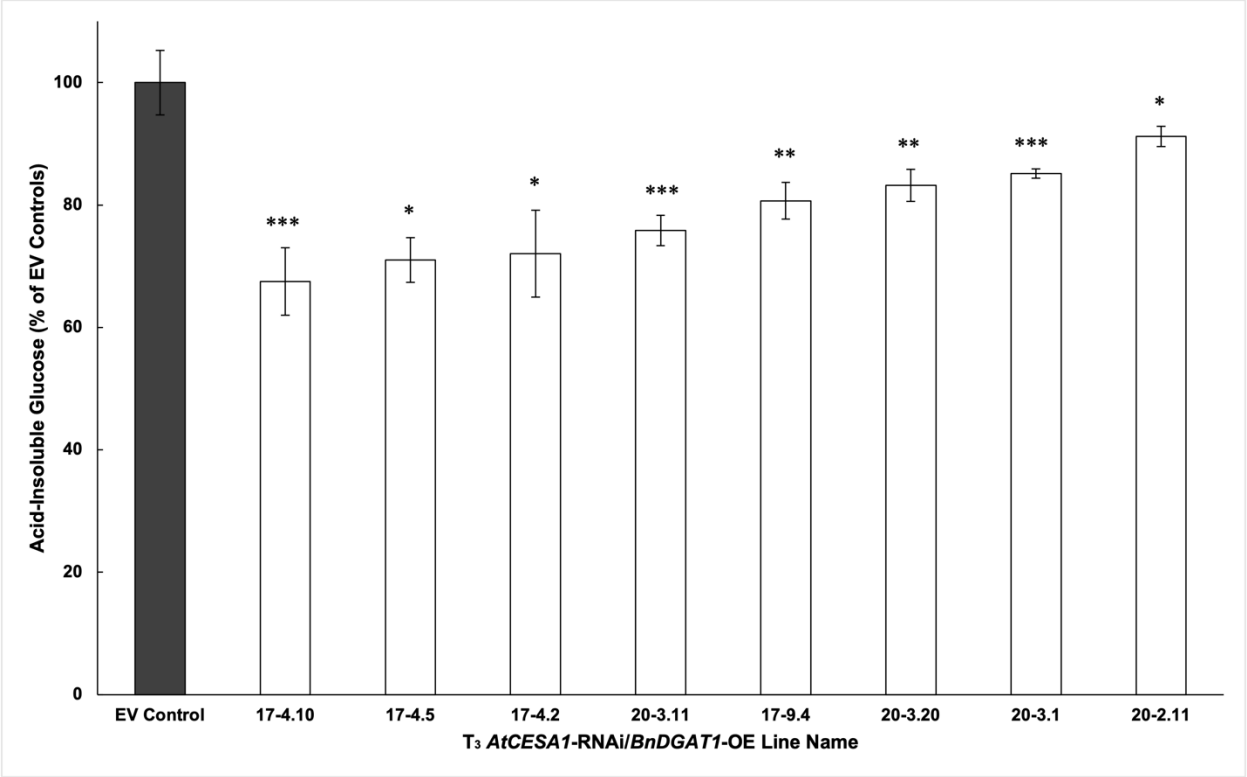

Figure 3.4.5 Cellulose-derived acid-insoluble glucose content of homozygous T3 *AtCESA1*-RNAi/*BnDGAT1*-OE lines
Averages are shown for 10 EV control and 9 selected *AtCESA1*-RNAi/*BnDGAT1*-OE lines as a percentage of the EV controls. Line names starting with 17, 19, and 20 refer to the WT, S112R, and L441P *BnDGAT1* variants, respectively. Three technical replicates were carried out for each line and bars denote standard error. Significant differences are designated by asterisks ($P \leq 0.05$ = *, $P \leq 0.01$ = **, $P \leq 0.001$= ***).

3.4.4 Combined Data and Selection of T3 *AtCESA1*-RNAi/*BnDGAT1*-OE lines

The seed lipid, protein, and cellulose data were assembled for the 8 reduced-cellulose lines for further analysis. Lipid and protein contents of all lines were equal or increased compared to the EV controls (Fig. 3.4.6). DAS 17-4.10 and 20-3.20 were selected for transformation with protein-related gene overexpression constructs as they represent lineages possessing the wild-type BnDGAT1 (DAS 17) and the L441P performance enhanced BnDGAT1 variant (DAS 20), as well as for their seed compositions. These two lines were selected because their CSP contents are equivalent to the EV controls, allowing evaluation of the effectiveness of

protein-related gene overexpression on CSP, they possessed equal or increased seed lipid contents relative to the EV controls, and they both had significantly reduced seed cellulose (Fig. 3.7).

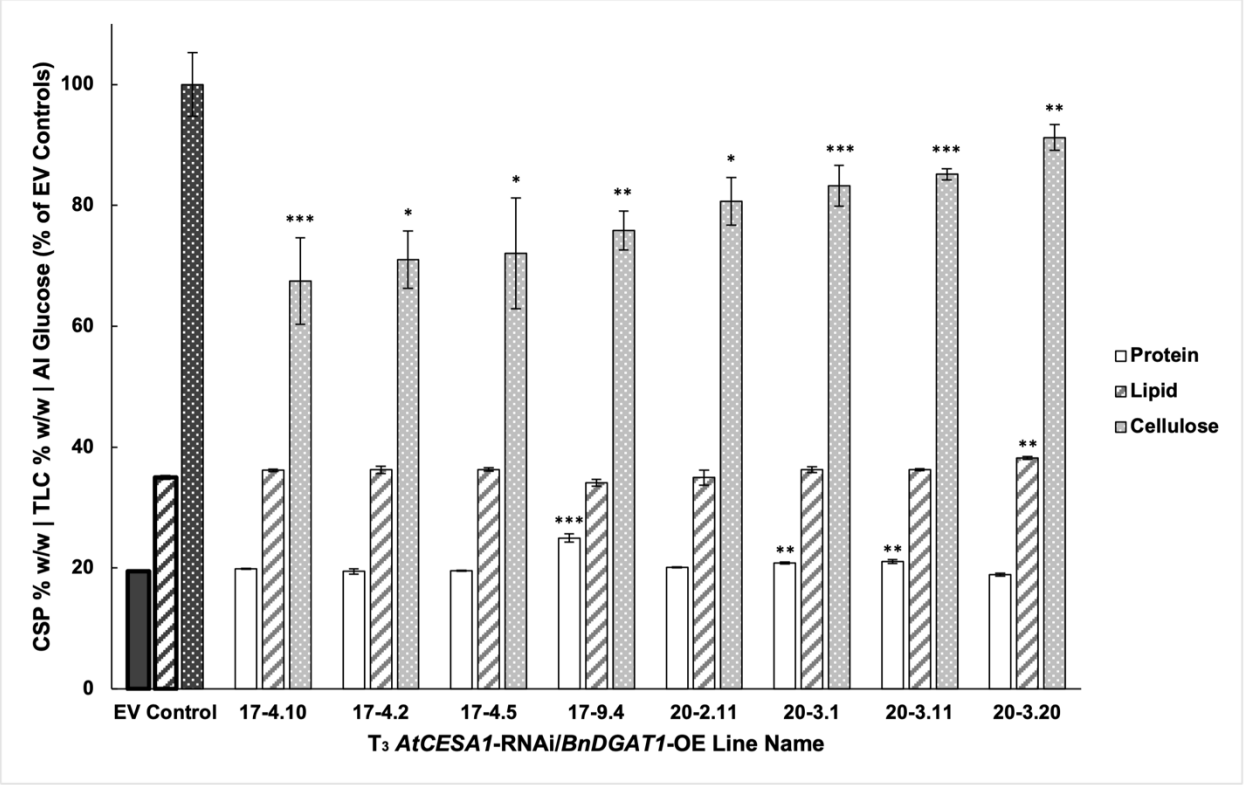

Figure 3.4.6 Combined crude seed protein (CSP, total lipid content (TLC), and cellulose (acid-insoluble glucose, AI Glucose) contents of EV control and T3 *AtCESA1*-RNAi/*BnDGAT1*-OE lines

Averages are shown on a mass/mass basis for independent control and transgenic lines, with 10 and 8 biological replicates of each, respectively. Line names starting with 17, 19, and 20 refer to the WT, S112R, and L441P *BnDGAT1* variants, respectively. Three technical replicates were carried out for protein and lipid content for each line, while two replicates were conducted for cellulose content. Bars denote standard error. Significant differences are indicated by asterisks ($P \leq 0.05$ = *, $P \leq 0.01$ = **, $P \leq 0.001$= ***).

3.4.5 Seed Size & 100-Seed Weight of T_3 *AtCESA1*-RNAi/*BnDGAT1*-OE lines

The T_3 *AtCESA1*-RNAi/*BnDGAT1*-OE lines with equal or increased seed lipid content, equal or increased seed protein, and reduced seed cellulose were imaged and processed in ImageJ for seed size and weight analysis. The average 2-dimensional size of the T_3 *AtCESA1*-RNAi/*BnDGAT1*-OE seeds was significantly greater than the EV controls by about 10,000 um^2, representing a 7.5% increase (Fig. 3.4.7). This increased seed size was mirrored in the 100 seed weight, with the average T_3 *AtCESA1*-RNAi/*BnDGAT1*-OE 100 seed weight increasing by nearly 0.3 mg (or 12%) above the EV controls (Fig. 3.4.8). Regrettably, overall seed yield data was not collected before seed mass was consumed by the lipid, protein, and cellulose analyses, therefore accurate seed yield data is not available for this generation.

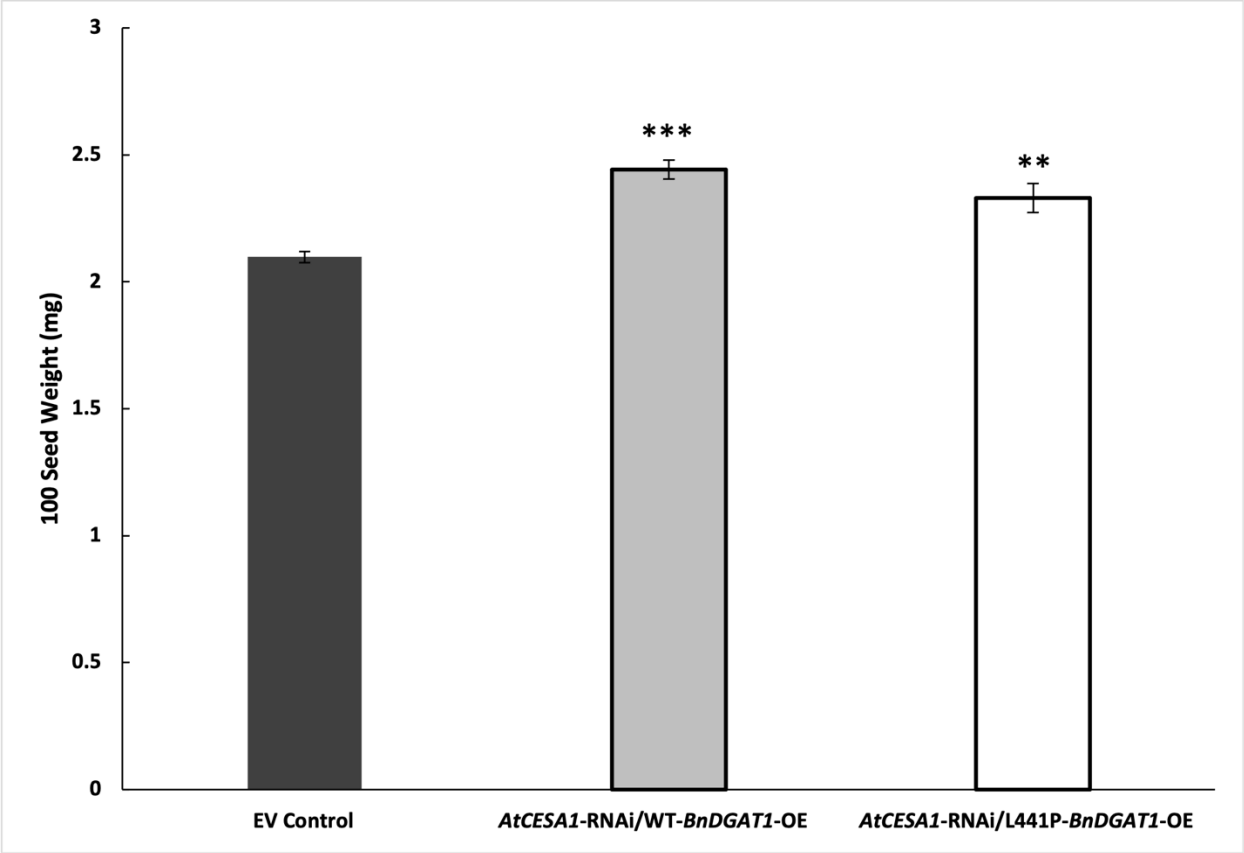

Figure 3.4.7 Average seed size (um^2) of EV control and T$_3$ *AtCESA1*-RNAi/*BnDGAT1*-OE seeds

Averages are shown for 10 independent control and 8 transgenics lines. Bars denote standard error. Significant differences are designated by asterisks ($P \leq 0.01$ = **, $P \leq 0.001$= ***).

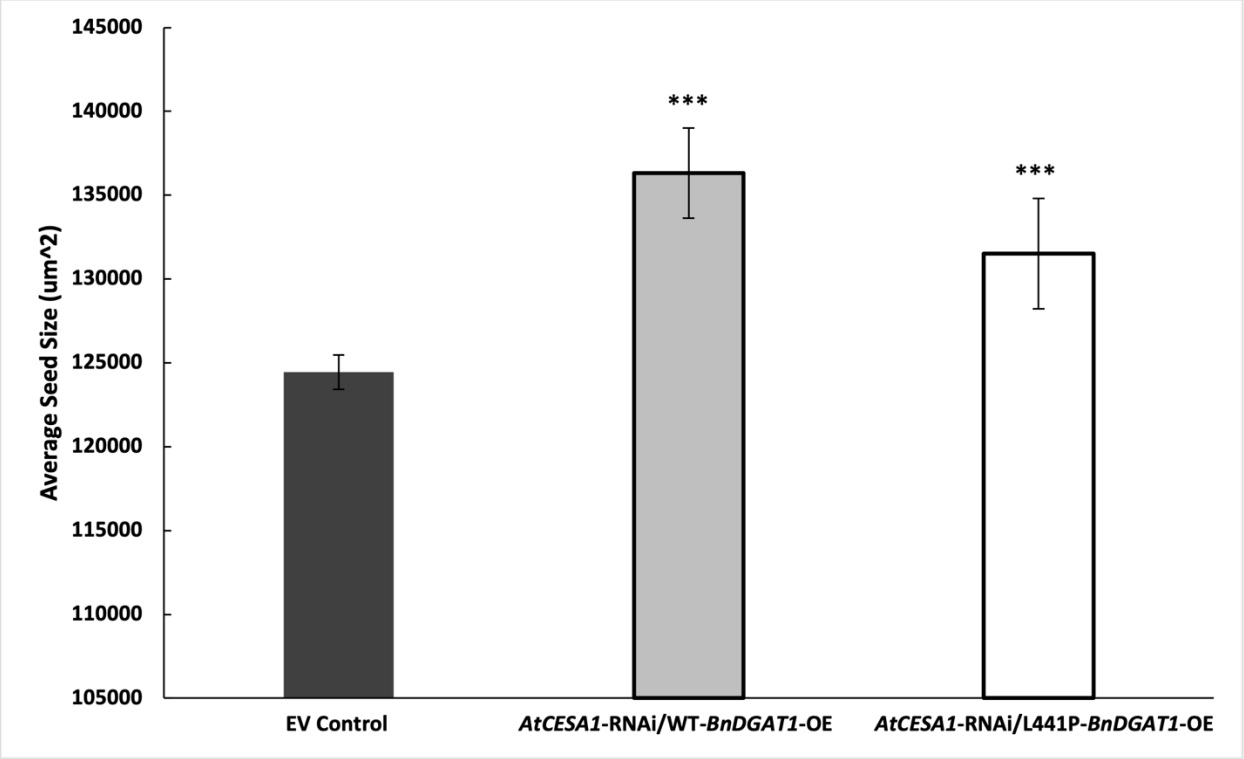

Figure 3.4.8 100 seed weight of EV control and T3 *AtCESA1*-RNAi/*BnDGAT1*-OE seeds
Averages are shown for 10 independent control and 8 transgenics lines. Bars denote standard error. Significant differences are designated by asterisks ($P \leq 0.001$= ***).

3.4.6 dsRed Fluorescent Screening of T_1 Transformants

The T_1 seed with *AtAAP1*-OE, *AtALAAT1*-OE, & *AtASN1*-OE were harvested and screened using the dsRed marker. The T_1 seeds were characterized by a scattering of distinct, brightly glowing (transformed) seeds amongst many non-glowing, untransformed seeds (Fig. 3.4.9, ai & bi). The dsRed T_1 seeds were carefully isolated and grown to the T_2 generation. Non-dsRed T_2 seeds lacked the red fluorescence phenotype (Fig 3.4.9, aii & bii). T_2 seeds produced from a heterozygous parent produced 75% glowing and 25% non-glowing progeny (Fig. 18, aiii & biii). Heterozygous T_2 lines that possessed only a single insertion of the transgene were advanced to the T_3 generation. T_3 seeds produced from homozygous, single-insertion lines produced 100% glowing progeny (Fig. 3.4.9, aiv & biv). This dsRed fluorescence screening

method was used to evaluate the transgene status of each line in every generation after the floral dip transformation. dsRed fluorescence can alternatively be visualized by the ChemiDoc MP Imaging System (Bio-Rad), allowing differentiation of homozygous, heterozygous, and non-segregant lines (Fig. 3.4.9, ci-cviii).

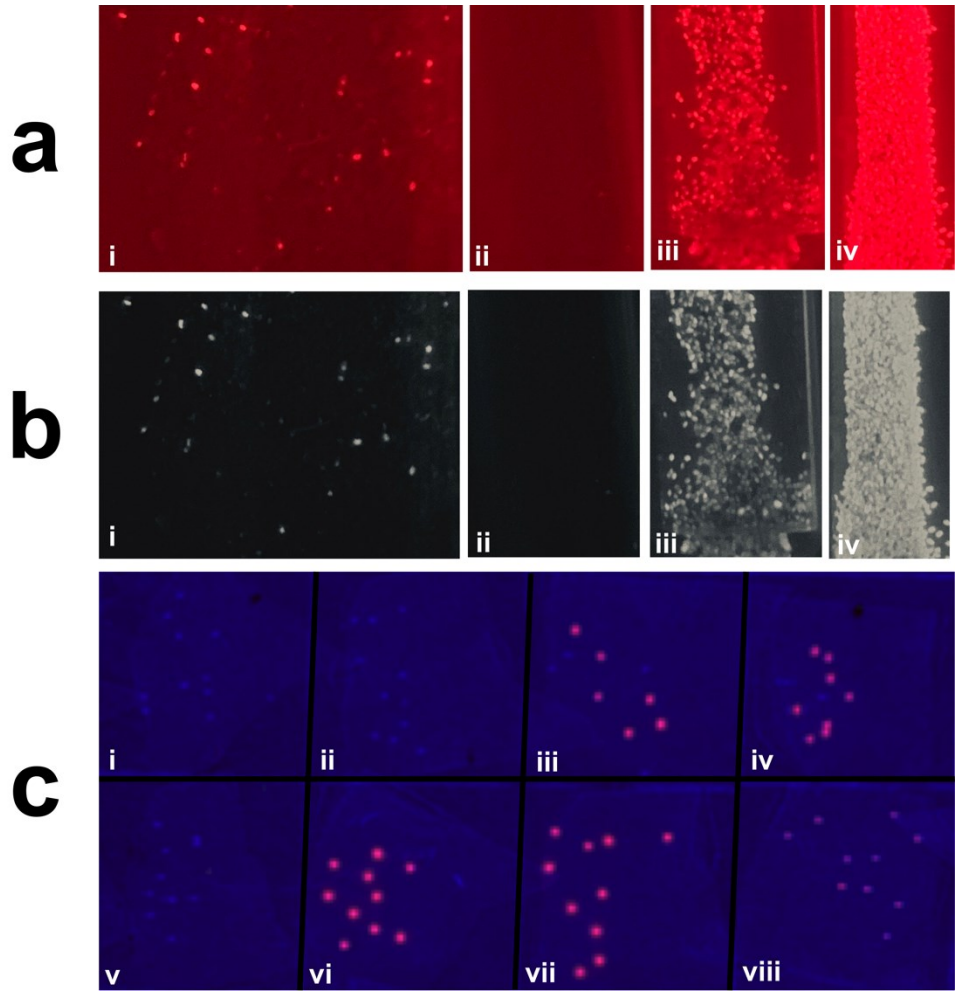

Figure 3.4.9 Screening of transformed seeds using dsRed fluorescence marker
Representative color and grayscale images of seeds from a T_1 line (ai & bi), a non-segregant line (aii & bii), a heterozygous line (aiii & biii) a homozygous line (aiv & biv) using a 595 nm green laser while viewing through red-lensed glasses. Alternative method of dsRed detection using ChemiDoc MP Imaging System (Bio-Rad) with blue and red filters (590 nm and 602 nm, respectively) (c). Non-segregant lines (ci, cii, & cv), heterozygous lines (ciii & civ), and homozygous lines (cvi, cvii, & cviii). Panel c credit: Dr. Limin Wu, Department of AFNS, Faculty of ALES, University of Alberta, Edmonton, Alberta.

3.4.7 Seed Lipid Analysis of T_3 *AtCESA1*-RNAi/*BnDGAT1*-OE/Protein Gene-OE lines

The seed lipid content data of the T_3 lines was organized into the following groups: EV controls, single protein-related gene (*AtAAP1*, *AtALAAT1*, or *AtASN1*) overexpressing lines, and carbon-reallocated lines (*AtCESA1*-RNAi/*BnDGAT1*-OE background with *AtAAP1*, *AtALAAT1*, or *AtASN1* overexpression).

Overexpression of *AtAAP1* alone resulted in reduced seed lipid accumulation (-4.8%) compared to the EV controls, while *AtCESA1*-RNAi/*BnDGAT1*-OE/*AtAAP1*-OE saw an increase in seed lipid content (+1.7) (Fig. 3.4.10). When comparing *AtAAP1*-OE alone with the *AtCESA1*-RNAi/*BnDGAT1*-OE/*AtAAP1*-OE lines, there was a substantial increase in seed lipid content (6.5%).

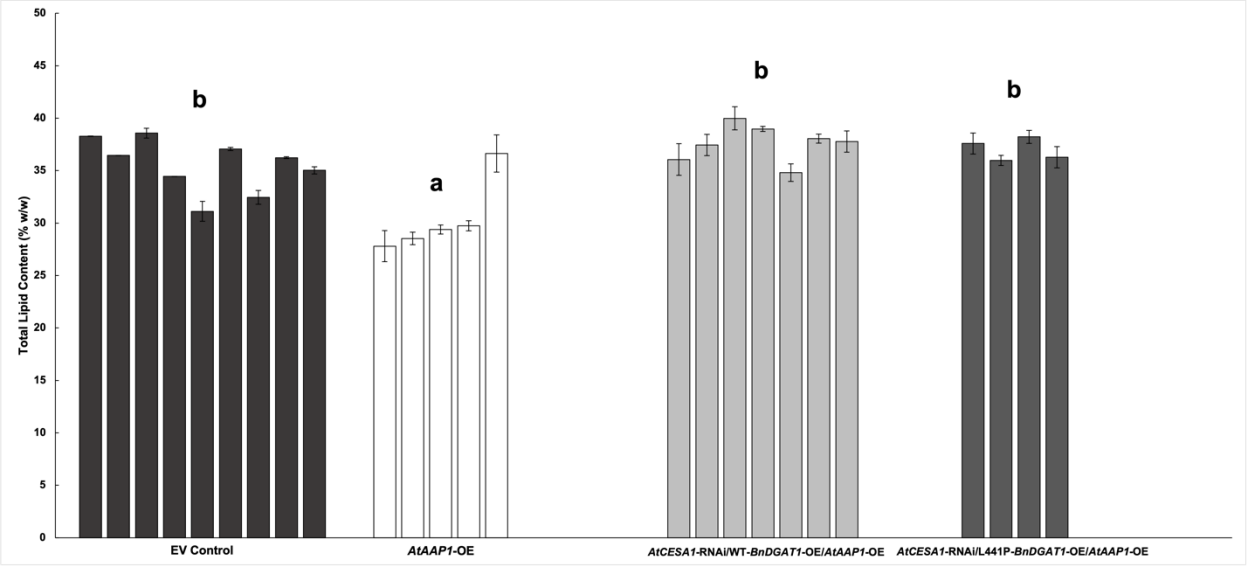

Figure 3.4.10 Seed lipid content of T_3 *AtCESA1*-RNAi/*BnDGAT1*-OE/*AtAAP1*-OE lines
Averages are shown for EV control, *AtAAP1*-OE, and two *AtCESA1*-RNAi/*BnDGAT1*/*AtAAP1*-OE groups with 9, 5, 7, and 4 independent biological replicates each, respectively. Three technical replicates were carried out for each line and bars denote standard error. Significant differences are indicated by different letters as determined by the Tukey test ($\alpha = 0.05$).

Several differences in seed FA composition were observed between the three groups. There was a small but significant increase (1.6%) in 18:1 in the L441P-*BnDGAT1*-OE lines, a substantial increase (5-5.5%) in 18:2 in all *BnDGAT1*-OE lines, a decrease (1.4-4.3%) in 18:3 (especially pronounced in the L441P-*BnDGAT1*-OE lines), and a decrease (2.9%) in 20:1 in all *BnDGAT1*-OE lines (Table 3.4.3). Significant but minor changes were detected in almost all remaining FA comparisons.

Table 3.4.3 Seed fatty acid composition of T_3 *AtCESA1*-RNAi/*BnDGAT1*-OE/*AtAAP1*-OE lines

Fatty acid	EV Control	*AtCESA1*-RNAi/WT-*BnDGAT1*-OE/*AtAAP1*-OE	*AtCESA1*-RNAi/L441P-*BnDGAT1*-OE/*AtAAP1*-OE
C16:0	8.14 (±0.47)	8.33 (±0.44)	9.31 (±0.56) ↑***
C16:1	0.22 (±0.05)	0.60 (±0.15) ↑***	0.75 (±0.20) ↑***
C18:0	2.81 (±0.21)	2.78 (±0.26)	3.00 (±0.31) ↑*
C18:1	18.41 (±1.01)	18.76 (±0.76)	19.96 (±0.80) ↑***
C18:2	32.99 (±0.27)	38.00 (±1.36) ↑***	38.54 (±1.66) ↑***
C18:3	18.61 (±1.32)	17.25 (±1.13) ↓***	14.36 (±1.34) ↓***
C20:0	1.34 (±0.20)	0.87 (±0.19) ↓***	0.84 (±0.13) ↓***
C20:1	15.42 (±0.1.61)	12.52 (±1.43) ↓***	12.45 (±1.70) ↓***
C20:2	1.17 (±0.22)	0.70 (±0.20) ↓***	0.60 (±0.15) ↓***
C22:1	0.89 (±0.16)	0.18 (±0.05) ↓***	0.20 (±0.07) ↓***

Average percentages (%) are shown for EV control, T_3 *AtCESA1*-RNAi/WT-*BnDGAT1*-OE/*AtAAP1*-OE lines, and T_3 *AtCESA1*-RNAi/L441P-*BnDGAT1*-OE/*AtAAP1*-OE lines with 9, 7, and 4 independent biological replicates each, respectively. Three technical replicates were carried out for each line and significant differences are designated by asterisks ($P \leq 0.05$ = *, $P \leq 0.001$= ***). The direction of the difference (increase or decrease) is indicated with arrows (↑ or ↓).

Overexpression of *AtALAAT1* did not impact seed lipid accumulation relative to the EV controls, nor was there any effect caused by *AtCESA1*-RNAi/*BnDGAT1*-OE/*AtALAAT1*-OE (Fig.

3.4.11). There was also no significant difference in lipid content when comparing *AtALAAT1*-OE alone with the *AtCESA1*-RNAi/*BnDGAT1*-OE/*AtALAAT1*-OE lines.

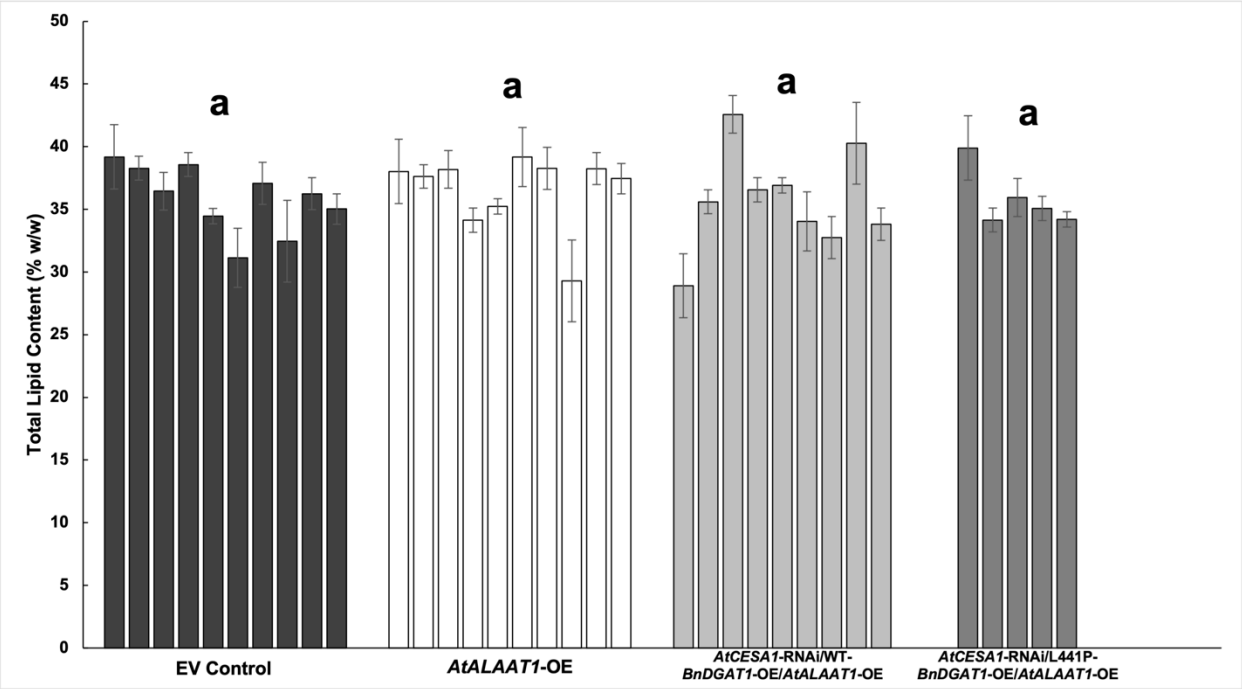

Figure 3.4.11 Seed lipid content of T$_3$ *AtCESA1*-RNAi/*BnDGAT1*-OE/*AtALAAT1*-OE lines Averages are shown for EV control, *AtALAAT1*-OE, and two *AtCESA1*-RNAi/*BnDGAT1*-OE/*AtALAAT1*-OE groups with 9, 10, 8, and 5 independent biological replicates each, respectively. Three technical replicates were carried out for each line and bars denote standard error. Significant differences are indicated by different letters as determined by the Tukey test ($\alpha = 0.05$).

Although the seed lipid content was not impacted, there were several significant shifts in FA composition in the *AtCESA1*-RNAi/*BnDGAT1*-OE/*AtALAAT1*-OE lines. There was a significant decrease (3%) in 18:1 in the WT-*BnDGAT1*-OE lines, a decrease in 18:3 in all *BnDGAT1*-OE lines, and a sizeable increase in 20:1 in all *BnDGAT1*-OE lines (Table 3.4.4). Several significant differences were observed in the proportions of the remaining FAs, though these were generally minor.

Table 3.4.4 Seed fatty acid composition of T$_3$ *AtCESA1*-RNAi/*BnDGAT1*-OE/*AtALAAT1*-OE lines

Fatty acid	EV Control	*AtCESA1*-RNAi/WT-*BnDGAT1*-OE/*AtALAAT1*-OE	*AtCESA1*-RNAi/L441P-*BnDGAT1*-OE/*AtALAAT1*-OE
C16:0	8.14 (±0.47)	8.41 (±0.22)↑*	7.67 (±0.13)↓***
C16:1	0.22 (±0.05)	0.29 (±0.07)↑**	0.26 (±0.02)↑**
C18:0	2.81 (±0.21)	3.21 (±0.09)↑***	2.69 (±0.14)
C18:1	18.41 (±1.01)	15.36 (±0.76) ↓***	18.62 (±0.41)
C18:2	32.99 (±0.27)	33.41 (±0.71)	32.2 (±0.48)↓*
C18:3	18.61 (±1.32)	16.95 (±0.86)↓***	16.83 (±0.82)↓***
C20:0	1.34 (±0.20)	1.16 (±0.12)↓***	1.27 (±0.12)
C20:1	15.42 (±0.1.61)	19.96 (±0.83)↑***	18.52 (±0.55)↑***
C20:2	1.17 (±0.22)	0.74 (±0.07)↓***	1.07 (±0.06)↓*
C22:1	0.89 (±0.16)	0.50 (±0.07)↓***	0.84 (±0.08)

Average percentages (%) are shown for EV control, T$_3$ *AtCESA1*-RNAi/WT-*BnDGAT1*-OE/*AtALAAT1*-OE lines, and T$_3$ *AtCESA1*-RNAi/L441P-*BnDGAT1*-OE/*AtALAAT1*-OE lines with 9, 8, and 5 independent biological replicates each, respectively. Three technical replicates were carried out for each line and significant differences are designated by asterisks ($P \leq 0.05$ = *, $P \leq 0.01$ = **, $P \leq 0.001$= ***). The direction of the difference (increase or decrease) is indicated with arrows (↑ or ↓).

There were no significant differences between seed lipid contents of the EV controls, T$_3$ *AtASN1*-OE lines, and T$_3$ *AtCESA1*-RNAi/*BnDGAT1*-OE/*AtASN1*-OE lines (Fig. 3.4.12).

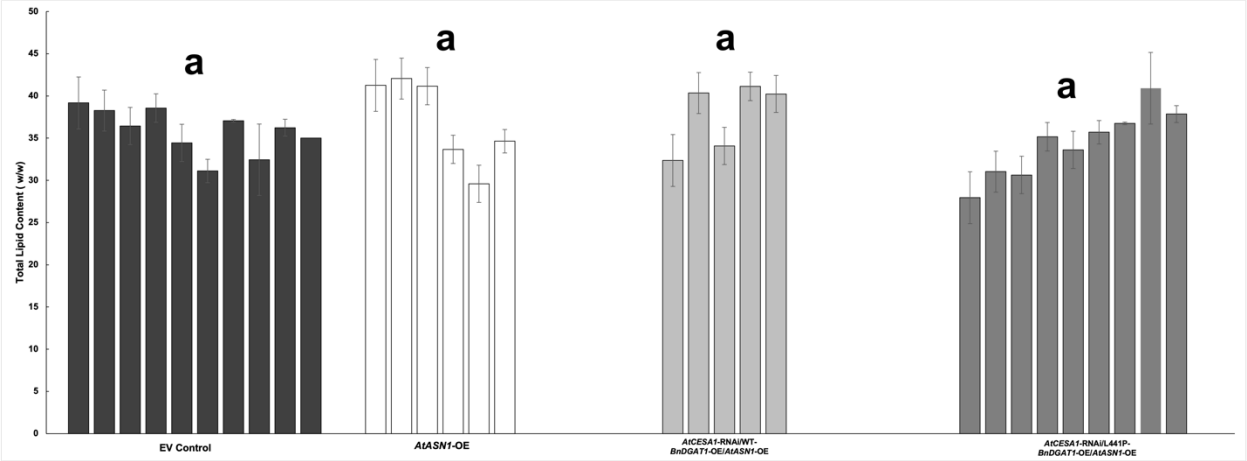

Figure 3.4.12 Seed lipid content of T3 *AtCESA1*-RNAi/*BnDGAT1*-OE/*AtASN1*-OE lines
Averages are shown for EV control, *AtASN1*-OE, and two *AtCESA1*-RNAi/*BnDGAT1*-OE/*AtASN1*-OE groups with 9, 6, 4, and 9 independent biological replicates each, respectively. Three technical replicates were carried out for each line and bars denote standard error. Significant differences are indicated by different letters as determined by the Tukey test (α = 0.05).

Although seed lipid content was not impacted, there were several significant shifts in FA composition in the *AtCESA1*-RNAi/*BnDGAT1*-OE/*AtASN1*-OE lines. There was a decrease (-1.9%) in 18:1 in the wildtype *BnDGAT1*-OE lines but an increase (+1.6%) in the L441P-*BnDGAT1*-OE lines, an increase (+1.9-2.9%) in 18:2 in all *BnDGAT1*-OE lines, a decrease (-2.3-6.5%) in 18:3 all *BnDGAT1*-OE lines (especially in the L441P-*BnDGAT1*-OE lines), and an increase (+2.6-2.8%) in 20:1 in all *BnDGAT1*-OE lines (Table 3.4.5). Several significant differences were observed in the proportions of the remaining FAs, though these were generally minor.

Table 3.4.5 Seed fatty acid composition of T3 *AtCESA1*-RNAi/*BnDGAT1*-OE/*AtASN1*-OE lines

Fatty acid	EV Control	*AtCESA1*-RNAi/WT-*BnDGAT1*-OE/*AtASN1*-OE	*AtCESA1*-RNAi/L441P-*BnDGAT1*-OE/*AtASN1*-OE

C16:0	8.14	(±0.47)	8.45	(±0.37)	8.26	(±0.17)
C16:1	0.22	(±0.05)	0.26	(±0.17)	0.27	(±0.11)
C18:0	2.81	(±0.21)	3.31	(±0.54)↑*	3.74	(±0.20)↑***
C18:1	18.41	(±1.01)	16.50	(±1.35)↓**	20.00	(±0.78)↑***
C18:2	32.99	(±0.27)	34.85	(±2.23)↑**	35.92	(±1.19)↑***
C18:3	18.61	(±1.32)	16.27	(±2.30)↓**	12.09	(±0.77)↓***
C20:0	1.34	(±0.20)	0.99	(±0.14)↓***	1.03	(±0.11)↓***
C20:1	15.42	(±1.61)	18.21	(±3.26)↑*	17.97	(±0.93)↑***
C20:2	1.17	(±0.22)	0.70	(±0.10)↓***	0.50	(±0.06)↓***
C22:1	0.89	(±0.16)	0.47	(±0.18)↓***	0.23	(±0.05)↓***

Average percentages (%) are shown for EV control, T_3 *AtCESA1*-RNAi/WT-*BnDGAT1*-OE/*AtASN1*-OE lines, and T_3 *AtCESA1*-RNAi/L441P-*BnDGAT1*-OE/*AtASN1*-OE lines with 9, 4, and 8 independent biological replicates each, respectively. Three technical replicates were carried out for each line and significant differences are designated by asterisks ($P \leq 0.05$ = *, $P \leq 0.01$ = **, $P \leq 0.001$= ***). The direction of the difference (increase or decrease) is indicated with arrows (↑ or ↓).

3.4.8 Crude Seed Protein Quantification of T_3 *AtCESA1*-RNAi/*BnDGAT1*-OE/Protein Gene-OE lines

Overexpression of *AtAAP1* alone increased the CSP by 1.4% compared to the EV controls, while *AtCESA1*-RNAi/*BnDGAT1*-OE/*AtAAP1*-OE yielded an increase of 2.3% (Fig. 3.4.13). When comparing *AtAAP1*-OE alone to *AtCESA1*-RNAi/*BnDGAT1*-OE/*AtAAP1*-OE, there was small but insignificant increase in CSP.

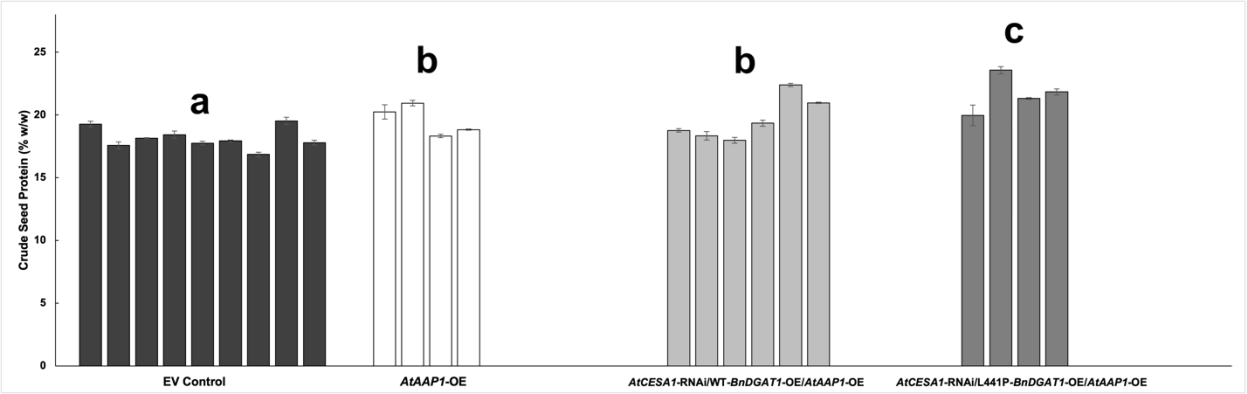

Figure 3.4.13 Crude seed protein content of T_3 *AtCESA1*-RNAi/*BnDGAT1*-OE/*AtAAP1*-OE lines

Averages are shown for EV control, *AtAAP1*-OE, and two *AtCESA1*-RNAi/*BnDGAT1*-OE/*AtAAP1*-OE groups with 9, 5, 6, and 5 independent biological replicates each, respectively. Three technical replicates were carried out for each line and bars denote standard error. Significant differences are indicated by different letters as determined by the Tukey test (α = 0.05).

Overexpression of *AtALAAT1* alone increased the CSP by 0.9% compared to the EV controls, while *AtCESA1*-RNAi/*BnDGAT1*-OE/*AtALAAT1*-OE yielded an increase of 2.6% (Fig. 3.4.14). When comparing *AtALAAT1*-OE alone to *AtCESA1*-RNAi/*BnDGAT1*-OE/*AtALAAT1*-OE, there was 1.7% increase in CSP.

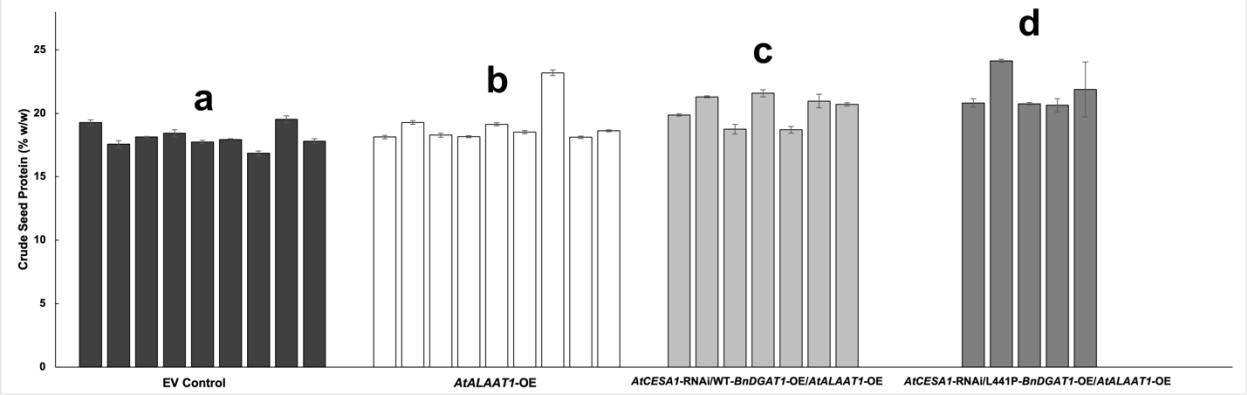

Figure 3.4.14 Crude seed protein content of T_3 *AtCESA1*-RNAi/*BnDGAT1*-OE/*AtALAAT1*-OE lines
Averages are shown for EV control, *AtALAAT1*-OE, and two *AtCESA1*-RNAi/*BnDGAT1*-OE/*AtALAAT1*-OE groups with 9, 9, 8, and 5 independent biological replicates each, respectively. Three technical replicates were carried out for each line and bars denote standard error. Significant differences are indicated by different letters as determined by the Tukey test (α = 0.05).

Overexpression of *AtASN1* alone decreased the CSP by 1.2% compared to the EV controls, while *AtCESA1*-RNAi/*BnDGAT1*-OE/*AtASN1*-OE yielded a small increase of 0.6% (Fig. 3.4.15). When comparing *AtASN1*-OE alone to *AtCESA1*-RNAi/*BnDGAT1*-OE/*AtASN1*-OE, there was 1.8% increase in CSP.

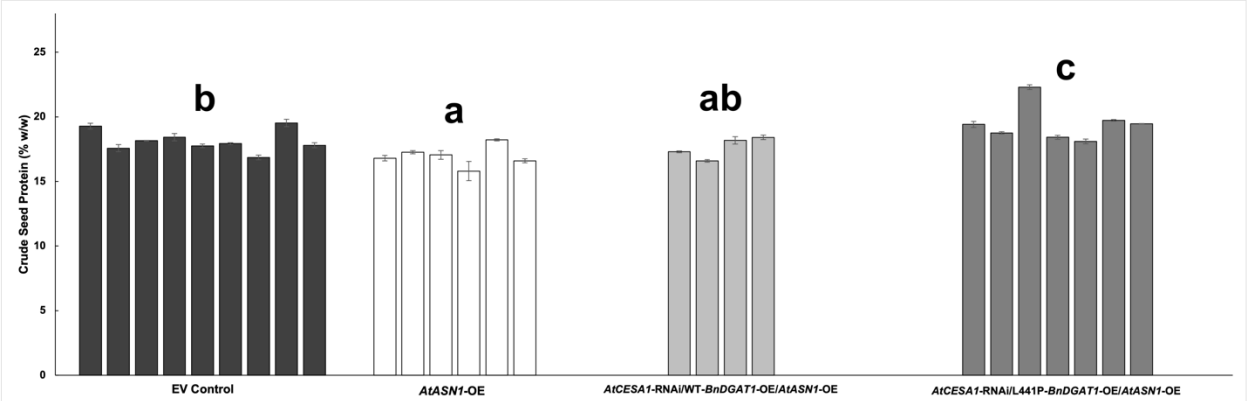

Figure 3.4.15 Crude seed protein content of T3 *AtCESA1*-RNAi/*BnDGAT1*-OE/*AtASN1*-OE lines
Averages are shown for EV control, *AtASN1*-OE, and two *AtCESA1*-RNAi/*BnDGAT1*-OE/*AtASN1*-OE groups with 9, 6, 4, and 7 independent biological replicates each, respectively. Three technical replicates were carried out for each line and bars denote standard error. Significant differences are indicated by different letters as determined by the Tukey test (α = 0.05).

Because the lipid, protein, and cellulose analyses consumed much of the seed from the T_3 lines, pooling of seed between independent transformants with the same genetics was required to ensure enough seed mass for at least three replicates per construct for AA analysis by HPLC. For example, seed was pooled together from fifteen different EV control lines, then split into ten technical replicates. Additionally, for the transgenic lines, seeds were pooled from both single protein-related gene overexpression lines the respective counterpart in the *AtCESA1*-RNAi/*BnDGAT1*-OE background. Due to an inability to chromatographically distinguish the signals for methionine and valine, they are represented as a single combined value.

Overall, there were almost no significant differences in the AA composition between transgenic and EV control lines (Table 3.4.6). The few differences that did reach statistical significance were minor, with the most notable being a 0.88% reduction in threonine in lines

with *AtALAAT1* overexpression. There were no significant differences in AA composition between *AtASN1*-OE lines and the EV controls.

Table 3.4.6 Seed amino acid composition of T$_3$ *AtCESA1*-RNAi/*BnDGAT1*-OE lines with *AtAAP1*-OE, *AtALAAT1*-OE, or *AtASN1*-OE

Amino Acid	EV Controls		*AtAAP1*-OE		*AtALAAT1*-OE		*AtASN1*-OE	
Aspartate	7.18	(±0.08)	7.32	(±0.11)↑*	7.44	(±0.46)	7.91	(±0.70)
Glutamate	15.24	(±0.32)	14.97	(±0.55)	15.13	(±0.46)	14.93	(±0.67)
Serine	6.68	(±0.18)	6.53	(±0.16)	6.62	(±0.21)	6.61	(±0.24)
Histidine	2.23	(±0.10)	2.08	(±0.09) ↓*	2.22	(±0.18)	2.12	(±0.11)
Glycine	12.10	(±0.25)	11.91	(±0.26)	11.94	(±0.28)	12.01	(±0.43)
Threonine	5.85	(±0.60)	5.41	(±0.41)	4.97	(±0.53)↓*	5.58	(±0.52)
Arginine	5.72	(±0.36)	5.60	(±0.24)	5.29	(±0.33)↓*	5.49	(±0.24)
Alanine	7.63	(±0.28)	7.51	(±0.19)	7.36	(±0.25)	7.60	(±0.26)
Tyrosine	1.64	(±0.17)	1.89	(±0.12) ↑*	1.86	(±0.21)↑*	1.73	(±0.35)
Met/Val	3.63	(±0.33)	3.62	(±0.12)	3.22	(±0.45)	3.66	(±0.18)
Phenala	3.98	(±0.20)	3.93	(±0.12)	3.78	(±0.21)	3.96	(±0.15)
Isoleucine	4.25	(±0.53)	4.27	(±0.14)	3.59	(±0.78)	4.30	(±0.19)
Leucine	7.22	(±0.35)	7.17	(±0.21)	6.87	(±0.39)	7.14	(±0.24)
Lysine	16.66	(±3.07)	17.80	(±2.27)	19.71	(±2.83)	16.95	(±2.98)

Values represent average percentages (%) and are shown for pooled samples consisting of seeds from EV control, *AtAAP1*-OE, *AtALAAT1*-OE, and *AtASN1*-OE lines (both single gene overexpression and in the *AtCESA1*-RNAi/*BnDGAT1*-OE background) with 10, 5, 6, and 6 replicates each, respectively. Pooling of seed between biological replicates was required to obtain sufficient sample mass for the analysis. Values for methionine and valine are combined due to chromatographic inability to separate the two signals. Significant differences are

designated by asterisks ($P \leq 0.05$ = *, $P \leq 0.01$ = **, $P \leq 0.001$= ***). The direction of the difference (increase or decrease) is indicated with arrows (↑ or ↓).

3.4.9 Crystalline Cellulose Quantification of T_3 *AtCESA1*-RNAi/*BnDGAT1*-OE/Protein Gene-OE lines.

To evaluate the seed cellulose content, the lines were organized into two groups: a non-*AtCESA1*-RNAi group consisting of EV control and all single protein-related gene overexpression lines, and a *AtCESA1*-RNAi group consisting of all *AtCESA1*-RNAi/*BnDGAT1*-OE/Protein Gene-OE lines. The cellulose-derived acid-insoluble glucose analysis found that the average cellulose content of all lines with *AtCESA1*-RNAi was reduced by 9.3 μg/mg (-20.8%) compared to the non-*AtCESA1*-RNAi lines (Fig. 3.4.16).

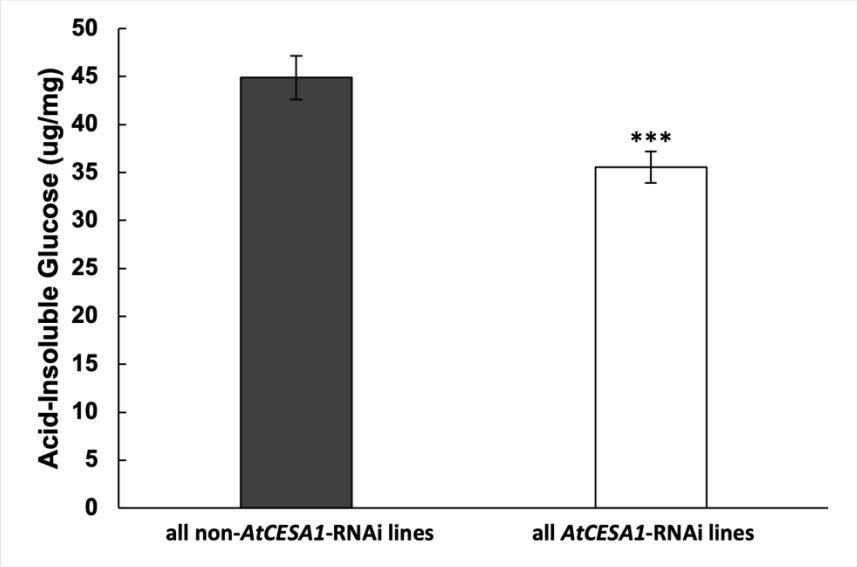

Figure 3.4.16 Acid-insoluble glucose contents of T_3 seeds with and without *AtCESA1*-RNAi
EV control, *AtAAP1*-OE, *AtALAAT1*-OE, and *AtASN1*-OE are shown in gray while *AtCESA1*-RNAi/*BnDGAT1*-OE/Protein Gene-OE lines are in white. A total of 24 and 34 independent biological replicates were used for the non-*AtCESA1*-RNAi and *AtCESA1*-RNAi groups, respectively. Three technical replicates were carried out for each line and bars denote standard error. Significant differences are designated by asterisks ($P \leq 0.05$ = *, $P \leq 0.01$ = **, $P \leq 0.001$= ***).

3.4.10 Yield, Seed Size & 100-Seed Weight of T_3 *AtCESA1*-RNAi/*BnDGAT1*-OE/Protein Gene-OE lines

The total mass of seed produced per plant (yield) was recorded after harvesting, followed by seed size and 100 seed weight analysis. There was high variability observed in the yield data between plants, likely resulting from a combination of factors such as natural plant-to-plant variation, static cling that caused some seeds to stick to the pollination tubes, and premature silique dehiscence.

Among the lines with *AtAAP1*-OE alone, there was increased seed yield (+26%) compared to the EV controls, though this finding did not quite reach statistical significance (Fig. 3.4.17A). There was, however, a significant increase in yield (+47%) for the *AtCESA1*-RNAi/L441P-*BnDGAT1*-OE/*AtAAP1*-OE lines. There was a small decrease in the 100 seed weight for the *AtCESA1*-RNAi/L441P-*BnDGAT1*-OE/*AtAAP1*-OE seeds (Fig. 3.4.17B). The seed size decreased slightly in all the transgenic seeds but no comparisons reached statistical significance (Fig. 3.4.17C).

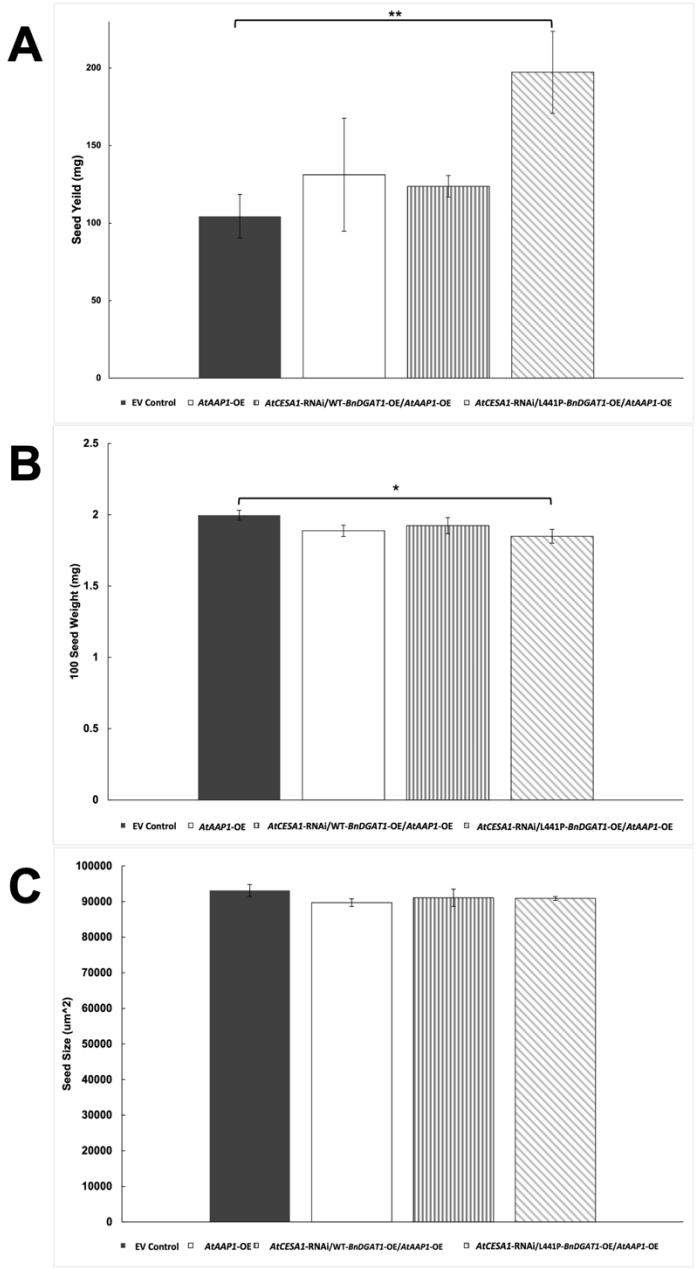

Figure 3.4.17 Seed yield (mg), 100-seed weight (mg), and seed size (μm^2) of T$_3$ *AtCESA1*-RNAi/*BnDGAT1*-OE/*AtAAP1*-OE lines

Averages are displayed for EV control, *AtAAP1*-OE, and *AtCESA1*-RNAi/*BnDGAT1*-OE/*AtAAP1*-OE lines with 9, 5, and 10 biological replicates each. Yield represents the total mass of seed produced and collected from a single mature plant. The 100-seed weights and seed sizes have been multiplied by 50 and divided by 1000, respectively, to accommodate display on a single y-axis. Bars denote standard error and significant differences are designated by asterisks ($P \leq 0.05$ = *, $P \leq 0.01$ = **).

Seed yield increased by 26% in the lines with *AtALAAT1*-OE alone compared to the EV controls but was not statistically significant, whereas the *AtCESA1*-RNAi/*BnDGAT1*-OE/*AtALAAT1*-OE lines saw a significant yield increase of nearly 60% (Fig. 3.4.18A). No significant differences were found between the 100 seed weights and seed sizes in any of the comparisons (Fig. 3.4.18B and C).

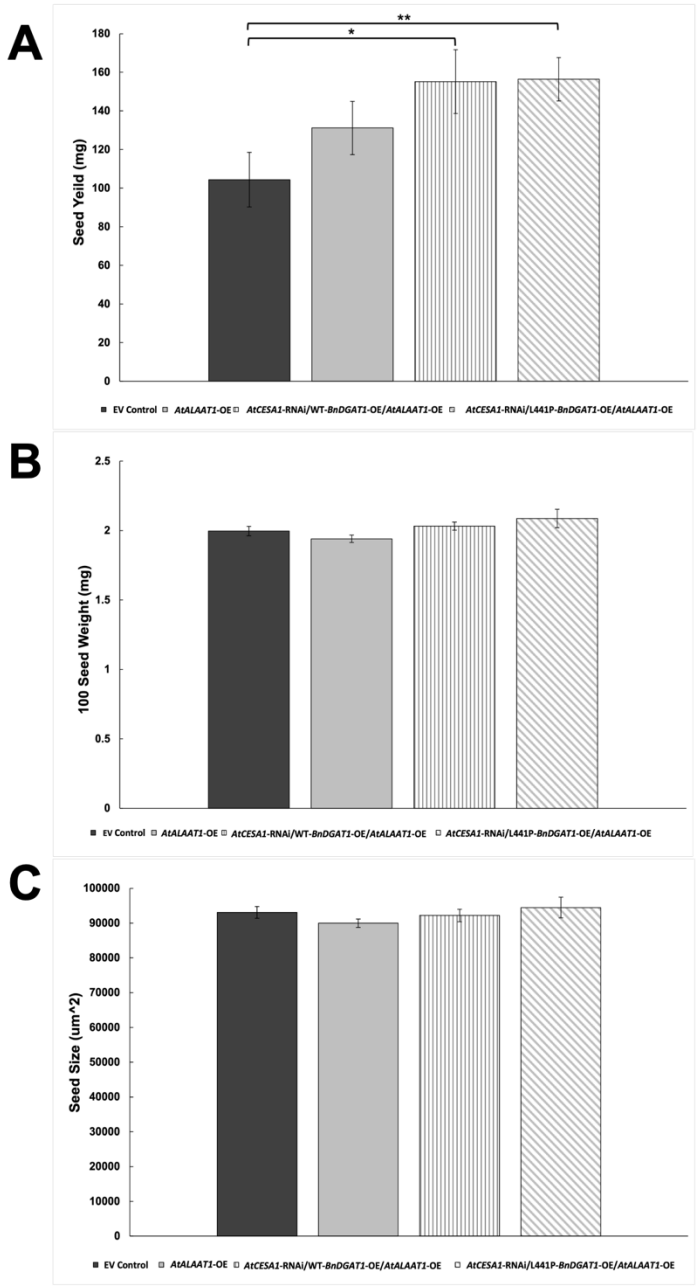

Figure 3.4.18 Seed yield (mg), 100-seed weight (mg), and seed size (μm^2) of T$_3$ *AtCESA1*-RNAi/*BnDGAT1*-OE/*AtALAAT1*-OE lines
Averages are displayed for EV control, *AtALAAT1*-OE, and *AtCESA1*-RNAi/*BnDGAT1*-OE/*AtALAAT1*-OE lines with 9, 9, and 12 biological replicates each. Yield represents the total mass of seed produced and collected from a single mature plant. The 100-seed weights and seed sizes have been multiplied by 50 and divided by 1000, respectively, to accommodate display on a single y-axis. Bars denote standard error and significant differences are designated by asterisks ($P \leq 0.05$ = *, $P \leq 0.01$ = **).

Seed yield increased for all three groups with *AtASN1*-OE, though only increase was statistically significant only in the *AtCESA1*-RNAi/L441P-*BnDGAT1*-OE background (Fig. 3.4.19A). The 100 seed weights and seed sizes of the *AtASN1*-OE alone and *AtCESA1*-RNAi/WT-*BnDGAT1*-OE/*AtASN1*-OE lines slightly decreased compared to the controls, though this was only significant for the latter comparison (Fig. 3.4.19B & C).

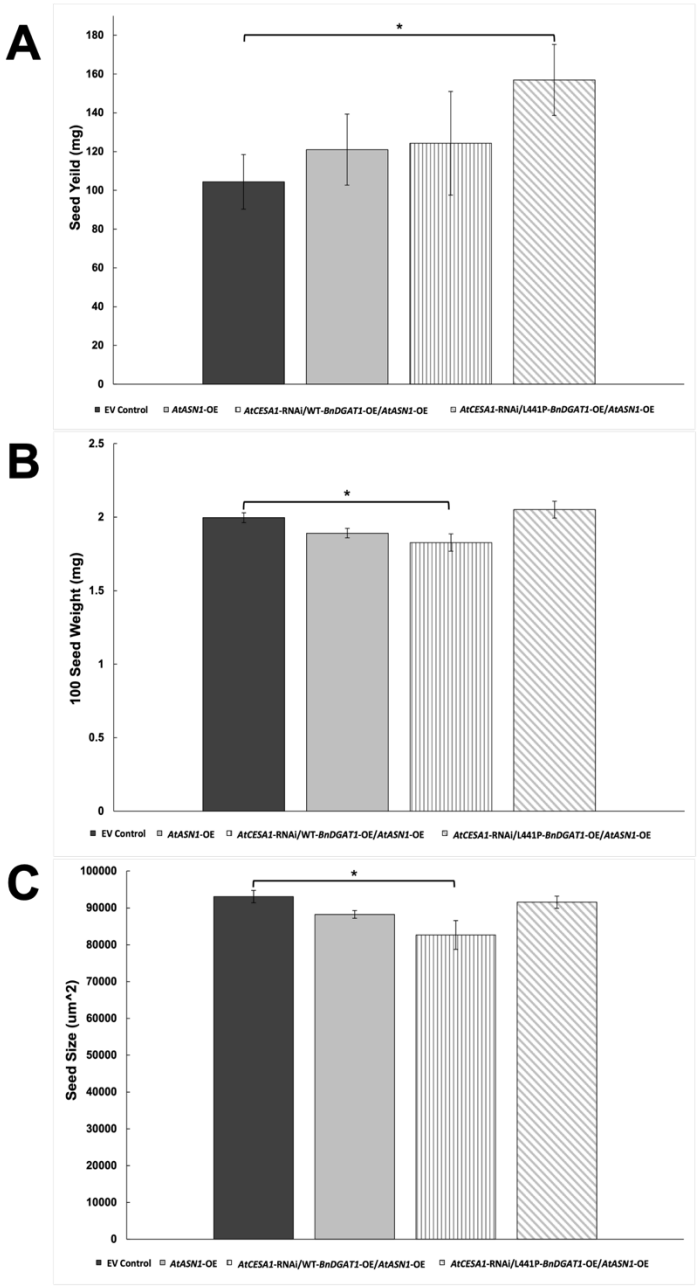

Figure 3.4.19 Seed yield (mg), 100-seed weight (mg), and seed size (μm^2) of T$_3$ *AtCESA1*-RNAi/*BnDGAT1*-OE/*AtASN1*-OE lines

Averages are displayed for EV control, *AtASN1*-OE, and *AtCESA1*-RNAi/*BnDGAT1*-OE/*AtASN1*-OE lines with 9, 6, and 11 biological replicates each. Yield represents the total mass of seed produced and collected from a single mature plant. The 100-seed weights and seed sizes have been multiplied by 50 and divided by 1000, respectively, to accommodate display on a single y-axis. Bars denote standard error and significant differences are designated by asterisks ($P \leq 0.05$ = *).

3.4.11 Seed Coat Permeability

A tetrazolium violet uptake assay was performed to evaluate the permeability of the seeds. Incubation of the seeds in the tetrazolium violet solution revealed that violet coloration was generally increased in the lines with *AtCESA1*-RNAi (Fig. 3.4.20B) compared to the EV controls (Fig. 3.4.20A). The EV control seeds exhibited a small amount of violet coloration mostly restricted to the micropylar region, whereas the seeds with *AtCESA1*-RNAi/exhibited substantially greater violet coloration, with the dye often spreading throughout the seed body (Fig. 3.4.20). Limited violet coloration appeared after 24 hours of imbibition in the dye solution, with modestly discernable differences between the control and transgenics lines (data now shown); by 44 hours, clear differences in dye permeation between the groups were observed.

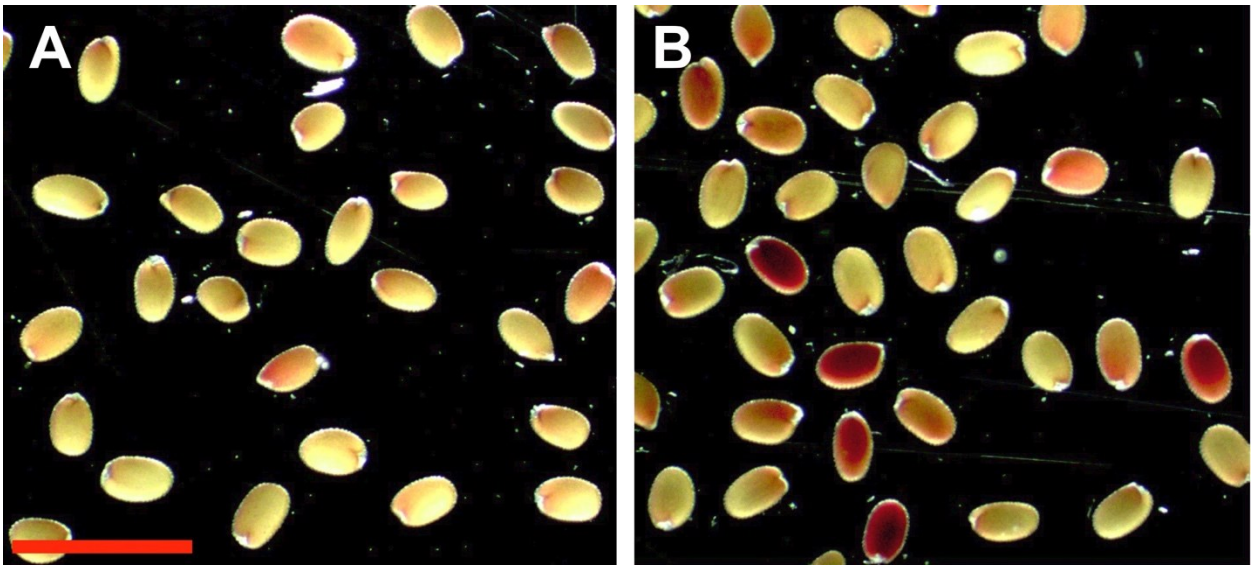

Figure 3.4.20 Permeability of EV control and T_3 *AtCESA1*-RNAi seeds to tetrazolium salt
EV control (A) and seeds with AtCESA1-RNAi (B) were imbibed in a 1% (w/v) aqueous solution of tetrazolium violet and imaged under a dissecting microscope after 44 hours. Representative photos are shown. Scale bar = 1.5mm.

3.4.12 Seedling Fresh Weight

EV Control and *AtCESA1*-RNAi/*BnDGAT1*-OE/Protein Gene-OE seeds were grown to evaluate differences in seedling fresh weight. After 12 days of growth, the average fresh weight of the transgenic carbon reallocated seedlings was smaller (from 10-60%) than the average EV control seedling fresh weight (Fig. 3.4.21).

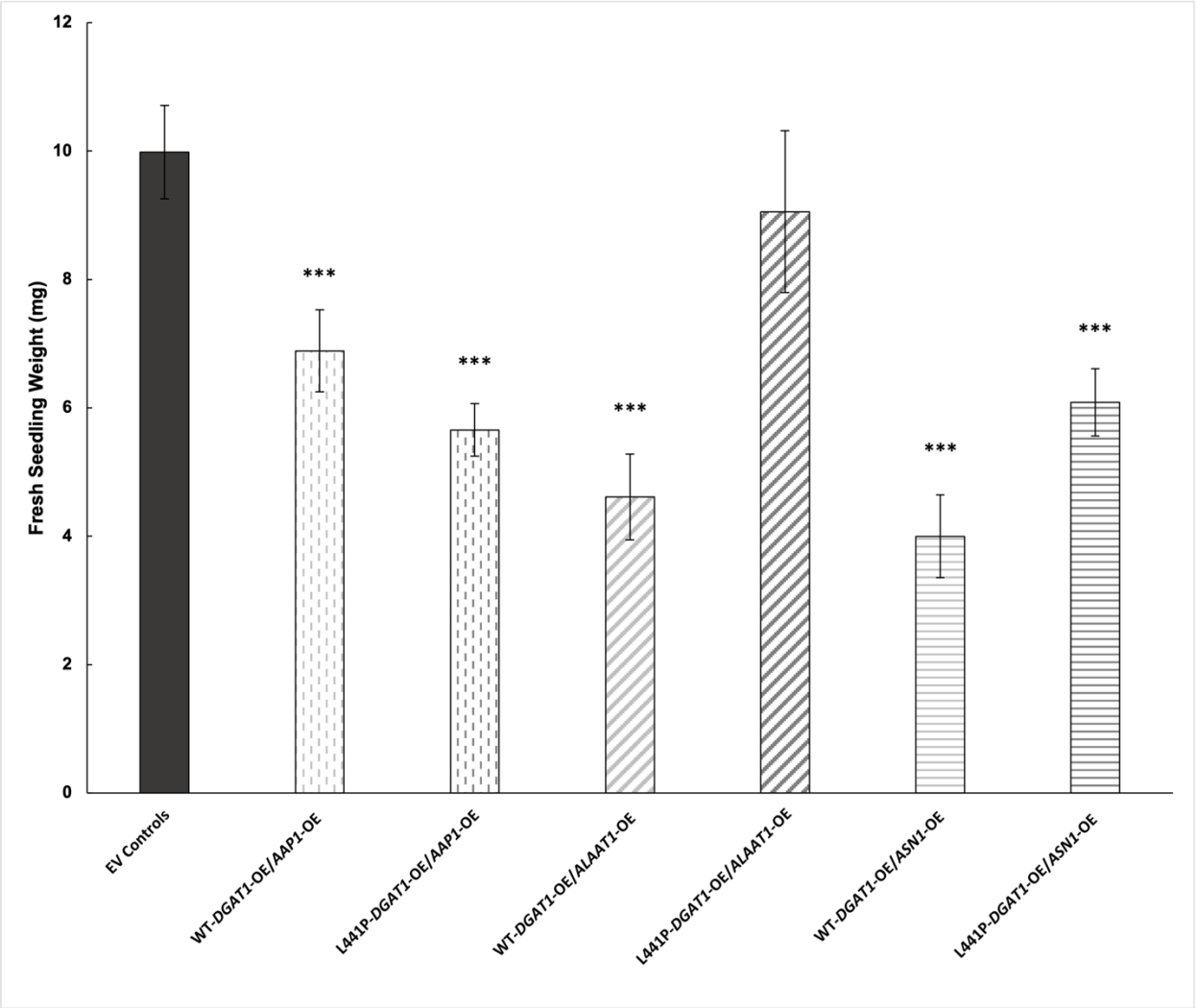

Figure 3.4.21 Seedling fresh weight of empty vector control and T_3 *AtCESA1*-RNAi/*BnDGAT1*-OE/Protein Gene-OE lines
Plants were grown on potting soil under fluorescent grow lights at 22°C for 12 days after germination. Averages are shown for 5 and 14 independent control and transgenic lines,

respectively, with 2-8 biological replicates each. Bars denote standard error. Significant differences are designated by asterisks ($P \leq 0.05$ = *, $P \leq 0.01$ = **, $P \leq 0.001$= ***).

3.4.13 Seedling Hypocotyl Length

The hypocotyl lengths of EV control and *AtCESA1*-RNAi/*BnDGAT1*-OE/Protein Gene-OE lines were assessed by growing seeds vertically on agar plates in the dark. After 6 days of etiolation, the average hypocotyl lengths were substantially shorter (4.5 mm or -26%) than the EV controls for several transgenic lines (Fig. 3.4.22). The reduced hypocotyl length phenotype was mildest in the lines with *AtAAP1*-OE. Interestingly, several *AtCESA1*-RNAi/*BnDGAT1*-OE/Protein Gene-OE lines exhibited large to extreme reductions in germination under the dark-grown condition, a phenomenon that was not observed in the germination, root length, and fresh seedling weight experiments, all of which were performed under light conditions.

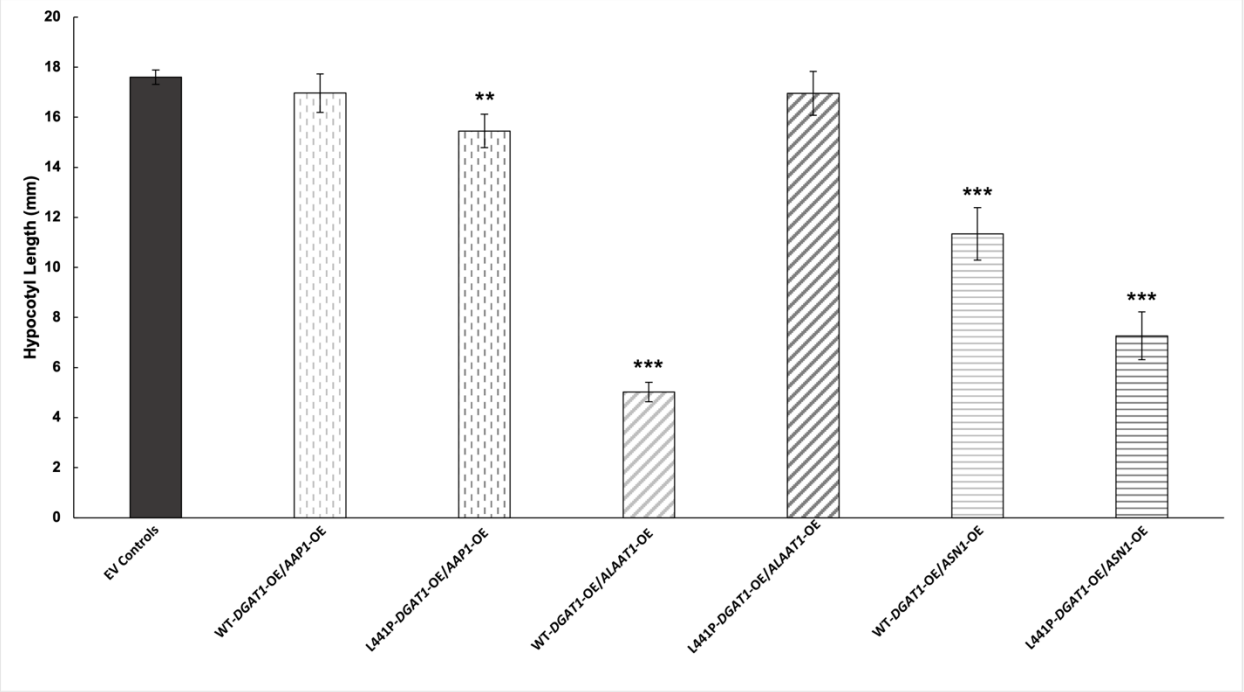

Figure 3.4.22 Hypocotyl length of etiolated empty vector control and T_3 *AtCESA1*-RNAi/*BnDGAT1*-OE/Protein Gene-OE lines

Seeds were imbibed for 2 days at 4°C, followed by 2 hours under fluorescent grow lights to synchronize germination. Plates were then wrapped in tinfoil and placed in a dark cabinet at 22°C for 6 days to allow etiolation. Averages are shown for 3 and 9 independent control and transgenic lines, respectively, with 2-8 biological replicates each. Bars denote standard error. Significant differences are designated by asterisks ($P \leq 0.05$ = *, $P \leq 0.01$ = **, $P \leq 0.001$= ***).

3.4.14 Germination Rate

A germination test was performed to determine whether there were differences in seed viability between the EV control and *AtCESA1*-RNAi/*BnDGAT1*-OE/Protein Gene-OE lines. Slightly reduced germination was observed in the *AtCESA1*-RNAi/*BnDGAT1*-OE/*AtAAP1*-OE (approximately -7%) and *AtCESA1*-RNAi/*BnDGAT1*-OE/*AtALAAT1*-OE (approximately -12%) lines compared to the EV controls (Fig. 3.4.23). There was also s reduction in germination in the *AtCESA1*-RNAi/L441P-*BnDGAT1*-OE/*AtASN1*-OE lines, though no negative effect was observed in the *AtCESA1*-RNAi/WT-*BnDGAT1*-OE/*AtASN1*-OE seeds (Fig. 3.4.23).

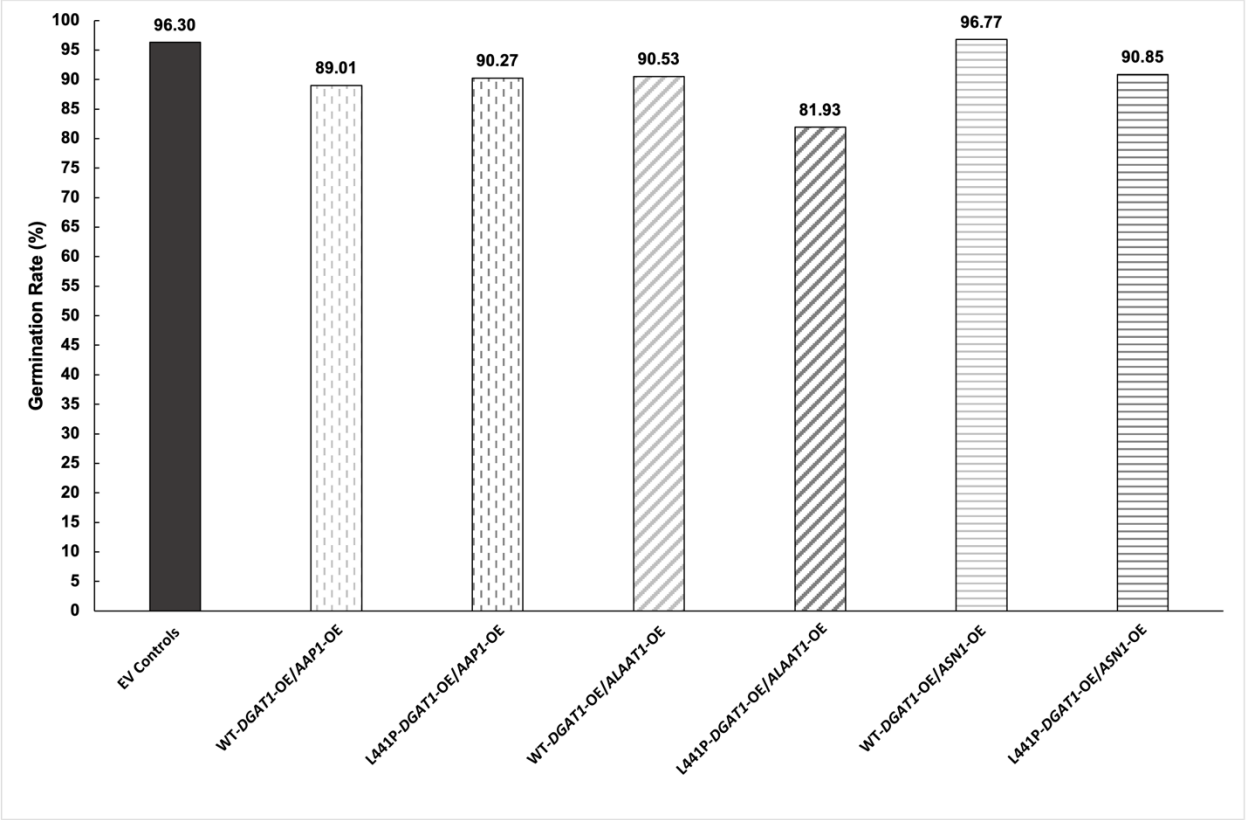

Figure 3.4.23 Percent germination of EV control and T$_3$ *AtCESA1*-RNAi/*BnDGAT1*-OE/Protein Gene-OE lines
Approximately 90 were used for each line and grown for 6 days under fluorescent lights at 25°C.

During the germination tests, somewhat delayed germination was reported in most of the *AtCESA1*-RNAi/*BnDGAT1*-OE/Protein Gene-OE lines. In general, germination and initial seedling growth appeared about 1-2 days slower than the EV controls. This can be observed in the reduced emergence, expansion, and greening of the cotyledons in the transgenic lines (Fig. 3.4.24B) relative to the EV controls (Fig. 3.4.24A).

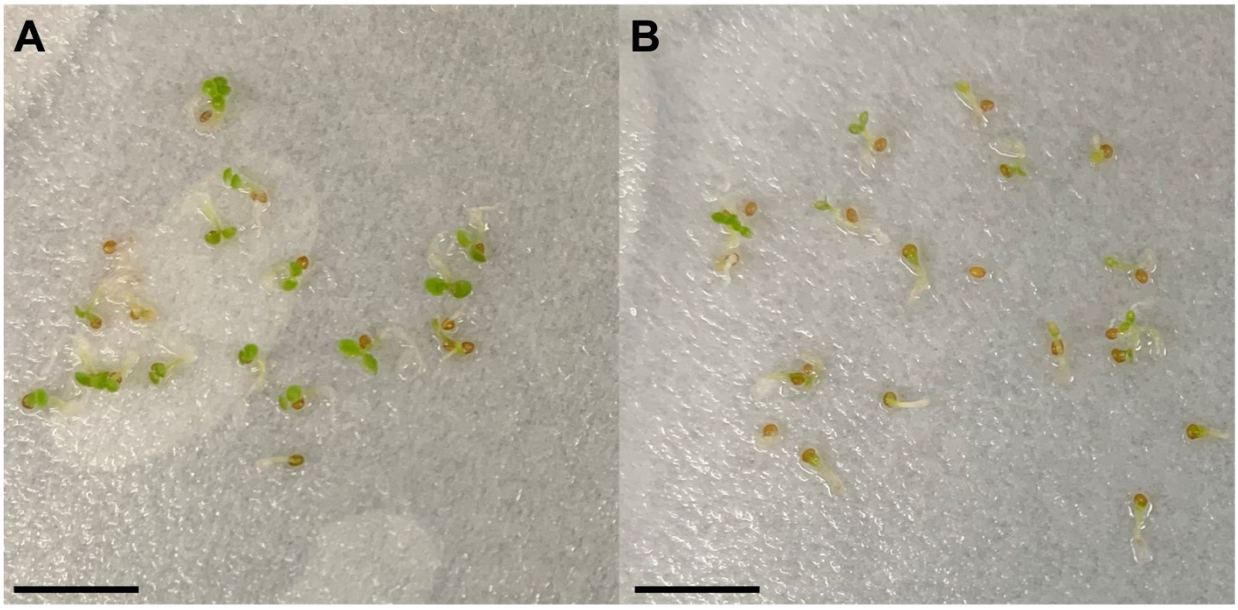

Figure 3.4.24 Delayed germination in T$_3$ *AtCESA1*-RNAi/*BnDGAT1*-OE/Protein Gene-OE seeds
EV control seedlings (a) and representative AtCESA1-RNAi/BnDGAT1-OE/Protein Gene-OE seeds. Scale bars represents 5 mm.

3.4.15 Seedling Root Length

The root lengths of EV control and *AtCESA1*-RNAi/*BnDGAT1*-OE/Protein Gene-OE lines were assessed by growing seeds vertically on agar plates under grow lights. Root lengths were recorded after 6, 8, and 10 days of growth under light conditions. The root lengths of the *AtCESA1*-RNAi/*BnDGAT1*-OE/*AtAAP1*-OE lines were slightly shorter than the EV controls only after 10 days (Fig. 3.4.25, 3.4.26a, 3.4.26b). There were more severe reductions in root lengths in both the *AtCESA1*-RNAi/*BnDGAT1*-OE/*AtASN1*-OE and *AtCESA1*-RNAi/*BnDGAT1*-OE/*AtALAAT1*-OE lines at all three timepoints, though the phenotype was most severe in the *AtCESA1*-RNAi/*BnDGAT1*-OE/*AtASN1*-OE lines at all timepoints (Fig. 3.4.25, 3.4.26c, 3.4.26d).

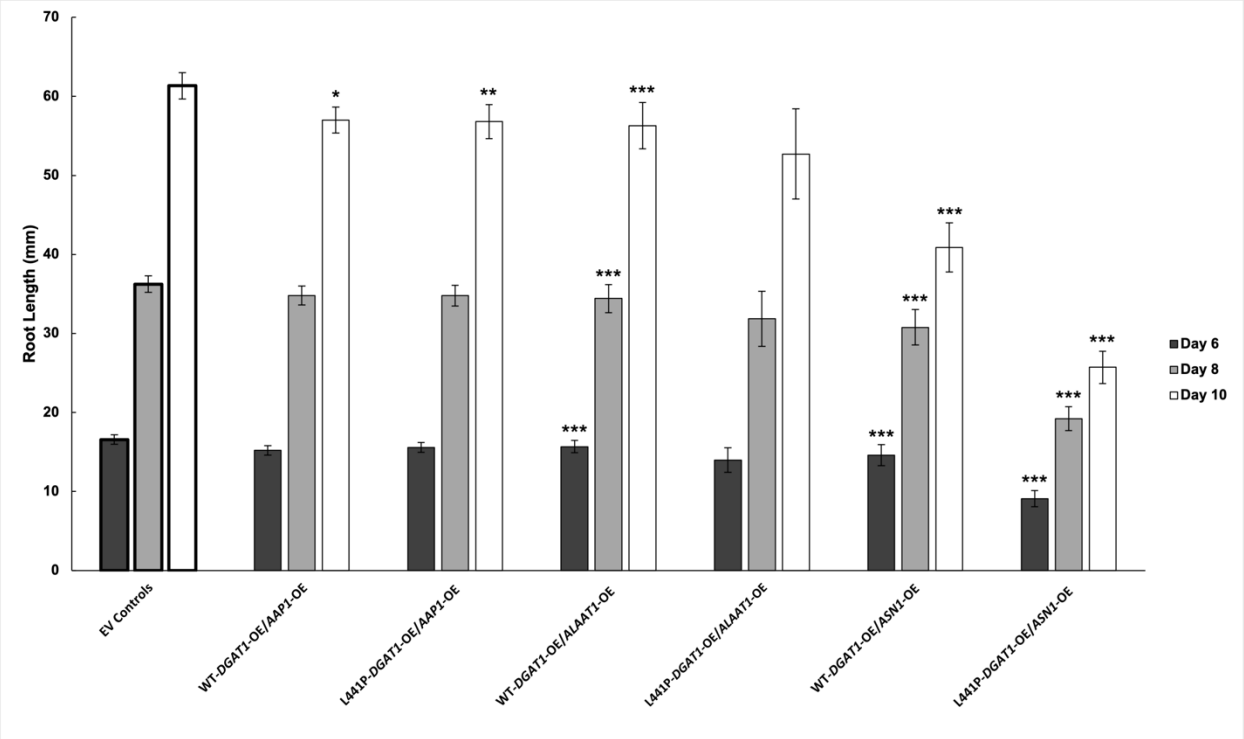

Figure 3.4.25 Average root lengths (mm) of EV control and T$_3$ *AtCESA1*-RNAi/*BnDGAT1*-OE/Protein Gene-OE lines

About 10-12 seeds were used from each line, in triplicate, and grown under fluorescent lights at 25°C. Root lengths were measured at 6, 8, and 10 days after the stratification treatment. Bars denote standard error. Significant differences are designated by asterisks ($P \leq 0.05$ = *, $P \leq 0.01$ = **, $P \leq 0.001$= ***).

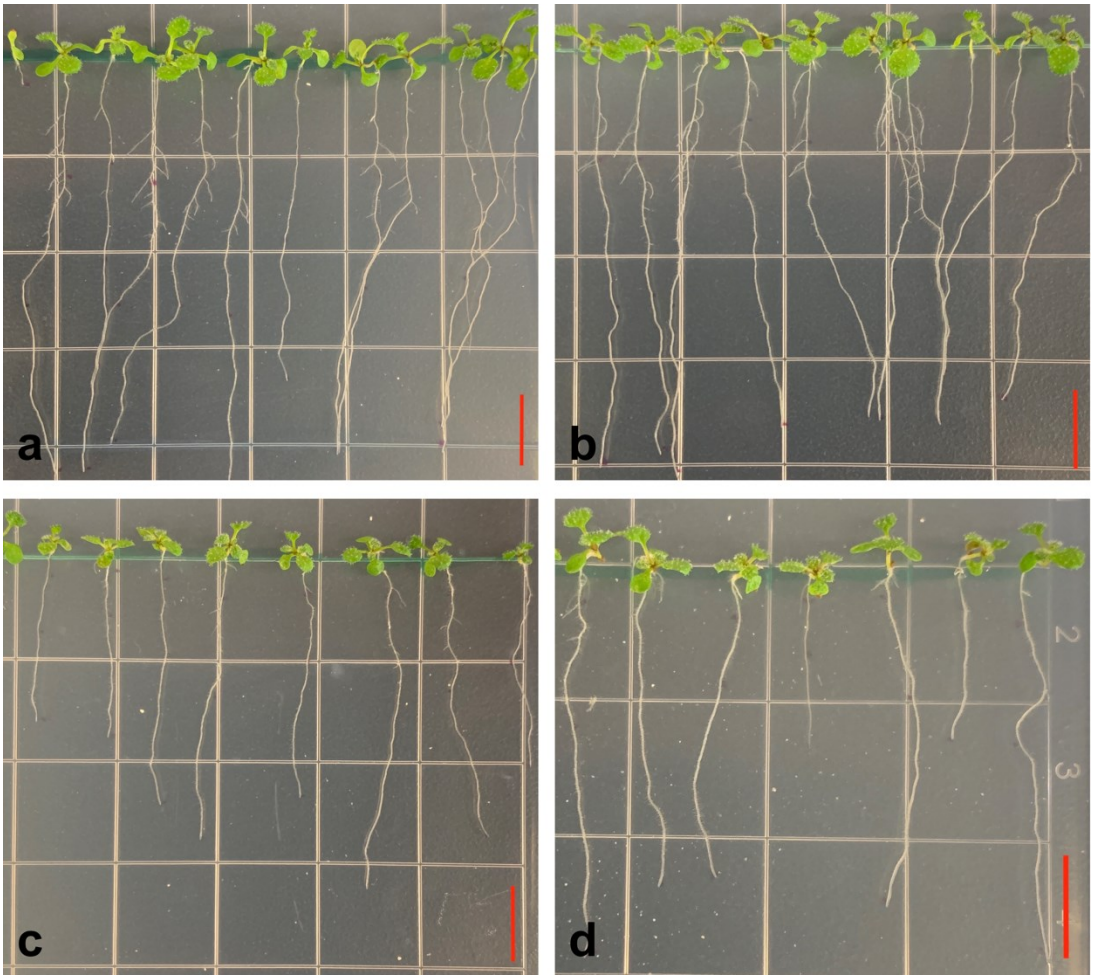

Figure 3.4.26 Representative seedling growth of EV control and T_3 *AtCESA1*-RNAi/*BnDGAT1*-OE/Protein Gene-OE lines
EV control seedlings (a), *AtCESA1*-RNAi/*BnDGAT1*-OE/*AtAAP1*-OE (b), *AtCESA1*-RNAi/*BnDGAT1*-OE/*AtASN1*-OE (c), and *AtCESA1*-RNAi/*BnDGAT1*-OE/*AtALAAT1*-OE (d). 10-12 seeds were used from each line, in triplicate, and grown under fluorescent lights at 25°C. Scale bars represent 1 cm.

3.4.16 Plant Growth & Development

Despite some phenotypic differences in the *AtCESA1*-RNAi/*BnDGAT1*-OE/Protein Gene-OE lines during early seedling growth, these differences did not seem to carry through into later development. During the growth of the T_3 generation, no clear differences emerged in terms of the mature rosettes, flowering time, inflorescence height, inflorescence branching, flower and silique morphology, pigmentation, and no other phenotypic abnormalities were observed (data

not shown). Representative seedling growth for the T_3 *AtCESA1*-RNAi/*BnDGAT1*-OE/Protein Gene-OE plants is shown in Figure 3.4.27.

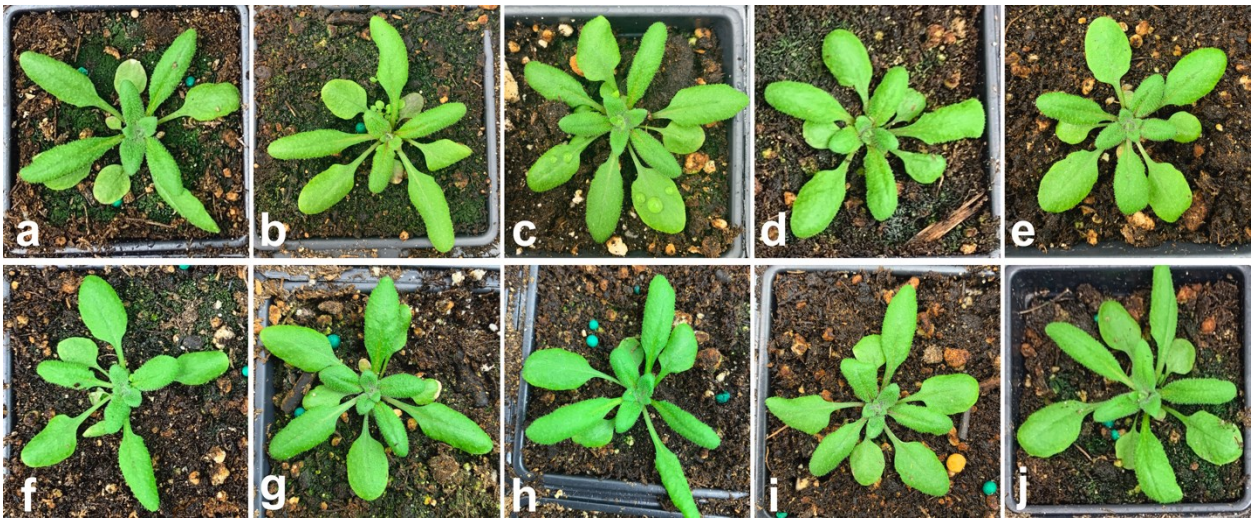

Figure 3.4.27 Representative growth of EV control and T_3 *AtCESA1*-RNAi/*BnDGAT1*-OE/Protein Gene-OE lines
EV control seedlings (a), *AtAAP1*-OE (b), *AtCESA1*-RNAi/WT-*BnDGAT1*-OE/*AtAAP1*-OE (c), and *AtCESA1*-RNAi/L441P-*BnDGAT1*-OE/*AtAAP1*-OE (d), *AtALAAT1*-OE (e), *AtCESA1*-RNAi/WT-*BnDGAT1*-OE/*AtALAAT1*-OE (f), and *AtCESA1*-RNAi/L441P-*BnDGAT1*-OE/*AtALAAT1*-OE (g), *AtASN1*-OE (h), *AtCESA1*-RNAi/WT-*BnDGAT1*-OE/ *AtASN1*-OE (i), and *AtCESA1*-RNAi/L441P-*BnDGAT1*-OE/ *AtASN1*-OE (j). 32 plants from each from each line were grown in a growth cabinet under standard conditions (22°C/18°C, 16hr light/18hr dark).

3.5 Discussion

The leftover meal from oilseeds provides a valuable feed source for animals, especially those with high protein contents. There has been increased research interest in recent years to reduce the fiber content of canola meal to enhance the digestibility of the seed protein for non-ruminant animals, as well as increase the amount of seed protein itself (Hansen et al., 2017; Tan et al., 2011). There is competition for carbon resources between biosynthetic pathways for cellulose, storage lipids, and storage proteins in seeds (Kambhampati et al., 2020; Li et al., 2018B; Liu et al., 2022), though the relationships between these pathways are not well

understood. Manipulation of the flow of carbon resources between these pathways is an emerging area of study (Jayawardhane et al., 2020) and we attempt to expand our understanding of this area through genetic engineering of *Arabidopsis* seeds. Reducing seed cellulose to liberate carbon for use by protein and lipid biosynthesis is a key aspect of this work (Jayawardhane et al., 2020).

The crystalline cellulose analysis found an average reduction in cellulose content by about -21% across all lines with *AtCESA1*-RNAi, compared to the non-*AtCESA1*-RNAi lines (Fig. 3.4.16), which suggests reduced resource allocation to cellulose biosynthesis. However, previous studies on the disruption of cellulose biosynthesis have reported a range of phenotypic abnormalities (Arioli et al., 1998; Beeckman et al., 2002; Persson et al., 2007; Zhang et al., 2022), even when only partially reduced through RNAi (Jayawardhane et al., 2020). Accordingly, we performed several seedling morphological and seed histochemical analyses to evaluate whether changes in early growth and development occurred due in response to the genetic manipulations. The increased tetrazolium violet staining in the *AtCESA1*-RNAi/*BnDGAT1*-OE/Protein Gene-OE seeds suggests increased seed coat permeability (Fig. 3.4.20), consistent with previous observations in *AtCESA1*-RNAi seeds (Jayawardhane et al., 2020). This provides evidence, in addition to the seed cellulose quantification, that the seed cellulose is decreased, likely manifested as thinner seed coats, in the transgenic lines.

Given that reduced cellulose biosynthesis in the seed may decrease the size of the embryo, I assessed the fresh seedling weights of the *Arabidopsis* lines. The significant decrease in the fresh seedling weights of all *AtCESA1*-RNAi/*BnDGAT1*-OE/Protein Gene-OE lines is a clear negative phenotype in the transgenic lines (Fig. 3.4.21). This phenotype may be explained by reduce embryo size due to *AtCESA1*-RNAi; alternatively, or perhaps in conjunction, the

slightly smaller transgenic seedlings may simply have been 1-2 days behind the EV controls in terms of growth and development due to slightly delayed seed germination (Figure 3.4.24. The latter may provide a more compelling explanation, given that reducing the seed cellulose content did not significantly reduce the 100 seed weights or seed sizes in any of the lines (Fig. 3.4.17-19). Microscopic analyses of the seed cell wall and embryo structures could provide further answers here, but such analyses were left for future research.

As with the fresh seedling weight, the seedling root and etiolated hypocotyl lengths were reduced in all *AtCESA1*-RNAi/*BnDGAT1*-OE/Protein Gene-OE lines (Fig. 3.4.25, Fig. 3.4.22), further suggesting a small but real negative effect on growth and development in the transgenic seedlings. These observations are also consistent with the early growth phenotypes of seedlings with *AtCESA1*-RNAi (Jayawardhane et al., 2020) and AtCESA1 phosphorylation mutants (Zhang et al., 2022). The reduced root and hypocotyl elongation may be functions of reduced embryo size in the transgenic lines and may partially explain reduced seedling fresh weight after 12 days of growth, though the slight delay in germination could also provide explanatory power here.

Seed cell walls play an important role in permeation of water into the embryo, thereby influencing the subsequent initiation of germination (Ezquer et al., 2016). Thus, altering seed properties, especially cell walls and the seed coat, may impact germination. There was an across-the-board decrease in germination rate of the transgenic seeds for all gene combinations, compared to the EV controls (Fig. 3.4.23), though the finding was not significant for the *AtCESA1*-RNAi/*BnDGAT1*-OE/*AtASN1*-OE seeds. These small but real decreases in germination rates were not observed in other studies involving *AtCESA1* (Jayawardhane et al., 2020; Zhang et al., 2022); thus, there may be a seed viability impact associated with manipulation of seed

storage reserves by *BnDGAT1*, *AtAAP1*, or *AtALAAT1*. Although seed storage lipids and proteins are useful to the embryo in terms of providing sustenance upon germination, there may perhaps be a limit to increasing these substances beyond which the embryo structure and viability is negatively impacted. The transgenic lines also exhibited somewhat delayed germination (Fig. 3.4.24), closely mirroring the delayed germination observed in *AtCESA1* phosphorylation mutants (Zhang et al., 2022). The emergence of the embryo radicle and cotyledon opening occurred about 1-2 days after the controls. This delay in germination may explain some of the reduced seedling fresh weight (Fig. 3.4.21), root length (Fig. 3.4.25), and hypocotyl length (Fig. 3.4.22), rather than reduced embryo size from *AtCESA1*-RNAi alone. Delayed germination could result from slower uptake of water, which itself may be a function of greater deposition of hydrophobic phenolic compounds (e.g. lignin), callose, cutin, or slower breakdown of these permeability-reducing seed coat components (Bhalla & Slattery, 1984; Serrato-Valenti & Modenesi, 1990; Kelly et al., 1992; Debeaujon et al., 2007; Smykal et al., 2014). However, the tetrazolium violet assay (Fig. 3.4.20) revealed increased seed coat permeability in the *AtCESA1*-RNAi lines, which contradicts the notion that increased seed coat hydrophobicity is involved in the observed germination delay. Alternatively, it is possible that synthesis of proanthocyanidins, which promote seed dormancy via abscisic acid signalling, may be associated with the observed germination delay (Jia et al., 2012A; Gao et al., 2018; Shah et al., 2018; Zhao et al., 2019C; Zhang et al., 2022; Zhao et al., 2022). Differences in the seed color may indicate changes in proanthocyanidins pigment levels (Zhang et al., 2022), though there were no apparent differences in seed color between EV control and *AtCESA1*-RNAi lines (Fig. 3.4.20). Although intriguing, this hypothesis was considered out of scope and was not investigated further. If a connection indeed exists between AtCESA1 and proanthocyanidins biosynthesis/ABA

signalling, the nature of the relationship is unclear. More in-depth research is needed to determine specific cell wall compositional changes in related to *AtCESA1*-RNAi, such as measurement of seed phenolics content, microscopy analysis to evaluate anatomical changes in the seeds, and determination of the relationship to pigments (such as proanthocyanidins) in the seed coat.

Accumulation of SSPs is vital for developing seeds as they provide the key source of nitrogen to fuel seedling growth upon germination. In the case of oilseed crops, such as canola, the protein- and fiber-rich seed meal left over from oil extraction provides a nutritious animal feed (Bell, 1984; Joehnke et al., 2018; Lannuzel et al., 2022). The nutritional and economic potential of seed protein has driven research interest in enhancing the protein fraction of the meal (Jayawardhane et al., 2020; Jia et al., 2012B; Slominski, 1997). We sought to increase seed protein content by drawing carbon into SSP biosynthesis through overexpression of three genes that encode proteins related to SSP biosynthesis, thereby increasing the carbon sink strength of the seeds. *AtAAP1*, *AtALAAT1*, and *AtASN1* contribute to AA biosynthesis and transport. These genes were chosen for overexpression in the *AtCESA1*-RNAi/*BnDGAT1*-OE background because previous studies have associated them with increased seed protein and nitrogen contents (Sanders et al., 2009; Lam et al., 2003; McAllister & Good, 2015). When overexpressed in the WT background, *AtAAP1* and *AtALAAT1* resulted in significantly increased seed protein accumulation, whereas protein decreased in the *AtASN1*-OE lines (Fig. 3.4.13-3.4.15), suggesting that *AtAAP1* and *AtALAAT1* would serve as the best candidates to test the ability of seed carbon reallocation (*AtCESA1*-RNAi/L441P-*BnDGAT1*-OE) for increasing seed protein content in crop seeds. In the carbon reallocated background, the seed protein contents increased significantly over both the EV controls and the WT lines overexpressing *AtAAP1*, *AtALAAT1*, or

AtASN1 alone (Fig. 3.4.13-3.4.15). The data demonstrate that manipulation of the flow of seed carbon away from cellulose biosynthesis (through *AtCESA1*-RNAi) towards lipid biosynthesis (*BnDGAT1*-OE) and storage protein biosynthesis (*AtAAP1*, *AtALAAT1*, or *AtASN1*) is a viable strategy for increasing seed protein content beyond the level achieved by *AtAAP1*, *AtALAAT1*, or *AtASN1* overexpression alone. *AtASN1*-OE was the least effective of the three protein-related genes at increasing protein content. AtASN1 contributes to AA synthesis, whereas AtAAP1 and AtALAAT1 are involved in AA transport, which may suggest that enhancing transport of AAs within the seed is more effective for increasing SSP biosynthesis than increasing the biosynthesis of AAs within the seed. However, the seed protein contents were significantly higher in the carbon reallocated lines with *AtASN1*-OE than without (Fig. 3.4.15), which further suggests that carbon reallocation through *AtCESA1*-RNAi and *BnDGAT1*-OE is an effective means of bolstering protein content, even when the chosen protein-related gene is ineffective by itself. With all three gene stacking approaches, the protein contents increased the most in the lines overexpressing the L441P variant of *BnDGAT1* (Fig 3.4.13-15), suggesting that although differences in lipid contents between WT and variant *BnDGAT1*-OE were not detectable, there may be some positive effect of the performance enhanced variant conferred on SSP accumulation.

Canola seed meal protein has a nutritious AA profile, with potential for human consumption (Anwar et al., 2015). Because we overexpressed genes that affected SSP biosynthesis, we accordingly evaluated whether the overexpression of these genes impacted the seed AA composition. Surprisingly, almost no changes in seed AA composition were detected in any of the transgenic lines, with only a handful of very minor but statistically significant changes in AA levels (Table 3.4.6). This suggests that the overall content of SSPs can be increased

without necessarily altering the AA composition. A possible explanation of the lack of change in the AA profile is that the biosynthesis of SSPs themselves (in *Arabidopsis*, mostly cruciferins and napins) operates independently of the dynamics of internal seed AA transport, even when *AtAAP1*, *AtALAAT1*, and *AtASN1* are overexpressed in the seeds.

When attempting to increase seed protein accumulation, it is important to consider potential trade-offs, given that seed lipid biosynthesis often competes with protein biosynthesis for carbon resources (Grami et al., 1977; Katepa-Mupondwa et al., 2005; Kambhampati et al., 2020). In an effort to neutralize the small, negative effect of *AtCESA1*-RNAi down-regulation on lipid content (reported by Jayawardhane et al., 2020), we chose to overexpress *BnDGAT1* to pull carbon resources towards storage lipid biosynthesis. The seed lipid analysis of the homozygous T_3 *AtCESA1*-RNAi/*BnDGAT1*-OE revealed that, overall, the lipid content was restored to slightly above WT levels in the transgenics lines (Fig. 3.4.2). This confirms that *BnDGAT1*-OE fulfills the intended purpose of restoring the seed lipid content and counteracting the lipid-reducing effect of *AtCESA1*-RNAi, likely by drawing carbon towards the TAG biosynthesis pathway and increasing the carbon sink strength of the seed. Similar changes in seed FA composition were observed between the T_2 and T_3 generations, with a sizeable decline in 18:3 abundance again associated with the L441P-*BnDGAT1* variant (Tables 3.4.1-2). As with the selected T_2 lines, the small increases in 18:1 and 18:2, and decrease in 20:1 suggest that the specific FA preferences of BnDGAT1 lead to altered FA abundances in the transgenic seeds. However, given that previous work has shown BnDGAT1's preference for 18:1 (Aznar-Moreno et al., 2015), it is curious that the 18:1 abundance did not increase further.

Comparison of the lines overexpressing WT and *BnDGAT1* variants found that the S112R variant did not out-perform the WT in terms of increasing oil accumulation, while the

L441P variant significantly outperformed both WT and S112R BnDGAT1 (Fig. 3.4.3). This suggests that the superior TAG-synthesizing ability of the L441P-BnDGAT1 variant observed in yeast is strong enough to be detected *in planta* (Chen et al., 2017; Xu et al., 2017). Although modest, this finding suggests that protein engineering may be a viable strategy to push the limits on increasing seed lipid accumulation. These findings, in tandem with the seed protein contents, illustrate that seed lipid accumulation can at least be increased back to WT levels while simultaneously increasing seed protein content (Fig. 3.4.2, Fig. 3.4.4). This is especially notable given the general finding that there is a trade-off between lipid and protein content in seeds. It should again be noted that the SSP contents of the carbon reallocated lines increased the most in seeds overexpressing the L441P-*BnDGAT1* variant, independent of which protein-related gene was being overexpressed (Fig. 3.4.13-15), suggesting some possible positive effect of the performance enhanced variant on protein synthesis.

Seed lipid analysis of the T_3 *AtCESA1*-RNAi/*BnDGAT1*-OE overexpressing the protein-related genes offered similarly positive findings. The analysis revealed that *AtAAP1*-OE alone has a significant negative effect on lipid accumulation (about -5%) compared to the EV controls (Fig. 3.4.10), which is consistent with the general finding that increasing seed protein results in a trade-off with seed oil content. Overexpression of *AtALAAT1* and *AtASN1* alone did not negatively impact seed lipid accumulation (Fig. 3.4.11, Fig. 3.4.12). The seed lipid contents in all the *AtCESA1*-RNAi/*BnDGAT1*-OE/Protein Gene-OE backgrounds were not lower than the EV controls (Fig. 3.4.10-12), demonstrating that *BnDGAT1*-OE continues to be effective at negating the lipid-reducing effect of *AtCESA1*-RNAi, independent of which protein biosynthesis-related gene is being overexpressed. Interestingly, when *AtAAP1* is overexpressed in the *AtCESA1*-RNAi/*BnDGAT1*-OE background, the lipid content instead increased (+1.2%) (Fig. 3.4.10),

suggesting that some genes may be for effective at overcoming the general rule of mutual exclusion between increasing seed lipid and protein contents simultaneously. These results demonstrate that *BnDGAT1*-OE continues to be an effective approach for resisting decreases in seed lipid content incurred by *AtCESA1*-RNAi. Unfortunately, the superior lipid-increasing effect of the L441P variant of *BnDGAT1* was no longer observed once the protein-related genes were overexpressed (Fig. 3.4.10-12).

The FA compositional changes in the *AtCESA1*-RNAi/*BnDGAT1*-OE/*AtAAP1*-OE were consistent with the T_2 and T_3 *AtCESA1*-RNAi/*BnDGAT1*-OE generations; proportions of both 18:1 and 18:2 increased, while 18:3 and 20:1 declined (Table 3.4.3). These findings suggest that *AtAAP1*-OE has minimal to no impact on FA incorporation into TAG. In contrast, several changes in FA composition in the *AtCESA1*-RNAi/*BnDGAT1*-OE/*AtALAAT1*-OE seeds were reversed compared to *AtCESA1*-RNAi/*BnDGAT1*-OE alone; 18:1 significantly decreased in the WT BnDGAT1-OE background, 18:2 was no longer increased, and 20:1 experienced an increase (Table 3.4.4). However, a decrease in 18:3 was observed, consistent with all other generations and genetic combinations. This suggests that *AtALAAT1*-OE does impact the incorporation of FAs into TAG, however the decrease in 18:3 seems to be independent of protein biosynthesis-related gene overexpression. The molecular mechanisms by which *AtALAAT1* affects seed FA composition are unclear. The FA changes in the *AtCESA1*-RNAi/*BnDGAT1*-OE/*AtASN1*-OE seeds were very similar to the *AtCESA1*-RNAi/*BnDGAT1*-OE generations, apart from decreased 18:1 in the WT *BnDGAT1*-OE background (Table 3.4.5). In all, these findings illustrate that manipulation of protein biosynthesis-related genes may influence the ultimate FA composition, though the scope and magnitude of the FA changes vary by gene.

Regarding the overall potential for seed-specific *BnDGAT1*-OE in *Arabidopsis*, the evidence suggests the gene has limited potential for raising the ceiling of seed lipid accumulation but is quite effective at raising the floor. This is evinced by the rescue of the lipid contents in the carbon-reallocated lines to wildtype levels when compared to the lines with only protein-related gene overexpression.

The seed size and 100 seed weight were both significantly increased in the seeds of the selected T_3 *AtCESA1*-RNAi/*BnDGAT1*-OE lines (Fig. 3.4.7, Fig. 3.4.8). No increase in seed size was observed in seeds with *AtCESA1*-RNAi alone (Jayawardhane et al., 2020), suggesting that *BnDGAT1* may have a secondary effect that contributes to increased seed size. The increases in both yield-related parameters bodes well for replicating this genetic approach in oilseed crops. At minimum, these findings demonstrated that the fundamental composition of *Arabidopsis* seeds can be manipulated in a deliberate and strategic manner that could increase the nutritional and economic properties of the seeds without compromising key yield metrics.

The seed yield, 100 seed weight, and seed size analysis of the *AtCESA1*-RNAi/*BnDGAT1*-OE/Protein Gene-OE lines revealed some differences in the transgenic lines. There were significant increases in total seed yield for all three of the protein-related genes when overexpressed in the *AtCESA1*-RNAi/*BnDGAT1*-OE background (Fig. 3.4.17-19), suggesting that seed carbon reallocation paired with increased seed protein may offer a promising avenue to boosting overall yield. This effect was strongest in the lines overexpressing the L441P-*BnDGAT1* variant. If replicated in crop plants, this would represent a valuable knock-on effect of increasing seed protein. However, the positive effects on seed weight and size observed in the *AtCESA1*-RNAi/*BnDGAT1*-OE lines were no longer present once the protein-related genes were overexpressed. In general, these metrics were slightly reduced in the transgenic lines compared

to the EV controls, though these changes were small and few of the reductions were statistically significant (Fig. 3.4.17-19). This contrasts with observations in *Atcesa1* phosphorylation mutants, which exhibited reduced seed weight and size (Zhang et al., 2022), perhaps suggesting that the overexpression of *BnDGAT1* and the protein biosynthesis-related genes may partially counter the negative effect on seed weight and size. The only other positive effect observed was slightly increased 100 seed weight in the *AtCESA1*-RNAi/*BnDGAT1*-OE/*AtALAAT1*-OE seeds (Fig. 3.4.18), suggesting that this genetic combination may be the most promising for increasing seed yield parameters.

In summary, we sought to manipulate the flow of carbon resources within *Arabidopsis* seeds through genetic engineering and determine the most promising gene combinations that could be replicated in major oilseed crops, such as canola. The combination of *AtCESA1*-RNAi/*BnDGAT1*-OE/*AtAAP1*-OE appears to be the most successful gene combination, given that the seed lipid and protein contents increased simultaneously, the seed yield increased slightly, and the seedling hypocotyl and root lengths experienced relatively small decreases compared to the other gene combinations. Although *AtCESA1*-RNAi/*BnDGAT1*-OE/*AtALAAT1*-OE seeds experienced the greatest increase in protein content, the germination rate decreased more than the other gene combinations and the seed lipid content was not increased above wildtype levels. For the *AtCESA1*-RNAi/*BnDGAT1*-OE/*AtASN1*-OE seeds, the protein content only increased marginally, which is the weakest observation for the most important metric in this study. Taken together, these findings demonstrate that overexpression of *AtAAP1* within the *AtCESA1*-RNAi/*BnDGAT1*-OE background leads to improved seed composition with mild negative seedling phenotypes, which represents a promising avenue for improvement in canola

seeds. However, it may be best for the results to be confirmed by growing another generation by plants and re-analyzing the seeds with a greater sample size.

4 Chapter 4 Conclusions & Future Directions

Understanding the flow of carbon resources within seeds, and how to manipulate this flow, is key to developing crops with enhanced nutritional and economic value. Canola is a highly valued oilseed crop, but the digestibility of the protein fraction of the seed meal is limited by an excess of fiber. In this work, we used genetic engineering in *Arabidopsis* seeds to redistribute carbon resources away from fiber and towards the most valuable seed components, storage lipids and proteins. We achieved this objective by reducing the seed fiber content through *AtCESA1*-RNAi downregulation, thereby liberating carbon resources that could then be reallocated towards seed lipid and protein biosynthesis through overexpression of selected genes (*BnDGAT1* for lipid; *AtAAP1*, *AtALAAT1*, and *AtASN1* for protein). We found that overexpression of *AtAAP1* in the *AtCESA1*-RNAi/*BnDGAT1*-OE background was most successful at increasing lipid and protein contents. Some modest negative seedling phenotypes were observed, including slightly reduced root length, hypocotyl length, seedling fresh weight, germination rate, as well as slightly delayed germination. There was an unexpected but welcome increase in seed yield in the lines overexpressing L441P-*BnDGAT1*, independently of which protein-related gene was overexpressed, which bodes well if replicated in oilseed crops.

One of the major analyses in this project was the quantification of seed lipid contents and FA compositions. Existing publications report a wide range of methods for plant lipid analysis, some of which are time and labor intense, consume expensive reagents, and produce excess chemical waste. Therefore, in Chapter 2, I optimized the method for a wide range of plant

species, culminating in a generalizable plant lipid analysis method: 2% sulfuric acid in methanol, 2 hours of transmethylation at 95°C reaction temperature, and grinding of dried samples with a mortar and pestle. Additionally, the results showed that convenient and easy-to-handle disposable plastic pipet tips and tubes are compatible with the reagents in this method, which dispels the convention of avoiding plastic wares in lipid analysis. This optimized method was used for analysis of the *Arabidopsis* seeds throughout this project and has been submitted for publication (currently under review).

Given the success of this carbon reallocation approach in *Arabidopsis*, we propose that this strategy should be evaluated in oilseed crops, such as canola. Additionally, the *Arabidopsis* lines bearing *AtCESA1*-RNAi/*BnDGAT1*-OE cassettes may serve as an effective background in which to accelerate the characterization of candidate genes identified in crop plants, such as those with putative involvement of storage protein biosynthesis (amino acid biosynthesis and transport, nitrogen use efficiency, transcriptional regulators, etc.), for increasing seed protein content. This will support the fast-tracked characterization of genes for developing value-added crop varieties, such as canola, with increased seed protein. Characterization of such genes has been identified as an important area of research for advancing the development of nutritious, high protein crops (Gacek et al., 2018; Le et al., 2016; McAllister et al., 2012; McAllister & Good, 2015; Meyer et al., 2012; Yang et al., 2023). However, further research is needed to understand whether the negative seedling phenotypes associated with carbon reallocation can be attenuated, as well as microscopic and cell wall composition analyses of the seeds to ascertain why these phenotypes occur. Verification of these results in another generation with a larger sample size may also be warranted. Additional protein-related genes may be identified by future experiments, such as RNA-Seq. Lastly, future studies should evaluate how effective this

approach is within crop plants and may consider approaches other than AA transportation for enhancing protein biosynthesis, such as increasing nitrogen use efficiency or enhancing transcriptional regulation of SSP genes.

References

Adhikari, N.D., Bates, P.D., and Browse, J. (2016). *WRINKLED1* rescues feedback inhibition of fatty acid synthesis in hydroxylase-expressing seeds. Plant Phys. **171**: 179–191. doi:10.1104/pp.15.01906.

AL-Amery, M., Downie, B., DeBolt, S., Crocker, M., Urschel, K., Goff, B., Teets, N., Gollihue, J., and Hildebrand, D. (2019). Proximate composition of enhanced DGAT high oil, high protein soybeans. Biocat. Ag. Biotech. **21**: 101303. doi:10.1016/j.bcab.2019.101303.

Alhomodi, A.F., Kasiga, T., Berhow, M., Brown, M.L., Gibbons, W.R., and Karki, B. (2022). Combined effect of mild pretreatment and fungal fermentation on nutritional characteristics of canola meal and nutrient digestibility of processed canola meal in rainbow trout. Food Bioprod. Proc. **133**: 57–66. doi:10.1016/j.fbp.2022.03.002.

Allen, D.K., and Young, J.D. (2013). Carbon and Nitrogen Provisions Alter the Metabolic Flux in Developing Soybean Embryos. Plant Phys. **161**: 1458–1475. doi:10.1104/pp.112.203299.

An, D., and Suh, M.C. (2015). Overexpression of *Arabidopsis* WRI1 enhanced seed mass and storage oil content in *Camelina sativa*. Plant Biotech. Rep. **9**: 137–148. doi:10.1007/s11816-015-0351-x.

Angeles-Núñez, J.G., and Tiessen, A. (2011). Mutation of the transcription factor LEAFY COTYLEDON 2 alters the chemical composition of *Arabidopsis* seeds, decreasing oil and protein content, while maintaining high levels of starch and sucrose in mature seeds. J. Plant Phys. **168**: 1891–1900. doi:10.1016/j.jplph.2011.05.003.

Annison, G., and Choct, M. (1991). Anti-nutritive activities of cereal non-starch polysaccharides in broiler diets and strategies minimizing their effects. World Poul. Sci. J. **47**: 232–242. doi:10.1079/WPS19910019.

Anwar, M.M., Ali, S.E., and Nasr, E.H. (2015). Improving the nutritional value of canola seed by gamma irradiation. J. Rad. Res. App. Sci. **8**: 328–333. doi:10.1016/j.jrras.2015.05.007.

Arioli T., Peng L., Betzner A.S., Burn J., Wittke W., Herth W., Camilleri C., Hofte H., Plazinski J., Birch R., Cork A., Glover J., Redmond J., and Williamson R.E. (1998). Molecular analysis of cellulose biosynthesis in *Arabidopsis*. Sci. **279**: 717–720. doi: 10.1126/science.279.5351.717.

Arondel, V., Lemieux, B., Hwang, I., Gibson, S., Goodman, H.M., and Somerville, C.R. (1992). Map-based cloning of a gene controlling omega-3 fatty acid desaturation in *Arabidopsis*. Sci. **258**: 1353–1355. doi:10.1126/science.1455229.

Aznar-Moreno, J.A., Sánchez, R., Gidda, S.K., Martínez-Force, E., Moreno-Pérez, A.J., Venegas Calerón, M., Garcés, R., Mullen, R.T., and Salas, J.J. (2018). New insights into sunflower (*Helianthus annuus* L.) FatA and FatB thioesterases, their regulation, structure and distribution. Fron. Plant Sci. **9**: 1496. doi:10.3389/fpls.2018.01496.

Bae, J.M., Kwak, M.S., Noh, S.A., Oh, M.-J., Kim, Y.-S., and Shin, J.S. (2014). Overexpression of sweetpotato expansin cDNA (*IbEXP1*) increases seed yield in *Arabidopsis*. Trans. Res. **23**: 657–667. doi:10.1007/s11248-014-9804-1.

Bai, Y., Jing, G., Zhou, J., Li, S., Bi, R., Zhao, J., Jia, Q., Zhang, Q., and Zhang, W. (2020). Overexpression of soybean GmPLDγ enhances seed oil content and modulates fatty acid composition in transgenic *Arabidopsis*. Plant Sci. **290**: 110298. doi:10.1016/j.plantsci.2019.110298.

Bai, Y., Shen, Y., Zhang, Z., Jia, Q., Xu, M., Zhang, T., Fang, H., Yu, X., Li, L., Liu, D., Qi, X., Chen, Z., Wu, S., Zhang, Q., and Liang, C. (2021). A *GPAT1* mutation in *Arabidopsis*

enhances plant height but impairs seed oil biosynthesis. Intl. J. Mol. Sci. **22**. doi:10.3390/ijms22020785.

Banas, W., Carlsson, A.S., and Banas, A. (2014). Effect of overexpression of PDAT gene on *Arabidopsis* growth rate and seed oil content. J. Ag. Sci. **6**: 65–79. doi:10.5539/jas.v6n5p65.

Bates, P.D., and Browse, J. (2012). The significance of different diacylgycerol synthesis ppathways on plant oil composition and bioengineering. Fron. Plant Sci. **3**: 147. doi:10.3389/fpls.2012.00147.

Bates, P.D. 2016. Understanding the control of acyl flux through the lipid metabolic network of plant oil biosynthesis. Bioch. Biophys. Acta **1861**: 1214–1225. doi:10.1016/j.bbalip.2016.03.021.

Baud, S., Dubreucq, B., Miquel, M., Rochat, C., and Lepiniec, L. (2008). Storage reserve accumulation in *Arabidopsis*: metabolic and developmental control of seed filling. The *Arabidopsis* Book **6**: e0113. doi:10.1199/tab.0113.

Bäumlein H., Miséra S., Luerßen H., Kölle K., Horstmann C., Wobus U., Andreas J. Müller A.J. (1994). The FUS3 gene of *Arabidopsis thaliana* is a regulator of gene expression during late embryogenesis. Plant J. **6**: 379-387.

Beeckman, T., Przemeck, G.K.H., Stamatiou, G., Lau, R., Terryn, N., De Rycke, R., Inzé, D., and Berleth, T. (2002). Genetic complexity of cellulose synthase A gene function in *Arabidopsis* embryogenesis. Plant Phys. **130**: 1883–1893. doi:10.1104/pp.102.010603.

Bell, J.M. (1984). Nutrients and toxicants in rapeseed meal: a review. J. An. Sci. **58**: 996–1010. doi:10.2527/jas1984.584996x.

Besnard, J., Zhao, C., Avice, J.-C., Vitha, S., Hyodo, A., Pilot, G., and Okumoto, S. (2018). *Arabidopsis* UMAMIT24 and 25 are amino acid exporters involved in seed loading. J. Exp. Bot. **69**: 5221–5232. doi:10.1093/jxb/ery302.

Bhalla, P.L., and Slattery, H.D. (1984). Callose deposits make clover seeds impermeable to water. Ann. Bot. **53**: 125–128. doi:10.1093/oxfordjournals.aob.a086661.

Bhunia, R.K., Chakraborty, A., Kaur, R., Maiti, M.K., and Sen, S.K. (2016). Enhancement of α-linolenic acid content in transgenic tobacco seeds by targeting a plastidial ω-3 fatty acid desaturase (*fad7*) gene of *Sesamum indicum* to ER. Plant Cell Rep. **35**: 213–226. doi:10.1007/s00299-015-1880-z.

Boston, R.S., Viitanen, P.V., and Vierling, E. (1996). Molecular chaperones and protein folding in plants. Plant Mol. Biol. **32**: 191–222.

Braybrook, S.A., Stone, S.L., Park, S., Bui, A.Q., Le, B.H., Fischer, R.L., Goldberg, R.B., and Harada, J.J. (2006). Genes directly regulated by LEAFY COTYLEDON2 provide insight into the control of embryo maturation and somatic embryogenesis. PNAS **103**: 3468–3473. doi:10.1073/pnas.0511331103.

Brown, A.P., Affleck, V., Fawcett., T, and Slabas, A.R. (2006). Tandem affinity purification tagging of fatty acid biosynthetic enzymes in *Synechocystis sp.* PCC6803 and *Arabidopsis thaliana*. J. Exp. Bot. **57**: 1563–1571. doi:10.1093/jxb/erj150.

Browse, J., and Somerville, C. (1991). Glycerolipid synthesis: biochemistry and regulation. An. Rev. Plant Phys. Plant Mol. Biol. **42**: 467–506.

Bryant, F.M., Munoz-Azcarate, O., Kelly, A.A., Beaudoin, F., Kurup, S., and Eastmond, P.J. (2016). ACYL-ACYL CARRIER PROTEIN DESATURASE2 and 3 are responsible for making omega-7 fatty acids in the *Arabidopsis* aleurone. Plant Phys. **172**: 154–162. doi:10.1104/pp.16.00836.

Burn J.E., Hocart C.H., Birch R.J., Cork A.C., and Williamson R.E. (2002). Functional analysis of the cellulose synthase genes CesA1, CesA2, and CesA3 in *Arabidopsis*. Plant Phys. **129**: 797–807. doi: 10.1104/pp.010931.

Cahoon, E.B., and Li-Beisson, Y. (2020). Plant unusual fatty acids: learning from the less common. Curr. Op. Plant Biol. **55**: 66–73. doi:10.1016/j.pbi.2020.03.007.

Cai, G., Wang, G., Kim, S.-C., Li, J., Zhou, Y., and Wang, X. (2021). Increased expression of fatty acid and ABC transporters enhances seed oil production in camelina. Biotech. Biof. **14**: 49. doi:10.1186/s13068-021-01899-w.

Cai, Y., Goodman, J.M., Pyc, M., Mullen, R.T., Dyer, J.M., and Chapman, K.D. (2015). *Arabidopsis* SEIPIN proteins modulate triacylglycerol accumulation and influence lipid droplet proliferation. Plant Cell **27**: 2616–2636. doi:10.1105/tpc.15.00588.

Caldo, K.M.P., Shen, W., Xu, Y., Hanley-Bowdoin, L., Chen, G., Weselake, R.J., and Lemieux, M.J. (2018). Diacylglycerol acyltransferase 1 is activated by phosphatidate and inhibited by SnRK1-catalyzed phosphorylation. Plant J. **96**: 287–299. doi:10.1111/tpj.14029.

Canola Council of Canada. (2019). Canola Meal Feeding Guide (6th Ed). Retrieved 2023-02-07 from: https://www.canolacouncil.org/canolamazing/wordpress/wp-content/uploads/2019/10/2019-Canola-Meal-Feed-Guide-Web.pdf

Carrapiso, A.I., and García, C. (2000). Development in lipid analysis: some new extraction techniques and in situ transesterification. Lipids **35**: 1167–1177. doi:10.1007/s11745-000-0633-8.

Chapman, K.D., Aziz, M., Dyer, J.M., and Mullen, R.T. (2019). Mechanisms of lipid droplet biogenesis. Bioch. J. **476**: 1929–1942. doi:10.1042/BCJ20180021.

Chen G., Harwood J.L., Lemieux M.J., Stone S.J., and Weselake R.J. (2022). Acyl-CoA:diacylglycerol acyltransferase: Properties, physiological roles, metabolic engineering and intentional control. Prog. Lipid Res. 88: 101181.

Chen, K., Yin, Y., Liu, S., Guo, Z., Zhang, K., Liang, Y., Zhang, L., Zhao, W., Chao, H., and Li, M. (2019). Genome-wide identification and functional analysis of oleosin genes in *Brassica napus* L. BMC Plant Biol. **19**: 294. doi:10.1186/s12870-019-1891-y.

Chen, M., Zhang, B., Li, C., Kulaveerasingam, H., Chew, F.T., and Yu, H. (2015). *TRANSPARENT TESTA GLABRA1* regulates the accumulation of seed storage reserves in *Arabidopsis*. Plant Phys. **169**: 391–402. doi:10.1104/pp.15.00943.

Chen, S., Ehrhardt, D.W., and Somerville, C.R. (2010). Mutations of cellulose synthase (CESA1) phosphorylation sites modulate anisotropic cell expansion and bidirectional mobility of cellulose synthase. PNAS **107**: 17188–17193. doi:10.1073/pnas.1012348107.

Chen, S., Lei, Y., Xu, X., Huang, J., Jiang, H., Wang, J., Cheng, Z., Zhang, J., Song, Y., Liao, B., and Li, Y. (2015). The peanut (*Arachis hypogaea* L.) gene *AhLPAT2* increases the lipid content of transgenic *Arabidopsis* seeds. PLoS ONE **10**: e0136170. doi:10.1371/journal.pone.0136170.

Chen, Y., Sun, A., Wang, M., Zhu, Z., and Ouwerkerk, P.B.F. (2014). Functions of the CCCH type zinc finger protein OsGZF1 in regulation of the seed storage protein GluB-1 from rice. Plant Mol. Biol. **84**: 621–634. doi:10.1007/s11103-013-0158-5.

Chen, Y., Cui, Q., Xu, Y., Yang, S., Gao, M., and Wang, Y. (2015). Effects of tung oilseed FAD2 and DGAT2 genes on unsaturated fatty acid accumulation in *Rhodotorula glutinis* and *Arabidopsis thaliana*. Mol. Genet. Genom. **290**: 1605–1613. doi:10.1007/s00438-015-1011-0.

Cheng, T., Zhao, P., Ren, Y., Zou, J., and Sun, M. (2021). AtMIF1 increases seed oil content by attenuating GL2 inhibition. New Phyt. **229**: 2152–2162. doi:10.1111/nph.17016.

Chhikara, S., Abdullah, H.M., Akbari, P., Schnell, D., and Dhankher, O.P. (2018). Engineering *Camelina sativa* (L.) Crantz for enhanced oil and seed yields by combining diacylglycerol acyltransferase1 and glycerol-3-phosphate dehydrogenase expression. Plant Biotech. J. **16**: 1034–1045. doi:10.1111/pbi.12847.

Chrispeels, M.J. (1991). Sorting of proteins in the secretory system. An. Rev. Plant Phys. Plant Mol. Biol. **42**: 21–53.

Corrales A.R., Carillo L., Nebauer S.G., Renau-Morata B., Sanchez-Perales M., Fernandez-Nohales P., Marques J., Granell A., Pollmann S., Vincente-Carbajosa J., Molina R.V., and Medina J. (2014). Salinity assay in *Arabidopsis*. Bio-Prot. **4**: e1216. doi: 10.21769/BioProtoc.1216.

Coulon, D., Brocard, L., Tuphile, K., and Bréhélin, C. (2020). *Arabidopsis* LDIP protein locates at a confined area within the lipid droplet surface and favors lipid droplet formation. Bioch. **169**: 29–40. doi:10.1016/j.biochi.2019.09.018.

Cui, Y., Liu, Z., Zhao, Y., Wang, Y., Huang, Y., Li, L., Wu, H., Xu, S., and Hua, J. (2017). Overexpression of heteromeric GhACCase subunits enhanced oil accumulation in Upland Cotton. Plant Mol. Biol. Rep. **35**: 287–297. doi:10.1007/s11105-016-1022-y.

Daras, G., Templalexis, D., Avgeri, F., Tsitsekian, D., Karamanou, K., and Rigas, S. (2021). Updating insights into the catalytic domain properties of plant cellulose synthase (CesA) and cellulose synthase-like (Csl) proteins. Mol. **26**: 4335. doi:10.3390/molecules26144335.

Debeaujon, I., Lepiniec, L., Pourcel, L., and Routaboul, J.-M. (2007). Seed coat development and dormancy. *In* Seed Development, Dormancy and Germination. *Edited by* K.J. Bradford and H. Nonogaki. Blackwell Publishing Ltd, Oxford, UK. pp. 25–49. doi:10.1002/9780470988848.ch2.

Dehesh, K., Tai, H., Edwards, P., Byrne, J., and Jaworski, J.G. (2001). Overexpression of 3-ketoacyl-acyl-carrier protein synthase IIIs in plants reduces the rate of lipid synthesis. Plant Phys. **125**: 1103–1114. doi:10.1104/pp.125.2.1103.

Desprez, T., Juraniec, M., Crowell, E.F., Jouy, H., Pochylova, Z., Parcy, F., Höfte, H., Gonneau, M., and Vernhettes, S. (2007). Organization of cellulose synthase complexes involved in primary cell wall synthesis in *Arabidopsis thaliana*. PNAS **104**: 15572–15577. doi:10.1073/pnas.0706569104.

Ding, L.-N., Gu, S.-L., Zhu, F.-G., Ma, Z.-Y., Li, J., Li, M., Wang, Z., and Tan, X.-L. (2020). Long-chain acyl-CoA synthetase 2 is involved in seed oil production in *Brassica napus*. BMC Plant Biol. **20**: 21. doi:10.1186/s12870-020-2240-x.

Dirisala, V.R., Nair, R.R., Srirama, K., Reddy, P.N., Rao, K.R.S.S., Satya Sampath Kumar, N., and Parvatam, G. (2017). Recombinant pharmaceutical protein production in plants: unraveling the therapeutic potential of molecular pharming. Acta Phys. Plant. **39**: 18. doi:10.1007/s11738-016-2315-3.

Du, H., Huang, M., Hu, J., and Li, J. (2016). Modification of the fatty acid composition in *Arabidopsis* and maize seeds using a stearoyl-acyl carrier protein desaturase-1 (*ZmSAD1*) gene. BMC Plant Biol. **16**: 137. doi:10.1186/s12870-016-0827-z.

El-Hamidi, M., and Zaher, F.A. (2018). Production of vegetable oils in the world and in Egypt: an overview. Bull. Nat. Res. Centre **42**: 1-19. doi:10.1186/s42269-018-0019-0.

Endler, A., Schneider, R., Kesten, C., Lampugnani, E.R., and Persson, S. (2016). The cellulose synthase companion proteins act non-redundantly with CELLULOSE SYNTHASE INTERACTING1/POM2 and CELLULOSE SYNTHASE 6. Plant Sig. Behav. **11**: e1135281. doi:10.1080/15592324.2015.1135281.

Ettaki, H., Troncoso-Ponce, M.A., To, A., Barthole, G., Lepiniec, L., and Baud, S. (2018). Overexpression of *MYB115*, *AAD2*, or *AAD3* in *Arabidopsis thaliana* seeds yields contrasting omega-7 contents. PLOS ONE **13**: e0192156. doi:10.1371/journal.pone.0192156.

Ezcurra, I., Ellerström, M., Wycliffe, P., Stålberg, K., and Rask, L. (1999). Interaction between composite elements in the napA promoter: both the B-box ABA-responsive complex and the RY/G complex are necessary for seed-specific expression. Plant Mol. Biol. **40**: 699–709.

Ezquer, I., Mizzotti, C., Nguema-Ona, E., Gotté, M., Beauzamy, L., Viana, V.E., Dubrulle, N., Costa de Oliveira, A., Caporali, E., Koroney, A.-S., Boudaoud, A., Driouich, A., and Colombo, L. (2016). The developmental regulator SEEDSTICK controls structural and mechanical properties of the *Arabidopsis* seed coat. Plant Cell **28**: 2478–2492. doi:10.1105/tpc.16.00454.

Fatihi, A., Boulard, C., Bouyer, D., Baud, S., Dubreucq, B., and Lepiniec, L. (2016). Deciphering and modifying LAFL transcriptional regulatory network in seed for improving yield and quality of storage compounds. Plant Sci. **250**: 198–204. doi:10.1016/j.plantsci.2016.06.013.

Focks N., and Benning, C. (1998). wrinkled1: A novel, low-seed-oil mutant of *Arabidopsis* with a deficiency in the seed-specific regulation of carbohydrate metabolism. Plant Phys. **118**: 91-101.

Frey-Wyssling, A., Grieshaber, E., and Mühlethaler, K. (1963). Origin of spherosomes in plant cells. J. Ult. Res. **8**: 506–516. doi:10.1016/S0022-5320(63)80052-0.

Frommer, W.B., Hummel, S., and Riesmeier, J.W. (1993). Expression cloning in yeast of a cDNA encoding a broad specificity amino acid permease from *Arabidopsis thaliana*. PNAS **90**: 5944–5948. doi:10.1073/pnas.90.13.5944.

Fujiwara, T., Nambara, E., Yamagishi, K., Goto, D.B., and Naito, S. (2002). Storage proteins. The *Arabidopsis* Book **1**: e0020. doi:10.1199/tab.0020.

Gacek, K., Bartkowiak-Broda, I., and Batley, J. (2018). Genetic and molecular regulation of seed storage proteins (SSPs) to improve protein nutritional value of oilseed rape (*Brassica napus* L.) Seeds. Fron. Plant Sci. **9**: 890. doi:10.3389/fpls.2018.00890.

Gao, C., Qi, S., Liu, K., Li, D., Jin, C., Li, Z., Huang, G., Hai, J., Zhang, M., and Chen, M. (2016). MYC2, MYC3, and MYC4 function redundantly in seed storage protein accumulation in *Arabidopsis*. Plant Phys. and Biochem. **108**: 63–70. doi:10.1016/j.plaphy.2016.07.004.

Gao, Y., Liu, J., Chen, Y., Tang, H., Wang, Y., He, Y., Ou, Y., Sun, X., Wang, S., and Yao, Y. (2018). Tomato SlAN11 regulates flavonoid biosynthesis and seed dormancy by interaction with bHLH proteins but not with MYB proteins. Hort. Res. **5**: 27. doi:10.1038/s41438-018-0032-3.

Gao, Y., An, K., Guo, W., Chen, Y., Zhang, R., Zhang, X., Chang, S., Rossi, V., Jin, F., Cao, X., Xin, M., Peng, H., Hu, Z., Guo, W., Du, J., Ni, Z., Sun, Q., and Yao, Y. (2021). The endosperm-specific transcription factor TaNAC019 regulates glutenin and starch accumulation and its elite allele improves wheat grain quality. Plant Cell **33**: 603–622. doi:10.1093/plcell/koaa040.

Garces R. and Mancha M. (1993). One-step lipid extraction and fatty acid methyl esters preparation from fresh plant tissues. An. Biochem. **211**: 139-143. doi: 10.1006/abio.1993.1244

Ghazani S.M., Garcia-Llatas G., and Marangoni A.G.. (2014). Micronutrient content of cold-pressed, hot-pressed, solvent extracted and RBD canola oil: Implications for nutrition and quality. Eur. J. Lipid Sci. **116**: 380-387. doi: 10.1002/ejlt.201300288

Goldberg, R.B., de Paiva, G., and Yadegari, R. (1994). Plant embryogenesis: zygote to seed. Sci. **266**: 605–614. doi:10.1126/science.266.5185.605.

Grami, B., Stefansson, B.R., and Baker, R.J. (1977). Genetics of protein and oil content in summer rape: heritability, number of effective factors, and correlations. Can. J. Plant Sci. **57**: 937–943. doi:10.4141/cjps77-134.

Grant, J.E., Ninan, A., Cripps-Guazzone, N., Shaw, M., Song, J., Petřík, I., Novák, O., Tegeder, M., and Jameson, P.E. (2021). Concurrent overexpression of amino acid permease *AAP1(3a)* and *SUT1* sucrose transporter in pea resulted in increased seed number and changed cytokinin and protein levels. Func. Plant Biol. **48**: 889-904. doi:10.1071/FP21011.

Greer, M.S., Cai, Y., Gidda, S.K., Esnay, N., Kretzschmar, F.K., Seay, D., McClinchie, E., Ischebeck, T., Mullen, R.T., Dyer, J.M., and Chapman, K.D. (2020). SEIPIN isoforms interact with the membrane-tethering protein VAP27-1 for lipid droplet formation. Plant Cell **32**: 2932–2950. doi:10.1105/tpc.19.00771.

Griffiths, J.S., Tsai, A.Y.-L., Xue, H., At Alin Voiniciuc, C., Šola, K., Seifert, G.J., Mansfield, S.D., and Haughn, G.W. (2014). SALT-OVERLY SENSITIVE5 mediates *Arabidopsis* seed coat mucilage adherence and organization through pectins. Plant Phys. **165**: 991–1004. doi: 10.1104/pp.114.239400.

Gu, J., Chao, H., Wang, H., Li, Y., Li, D., Xiang, J., Gan, J., Lu, G., Zhang, X., Long, Y., and Li, M. (2017). Identification of the relationship between oil body morphology and oil content by microstructure comparison combining with QTL analysis in *Brassica napus*. Fron. Plant Sci. **7**: 1989. doi:10.3389/fpls.2016.01989.

Gu, Y., Kaplinsky, N., Bringmann, M., Cobb, A., Carroll, A., Sampathkumar, A., Baskin, T.I., Persson, S., and Somerville, C.R. (2010). Identification of a cellulose synthase-associated protein required for cellulose biosynthesis. PNAS **107**: 12866–12871. doi:10.1073/pnas.1007092107.

Guo, Z., Haslam, R.P., Michaelson, L.V., Yeung, E.C., Lung, S., Napier, J.A., and Chye, M. (2019B). The overexpression of rice *ACYL-CoA-BINDING PROTEIN 2* increases grain size and bran oil content in transgenic rice. Plant J. **100**: 1132–1147. doi:10.1111/tpj.14503.

Guo, Z., Ye, Z., Haslam, R.P., Michaelson, L.V., Napier, J.A., and Chye, M. (2019). *Arabidopsis* cytosolic acyl-CoA-binding proteins function in determining seed oil composition. Plant Dir. **3**: 1-9. doi:10.1002/pld3.182.

Hansen, J.Ø., Skrede, A., Mydland, L.T., and Øverland, M. (2017). Fractionation of rapeseed meal by milling, sieving and air classification - effect on crude protein, amino acids and fiber content and digestibility. An. Feed Sci. Tech. **230**: 143–153. doi:10.1016/j.anifeedsci.2017.05.007.

Hara A., Radin N.S. (1978). Lipid extraction of tissues with a low-toxicity solvent. An. Bioch. **90**: 420-426.

Hardouin C., and Lemaitre S. (2020). Safety case study. Intrinsic instability of concentrated solutions of alcoholic hydrogen chloride: potential hazards associated with methanol. Org. Process. Res. Dev. **24**: 867-871. doi:10.1021/acs.oprd.0c00034.

Harrington, K.J., and D'Arcy-Evans, C. (1985). A comparison of conventional and in situ methods of transesterification of seed oil from a series of sunflower cultivars. J. Am. Oil Chem. Soc. **62**: 1009–1013. doi:10.1007/BF02935703.

Henchion, M., Hayes, M., Mullen, A., Fenelon, M., and Tiwari, B. (2017). Future protein supply and demand: strategies and factors influencing a sustainable equilibrium. Foods **6**: 53. doi:10.3390/foods6070053.

Herman, E.M., and Larkins, B.A. (1999). Protein storage bodies and vacuoles. Plant Cell **11**: 601–613.

Hu, Y., Zhou, L., Yang, Y., Zhang, W., Chen, Z., Li, X., Qian, Q., Kong, F., Li, Y., Liu, X., and Hou, X. (2021). The gibberellin signaling negative regulator RGA-LIKE3 promotes seed storage protein accumulation. Plant Phys. **185**: 1697–1707. doi:10.1093/plphys/kiaa114.

Huai, D., Zhang, Y., Zhang, C., Cahoon, E.B., and Zhou, Y. (2015). Combinatorial effects of fatty acid elongase enzymes on nervonic acid production in *Camelina sativa*. PLOS ONE **10**: e0131755. doi:10.1371/journal.pone.0131755.

Huang, A.H.C. (1992). Oil bodies and oleosins in seeds. An. Rev. Plant Phys. Plant Mol. Biol. **43**: 177-200.

Huang, C.-Y., and Huang, A.H.C. (2017). Unique motifs and length of hairpin in oleosin target the cytosolic side of endoplasmic reticulum and budding lipid droplet. Plant Phys. **174**: 2248–2260. doi:10.1104/pp.17.00366.

Ivarson, E., Leiva-Eriksson, N., Ahlman, A., Kanagarajan, S., Bülow, L., and Zhu, L.-H. (2017). Effects of overexpression of *WRI1* and hemoglobin genes on the seed oil content of *Lepidium campestre*. Fron. Plant Sci. **7**: 2032. doi:10.3389/fpls.2016.02032.

Jain, R.K., Coffey, M., Lai, K., Kumar, A., and MacKenzie, S.L. (2000). Enhancement of seed oil content by expression of glycerol-3-phosphate acyltransferase genes. Biochem. Soc. Trans. **28**: 4.

Jako, C., Kumar, A., Wei, Y., Zou, J., Barton, D.L., Giblin, E.M., Covello, P.S., and Taylor, D.C. (2001). Seed-specific over-expression of an *Arabidopsis* cDNA encoding a diacylglycerol acyltransferase enhances seed oil content and seed weight. Plant Phys. **126**: 861–874. doi:10.1104/pp.126.2.861.

Jayawardhane, K.N., Singer, S.D., Weselake, R.J., and Chen, G. (2018). Plant *sn*-glycerol-3-phosphate acyltransferases: biocatalysts involved in the biosynthesis of intracellular and extracellular lipids. Lipids **53**: 469–480. doi:10.1002/lipd.12049.

Jayawardhane, K.N., Singer, S.D., Ozga, J.A., Rizvi, S.M., Weselake, R.J., and Chen, G. (2020). Seed-specific downregulation of *Arabidopsis CELLULOSE SYNTHASE 1* or *9* reduces seed cellulose content and differentially affects carbon partitioning. Plant Cell Rep. **39**: 953–969. doi:10.1007/s00299-020-02541-z.

Jessen, D., Roth, C., Wiermer, M., and Fulda, M. (2015). Two activities of long-chain acyl-coenzyme a synthetase are involved in lipid trafficking between the endoplasmic reticulum and the plastid in *Arabidopsis*. Plant Phys. **167**: 351–366. doi:10.1104/pp.114.250365.

Jia, L., Wu, Q., Ye, N., Liu, R., Shi, L., Xu, W., Zhi, H., Rahman, A.N.M.R.B., Xia, Y., and Zhang, J. (2012A). Proanthocyanidins inhibit seed germination by maintaining a high level of abscisic acid in *Arabidopsis thaliana*. J. Int. Plant Biol. **54**: 663–673. doi:10.1111/j.1744-7909.2012.01142.x.

Jia, W., Mikulski, D., Rogiewicz, A., Zduńczyk, Z., Jankowski, J., and Slominski, B.A. (2012B). Low-fiber canola. Part 2. Nutritive value of the meal. J. Ag. Food Chem. **60**: 12231–12237. doi:10.1021/jf302118c.

Jiang, Y., and Deyholos, M.K. (2010). Transcriptome analysis of secondary-wall-enriched seed coat tissues of canola (*Brassica napus* L.). Plant Cell Rep. **29**: 327–342. doi:10.1007/s00299-010-0824-x.

Jin, Y., Yuan, Y., Gao, L., Sun, R., Chen, L., Li, D., and Zheng, Y. (2017). Characterization and functional analysis of a type 2 diacylglycerol acyltransferase (dgat2) gene from oil palm (*Elaeis guineensis* Jacq.) mesocarp in *Saccharomyces cerevisiae* and transgenic *Arabidopsis thaliana*. Fron. Plant Sci. **8**: 1791. doi:10.3389/fpls.2017.01791.

Jing, G., Tang, D., Yao, Y., Su, Y., Shen, Y., Bai, Y., Jing, W., Zhang, Q., Lin, F., Guo, D., and Zhang, W. (2021). Seed specifically over-expressing *DGAT2A* enhances oil and linoleic acid

contents in soybean seeds. Biochem. Biophys. Res. Comm. **568**: 143–150. doi:10.1016/j.bbrc.2021.06.087.

Joehnke, M., Sørensen, S., Bjergegaard, C., Markedal, K., and Sørensen, J. (2018). Effect of dietary fibre fractions on in vitro digestibility of rapeseed napin proteins. Pol. J. Food Nutr. Sci. **68**: 335–345. doi:10.2478/pjfns-2018-0005.

Jolivet, P., Roux, E., d'Andrea, S., Davanture, M., Negroni, L., Zivy, M., and Chardot, T. (2004). Protein composition of oil bodies in *Arabidopsis thaliana* ecotype WS. Plant Phys. Biochem. **42**: 501–509. doi:10.1016/j.plaphy.2004.04.006.

Jones, D.B. (1941). Factors for converting percentages of nitrogen in foods and feeds into percentages of protein. USDA Circular **183**: 1-22.

Jung, S.H., Kim, R.J., Kim, K.J., Lee, D.H., and Suh, M.C. (2019). Plastidial and mitochondrial malonyl CoA-ACP malonyltransferase is essential for cell division and its overexpression increases storage oil content. Plant Cell Phys. **60**: 1239–1249. doi:10.1093/pcp/pcz032.

Kagaya, Y., Toyoshima, R., Okuda, R., Usui, H., Yamamoto, A., and Hattori, T. (2005). LEAFY COTYLEDON1 controls seed storage protein genes through its regulation of FUSCA3 and ABSCISIC ACID INSENSITIVE3. Plant Cell Phys. **46**: 399–406. doi:10.1093/pcp/pci048.

Kail, B.W., Link, D.D., and Morreale, B.D. (2012). Determination of free fatty acids and triglycerides by gas chromatography using selective esterification reactions. J. Chrom. Sci. **50**: 934–939. doi:10.1093/chromsci/bms093.

Kámán-Tóth, E., Pogány, M., Dankó, T., Szatmári, Á., and Bozsó, Z. (2018). A simplified and efficient *Agrobacterium tumefaciens* electroporation method. 3 Biotech **8**: 148. doi:10.1007/s13205-018-1171-9.

Kambhampati, S., Aznar-Moreno, J.A., Hostetler, C., Caso, T., Bailey, S.R., Hubbard, A.H., Durrett, T.P., and Allen, D.K. (2019). On the inverse correlation of protein and oil: examining the effects of altered central carbon metabolism on seed composition using soybean fast neutron mutants. Metab. **10**: 18. doi:10.3390/metabo10010018.

Kanai, M., Mano, S., Kondo, M., Hayashi, M., and Nishimura, M. (2016). Extension of oil biosynthesis during the mid-phase of seed development enhances oil content in *Arabidopsis* seeds. Plant Biotech. J. **14**: 1241–1250. doi:10.1111/pbi.12489.

Katepa-Mupondwa, F., Raney, J.P., and Rakow, G. (2005). Recurrent selection for increased protein content in yellow mustard (*Sinapis alba* L.). Plant Breed. **124**: 382–387. doi:10.1111/j.1439-0523.2005.01131.x.

Kawakatsu, T., Yamamoto, M.P., Touno, S.M., Yasuda, H., and Takaiwa, F. (2009). Compensation and interaction between RISBZ1 and RPBF during grain filling in rice. Plant J. **59**: 908–920. doi:10.1111/j.1365-313X.2009.03925.x.

Kawakatsu, T., Hirose, S., Yasuda, H., and Takaiwa, F. (2010). Reducing rice seed storage protein accumulation leads to changes in nutrient quality and storage organelle formation. Plant Phys. **154**: 1842–1854. doi:10.1104/pp.110.164343.

Ke, J., Behal, R.H., Back, S.L., Nikolau, B.J., Wurtele, E.S., and Oliver, D.J. (2000). The role of pyruvate dehydrogenase and acetyl-coenzyme A synthetase in fatty acid synthesis in developing *Arabidopsis* seeds. Plant Phys. **123**: 497–508. doi:10.1104/pp.123.2.497.

Kelly, K.M., Van Staden, J., and Bell, W.E. (1992). Seed coat structure and dormancy. Plant Gro. Reg. **11**: 201–209. doi:10.1007/BF00024559.

Kennedy E.P., Weiss, S.B. (1956). The function of cytidine coenzymes in the biosynthesis of phospholipides. J. Biol. Chem. 222, 193-214.

Keereetaweep, J., Liu, H., Zhai, Z., and Shanklin, J. (2018). Biotin attachment domain-containing proteins irreversibly inhibit acetyl CoA carboxylase. Plant Phys. **177**: 208–215. doi:10.1104/pp.18.00216.

Kim, H.U., Jung, S.-J., Lee, K.-R., Kim, E.H., Lee, S.-M., Roh, K.H., and Kim, J.-B. (2014). Ectopic overexpression of castor bean *LEAFY COTYLEDON2* (*LEC2*) in *Arabidopsis* triggers the expression of genes that encode regulators of seed maturation and oil body proteins in vegetative tissues. FEBS Open Bio **4**: 25–32. doi:10.1016/j.fob.2013.11.003.

Kim, H.J., Silva, J.E., Vu, H.S., Mockaitis, K., Nam, J.-W., and Cahoon, E.B. (2015). Toward production of jet fuel functionality in oilseeds: identification of FatB acyl-acyl carrier protein thioesterases and evaluation of combinatorial expression strategies in *Camelina* seeds. J. Exp. Bot. **66**: 4251–4265. doi:10.1093/jxb/erv225.

Kim, H., Park, J.H., Kim, D.J., Kim, A.Y., and Suh, M.C. (2016A). Functional analysis of diacylglycerol acyltransferase1 genes from *Camelina sativa* and effects of *CsDGAT1B* overexpression on seed mass and storage oil content in *C. sativa*. Plant Biotech. Rep. **10**: 141–153. doi:10.1007/s11816-016-0394-7.

Kim, M.J., Jang, I.-C., and Chua, N.-H. (2016B). The mediator complex MED15 subunit mediates activation of downstream lipid-related genes by the WRINKLED1 transcription factor. Plant Phys. **171**: 1951–1964. doi:10.1104/pp.16.00664.

Kim, R.J., Kim, H.U., and Suh, M.C. (2019). Development of camelina enhanced with drought stress resistance and seed oil production by co-overexpression of *MYB96A* and *DGAT1C*. Ind. Crops Prod. **138**: 111475. doi:10.1016/j.indcrop.2019.111475.

Kim, S., Yamaoka, Y., Ono, H., Kim, H., Shim, D., Maeshima, M., Martinoia, E., Cahoon, E.B., Nishida, I., and Lee, Y. (2013). AtABCA9 transporter supplies fatty acids for lipid synthesis to the endoplasmic reticulum. PNAS **110**: 773–778. doi:10.1073/pnas.1214159110.

Kong, Q., and Ma, W. (2018). WRINKLED1 as a novel 14-3-3 client: function of 14-3-3 proteins in plant lipid metabolism. Plant Sig. Behav. **13**: e1482176. doi:10.1080/15592324.2018.1482176.

Kong, Q., Yuan, L., and Ma, W. (2019). WRINKLED1, a "master regulator" in transcriptional control of plant oil biosynthesis. Plants **8**: 238. doi:10.3390/plants8070238.

Kong, Q., Yang, Y., Guo, L., Yuan, L., and Ma, W. (2020A). molecular basis of plant oil biosynthesis: insights gained from studying the WRINKLED1 transcription factor. Fron. Plant Sci. **11**: 24. doi:10.3389/fpls.2020.00024.

Kong, Q., Yang, Y., Low, P.M., Guo, L., Yuan, L., and Ma, W. (2020B). The function of the WRI1-TCP4 regulatory module in lipid biosynthesis. Plant Sig. Behav. **15**: e1812878. doi:10.1080/15592324.2020.1812878.

Konishi, T., Shinohara, K., Yamada, K., and Sasaki, Y. (1996). Acetyl-CoA carboxylase in higher plants: most plants other than Gramineae have both the prokaryotic and the eukaryotic forms of this enzyme. Plant Cell Phys **37**: 117–122. doi:10.1093/oxfordjournals.pcp.a028920.

Kroj, T., Savino, G., Valon, C., Giraudat, J., and Parcy, F. (2003). Regulation of storage protein gene expression in *Arabidopsis*. Dev. **130**: 6065–6073. doi:10.1242/dev.00814.

Kwak, J.S., Kim, S.-I., Park, S.W., Song, J.T., and Seo, H.S. (2019). E3 SUMO ligase AtSIZ1 regulates the cruciferin content of *Arabidopsis* seeds. Biochem. Biophys. Res. Comm. **519**: 761–766. doi:10.1016/j.bbrc.2019.09.064.

Ladwig, F., Stahl, M., Ludewig, U., Hirner, A.A., Hammes, U.Z., Stadler, R., Harter, K., and Koch, W. (2012). *Siliques Are Red1* from *Arabidopsis* acts as a bidirectional amino acid

transporter that is crucial for the amino acid homeostasis of siliques. Plant Phys. **158**: 1643–1655. doi:10.1104/pp.111.192583.

Lam, H.-M., Wong, P., Chan, H.-K., Yam, K.-M., Chen, L., Chow, C.-M., and Coruzzi, G.M. (2003). Overexpression of the *ASN1* gene enhances nitrogen status in seeds of *Arabidopsis*. Plant Phys. **132**: 926–935. doi:10.1104/pp.103.020123.

Lannuzel, C., Smith, A., Mary, A.L., Della Pia, E.A., Kabel, M.A., and de Vries, S. (2022). Improving fiber utilization from rapeseed and sunflower seed meals to substitute soybean meal in pig and chicken diets: A review. An. Feed Sci. Tech. **285**: 115213. doi:10.1016/j.anifeedsci.2022.115213.

Lara, P., Oñate-Sánchez, L., Abraham, Z., Ferrándiz, C., Díaz, I., Carbonero, P., and Vicente-Carbajosa, J. (2003). Synergistic activation of seed storage protein gene expression in *Arabidopsis* by ABI3 and two bZIPs related to OPAQUE2. J. Biol. Chem. **278**: 21003–21011. doi:10.1074/jbc.M210538200.

Lassner, M.W., Levering, C.K., Davies, H.M., and Knutzon, D.S. (1995). Lysophosphatidic acid acyltransferase from Meadowfoam mediates insertion of erucic acid at the *sn*-2 position of triacylglycerol in transgenic rapeseed oil. Plant Phys. **109**: 1389–1394. doi:10.1104/pp.109.4.1389.

Lee, E.-J., Oh, M., Hwang, J.-U., Li-Beisson, Y., Nishida, I., and Lee, Y. (2017). Seed-Specific Overexpression of the pyruvate transporter BASS2 increases oil content in *Arabidopsis* Seeds. Fron. Plant Sci. **8**: 194. doi:10.3389/fpls.2017.00194.

Lee, H.G., Park, B.-Y., Kim, H.U., and Seo, P.J. (2015). MYB96 stimulates C18 fatty acid elongation in *Arabidopsis* seeds. Plant Biotech. Rep. **9**: 161–166. doi:10.1007/s11816-015-0352-9.

Lee, J., Welti, R., Schapaugh, W.T., and Trick, H.N. (2011). Phospholipid and triacylglycerol profiles modified by PLD suppression in soybean seed: PLD suppression in transgenic soybean. Plant Biotech. J. **9**: 359–372. doi:10.1111/j.1467-7652.2010.00562.x.

Lee, S., Park, J., Lee, J., Shin, D., Marmagne, A., Lim, P.O., Masclaux-Daubresse, C., An, G., and Nam, H.G. (2020). OsASN1 overexpression in rice increases grain protein content and yield under nitrogen-limiting conditions. Plant Cell Phys. **61**: 1309–1320. doi:10.1093/pcp/pcaa060.

Lehman, T.A., and Sanguinet, K.A. (2019). Auxin and cell wall crosstalk as revealed by the *Arabidopsis thaliana* cellulose synthase mutant radially swollen 1. Plant Cell Phys. **60**: 1487–1503. doi:10.1093/pcp/pcz055.

Li, C., Yue, Y., Chen, H., Qi, W., and Song, R. (2018A). The ZmbZIP22 transcription factor regulates 27-kD γ-zein gene transcription during maize endosperm development. Plant Cell **30**: 2402–2424. doi:10.1105/tpc.18.00422.

Li, C., and Song, R. (2020). The regulation of zein biosynthesis in maize endosperm. Theo. App. Genet. **133**: 1443–1453. doi:10.1007/s00122-019-03520-z.

Li, C., Zhang, B., Chen, B., Ji, L., and Yu, H. (2018B). Site-specific phosphorylation of TRANSPARENT TESTA GLABRA1 mediates carbon partitioning in *Arabidopsis* seeds. Nat. Comm. **9**: 571. doi:10.1038/s41467-018-03013-5.

Li, D., Jin, C., Duan, S., Zhu, Y., Qi, S., Liu, K., Gao, C., Ma, H., Zhang, M., Liao, Y., and Chen, M. (2017A). MYB89 transcription factor represses seed oil accumulation. Plant Phys. **173**: 1211–1225. doi:10.1104/pp.16.01634.

Li, F., Xie, G., Huang, J., Zhang, R., Li, Y., Zhang, M., Wang, Y., Li, A., Li, X., Xia, T., Qu, C., Hu, F., Ragauskas, A.J., and Peng, L. (2017B). *OsCESA9* conserved-site mutation leads to

largely enhanced plant lodging resistance and biomass enzymatic saccharification by reducing cellulose DP and crystallinity in rice. Plant Biotech. J. **15**: 1093–1104. doi:10.1111/pbi.12700.

Li, M., Wei, F., Tawfall, A., Tang, M., Saettele, A., and Wang, X. (2015A). Overexpression of patatin-related phospholipase AIII δ altered plant growth and increased seed oil content in camelina. Plant Biotech. J. **13**: 766–778. doi:10.1111/pbi.12304.

Li, N., Gügel, I.L., Giavalisco, P., Zeisler, V., Schreiber, L., Soll, J., and Philippar, K. (2015B). FAX1, a novel membrane protein mediating plastid fatty acid export. PLOS Biol. **13**: e1002053. doi:10.1371/journal.pbio.1002053.

Li, N., Meng, H., Li, S., Zhang, Z., Zhao, X., Wang, S., Liu, A., Li, Q., Song, Q., Li, X., Guo, L., Li, H., Zuo, J., and Luo, K. (2020). Two plastid fatty acid exporters contribute to seed oil accumulation in *Arabidopsis*. Plant Physiology **182**: 1910–1919. doi:10.1104/pp.19.01344.

Li, X., Mei, D., Liu, Q., Fan, J., Singh, S., Green, A., Zhou, X.-R., and Zhu, L.-H. (2016). Downregulation of crambe fatty acid desaturase and elongase in *Arabidopsis* and crambe resulted in significantly increased oleic acid content in seed oil. Plant Biotech. J. **14**: 323–331. doi:10.1111/pbi.12386.

Li, Y., Beisson, F., Pollard, M., and Ohlrogge, J. (2006). Oil content of *Arabidopsis* seeds: The influence of seed anatomy, light and plant-to-plant variation. Phyt. **67**: 904–915. doi:10.1016/j.phytochem.2006.02.015.

Liang S., Yang G., and Ma Y. (2010). Chemical characteristics and fatty acid profile of foxtail millet bran oil. J. Am. Oil Chem. Soc. **87**: 63-67. doi: 10.1007/s11746-009-1475-3

Liu, B., Hua, C., Song, G., Wu, M., Cui, R., Zhang, A., Liu, Y., Huang, L., Yan, A., Ali, I., Khan, A.R., and Gan, Y. (2017). The SPATULA transcription factor regulates seed oil content by

controlling seed specific genes in *Arabidopsis thaliana*. Plant Growth Reg. **82**: 111–121. doi:10.1007/s10725-016-0243-2.

Liu, F., Xia, Y., Wu, L., Fu, D., Hayward, A., Luo, J., Yan, X., Xiong, X., Fu, P., Wu, G., and Lu, C. (2015). Enhanced seed oil content by overexpressing genes related to triacylglyceride synthesis. Gene **557**: 163–171. doi:10.1016/j.gene.2014.12.029.

Liu, H., Zhai, Z., Kuczynski, K., Keereetaweep, J., Schwender, J., and Shanklin, J. (2019A). WRINKLED1 regulates BIOTIN ATTACHMENT DOMAIN-CONTAINING proteins that inhibit fatty acid synthesis. Plant Phys. **181**: 55–62. doi:10.1104/pp.19.00587.

Liu, K., Liu Y., and Chen F. (2019). Effects of storage temperature on lipid oxidation and changes in nutrient contents in peanuts. Food Sci. Nutr. **7**: 2280-2290. doi: 10.1002/fsn3.1069

Liu, S., Wang, D., Mei, Y., Xia, T., Xu, W., Zhang, Y., You, X., Zhang, X., Li, L., and Wang, N.N. (2020). Overexpression of *GmAAP6a* enhances tolerance to low nitrogen and improves seed nitrogen status by optimizing amino acid partitioning in soybean. Plant Biotech. J. **18**: 1749–1762. doi:10.1111/pbi.13338.

Liu, Y.-F., Li, Q.-T., Lu, X., Song, Q.-X., Lam, S.-M., Zhang, W.-K., Ma, B., Lin, Q., Man, W.-Q., Du, W.-G., Shui, G.-H., Chen, S.-Y., and Zhang, J.-S. (2014). Soybean GmMYB73 promotes lipid accumulation in transgenic plants. BMC Plant Biol. **14**: 73. doi:10.1186/1471-2229-14-73.

Liu, Z., Liu, H., Zheng, L., Xu, F., Wu, Y., Pu, L., and Zhang, G. (2022). Enolase2 regulates seed fatty acid accumulation via mediating carbon partitioning in *Arabidopsis thaliana*. Phys. Plant. **174**. doi:10.1111/ppl.13797.

Lopes M.A., and Larkins B.A. (1993). Endosperm origin, development, and function. Plant Cell **5**: 1383-1399.

Lu, C., Xin, Z., Ren, Z., Miquel, M., and Browse, J. (2009). An enzyme regulating triacylglycerol composition is encoded by the ROD1 gene of *Arabidopsis*. PNAS **106**: 18837–18842. doi:10.1073/pnas.0908848106.

Lu, L., Wei, W., Li, Q., Bian, X., Lu, X., Hu, Y., Cheng, T., Wang, Z., Jin, M., Tao, J., Yin, C., He, S., Man, W., Li, W., Lai, Y., Zhang, W., Chen, S., and Zhang, J. (2021). A transcriptional regulatory module controls lipid accumulation in soybean. New Phyt. **231**: 661–678. doi:10.1111/nph.17401.

Lu, Y., Chi, M., Li, L., Li, H., Noman, M., Yang, Y., Ji, K., Lan, X., Qiang, W., Du, L., Li, H., and Yang, J. (2018). Genome-wide identification, expression profiling, and functional validation of oleosin gene family in *Carthamus tinctorius* L. Fron. Plant Sci. **9**: 1393. doi:10.3389/fpls.2018.01393.

Lunn, D., Wallis, J.G., and Browse, J. (2018). Overexpression of Seipin1 increases oil in hydroxy fatty acid-accumulating seeds. Plant Cell Phys. **59**: 205–214. doi:10.1093/pcp/pcx177.

Luo, G., Shen, L., Song, Y., Yu, K., Ji, J., Zhang, C., Yang, W., Li, X., Sun, J., Zhan, K., Cui, D., Wang, Y., Gao, C., Liu, D., and Zhang, A. (2021). The MYB family transcription factor *TuODORANT1* from *Triticum urartu* and the homolog *TaODORANT1* from *Triticum aestivum* inhibit seed storage protein synthesis in wheat. Plant Biotech. J. **19**: 1863–1877. doi:10.1111/pbi.13604.

Lyzenga, W.J., Harrington, M., Bekkaoui, D., Wigness, M., Hegedus, D.D., and Rozwadowski, K.L. (2019). CRISPR/Cas9 editing of three CRUCIFERIN C homoeologues alters the seed protein profile in Camelina sativa. BMC Plant Biol. **19**: 292. doi:10.1186/s12870-019-1873-0.

Ma S., Du C., Ohlrogge J., and Zhang, M. (2020). Accelerating gene function discovery by rapid phenotyping of fatty acid composition and oil content of single transgenic T_1 *Arabidopsis* and camelina seeds. Plant Dir. **4**: 1-15. doi: 10.1002/pld3.253

Ma, W., Kong, Q., Mantyla, J.J., Yang, Y., Ohlrogge, J.B., and Benning, C. (2016). 14-3-3 protein mediates plant seed oil biosynthesis through interaction with AtWRI1. Plant J. **88**: 228–235. doi:10.1111/tpj.13244.

Maeo, K., Tokuda, T., Ayame, A., Mitsui, N., Kawai, T., Tsukagoshi, H., Ishiguro, S., and Nakamura, K. (2009). An AP2-type transcription factor, WRINKLED1, of *Arabidopsis thaliana* binds to the AW-box sequence conserved among proximal upstream regions of genes involved in fatty acid synthesis. Plant J. **60**: 476–487. doi:10.1111/j.1365-313X.2009.03967.x.

Manan, S., Ahmad, M.Z., Zhang, G., Chen, B., Haq, B.U., Yang, J., and Zhao, J. (2017). Soybean LEC2 regulates subsets of genes involved in controlling the biosynthesis and catabolism of seed storage substances and seed development. Fron. Plant Sci. **8**: 1604. doi:10.3389/fpls.2017.01604.

Mansfield, S.G., and Briarty, L.G. (1992). Cotyledon cell development in *Arabidopsis thaliana* during reserve deposition. Can. J. Bot. **70**: 151–164. doi:10.1139/b92-021.

Matthäus, B. (1998). Effect of dehulling on the composition of antinutritive compounds in various cultivars of rapeseed. Lipid/Fett (Eur. J. Lipid Sci. Tech.) **100**: 295–301. doi:10.1002/(SICI)1521-4133(199807)100:7<295::AID-LIPI295>3.0.CO;2-G.

McAllister, C.H., Beatty, P.H., and Good, A.G. (2012). Engineering nitrogen use efficient crop plants: the current status: Engineering nitrogen use efficient crop plants. Plant Biotech. J. **10**: 1011–1025. doi:10.1111/j.1467-7652.2012.00700.x.

McAllister, C.H., and Good, A.G. (2015). Alanine Aminotransferase Variants Conferring Diverse NUE Phenotypes in Arabidopsis thaliana. PLoS ONE **10**: e0121830. doi:10.1371/journal.pone.0121830.

Meyer, K., Stecca, K.L., Ewell-Hicks, K., Allen, S.M., and Everard, J.D. (2012). Oil and protein accumulation in developing seeds is influenced by the expression of a cytosolic pyrophosphatase in *Arabidopsis*. Plant Phys. **159**: 1221–1234. doi:10.1104/pp.112.198309.

Mhaske, V., Beldjilali, K., Ohlrogge, J., and Pollard, M. (2005). Isolation and characterization of an *Arabidopsis thaliana* knockout line for phospholipid: diacylglycerol transacylase gene (At5g13640). Plant Phys. Biochem. **43**: 413–417. doi:10.1016/j.plaphy.2005.01.013.

Miranda, M., Borisjuk, L., Tewes, A., Heim, U., Sauer, N., Wobus, U., and Weber, H. (2001). Amino acid permeases in developing seeds of *Vicia faba* L.: expression precedes storage protein synthesis and is regulated by amino acid supply: amino acid permeases in *V. faba* seeds. Plant J. **28**: 61–71. doi:10.1046/j.1365-313X.2001.01129.x.

Mönke, G., Altschmied, L., Tewes, A., Reidt, W., Mock, H.-P., B  **umlein, H., and Conrad, U.** (2004). Seed-specific transcription factors ABI3 and FUS3: molecular interaction with DNA. Planta **219**: 158–166. doi:10.1007/s00425-004-1206-9.

Moreau, R.A., and Stumpf, P.K. (1981). Recent studies of the enzymic synthesis of ricinoleic acid by developing castor beans. Plant Phys. **67**: 672–676. doi:10.1104/pp.67.4.672.

Müller, B., Fastner, A., Karmann, J., Mansch, V., Hoffmann, T., Schwab, W., Suter-Grotemeyer, M., Rentsch, D., Truernit, E., Ladwig, F., Bleckmann, A., Dresselhaus, T., and Hammes, U.Z. (2015). Amino acid export in developing *Arabidopsis* seeds depends on UmamiT facilitators. Curr. Biol. **25**: 3126–3131. doi:10.1016/j.cub.2015.10.038.

Murashige T., and Skoog F. (1962). A revised medium for rapid growth and bio assays with tobacco tissue cultures. Physiol. Plant. **15**: 473-497. doi: 10.1111/j.1399-3054.1962.tb08052.x

Murphy, D.J., and Cummins, I. (1989). Biosynthesis of seed storage products during Embryogenesis in Rapeseed, *Brassica napus*. J. Plant Phys. **135**: 63–69. doi:10.1016/S0176-1617(89)80225-1.

Murphy, D.J., Cummins, I., and Kang, A.S. (1989). Synthesis of the major oil-body membrane protein in developing rapeseed (*Brassica napus*) embryos. Integration with storage-lipid and storage-protein synthesis and implications for the mechanism of oil-body formation. Biochem. J. **258**: 285–293. doi:10.1042/bj2580285.

Nakamura, Y., Koizumi, R., Shui, G., Shimojima, M., Wenk, M.R., Ito, T., and Ohta, H. (2009). *Arabidopsis* lipins mediate eukaryotic pathway of lipid metabolism and cope critically with phosphate starvation. PNAS **106**: 20978–20983. doi:10.1073/pnas.0907173106.

Nauerby B., Billing K., and Wyndaele R. (1997). Influence of the antibiotic timentin on plant regeneration compared to carbenicillin and cefotaxime in concentrations suitable for elimination of *Agrobacterium tumefaciens*. Plant Sci. **123**: 169-177.

Nguyen, T.-P., Cueff, G., Hegedus, D.D., Rajjou, L., and Bentsink, L. (2015). A role for seed storage proteins in *Arabidopsis* seed longevity. J. Exp. Bot. **66**: 6399–6413. doi:10.1093/jxb/erv348.

Novotna, Z., Valentova, O., Martinec, J., Feltl, T., and Nokhrina, K. (2000). Study of phospholipases D and C in maturing and germinating seeds of *Brassica napus*. Biochem. Soc. Trans. **28**: 817–818. doi:10.1042/bst0280817.

Ohlrogge, J.B., Kuhn, D.N., and Stumpf, P.K. (1979). Subcellular localization of acyl carrier protein in leaf protoplasts of Spinacia oleracea. PNAS **76**: 1194–1198. doi:10.1073/pnas.76.3.1194.

Ohlrogge, J. (1994). Design of new plant products: engineering of fatty acid metabolism. Plant Phys. **104**: 821–826.

Okuley, J., Lightner, J., Feldmann, K., and Browse, J. (1994). *Arabidopsis* FAD2 gene encodes the enzyme that is essential for polyunsaturated lipid synthesis. Plant Cell **6**: 147–158.

Okuzaki, A., Ogawa, T., Koizuka, C., Kaneko, K., Inaba, M., Imamura, J., and Koizuka, N. (2018). CRISPR/Cas9-mediated genome editing of the fatty acid desaturase 2 gene in *Brassica napus.* Plant Phys. Biochem. **131**: 63–69. doi:10.1016/j.plaphy.2018.04.025.

Opazo-Navarrete, M., Tagle Freire, D., Boom, R.M., and Janssen, A.E.M. (2019). The influence of starch and fibre on in vitro protein digestibility of dry fractionated quinoa seed (riobamba variety). Food Biophys. **14**: 49–59. doi:10.1007/s11483-018-9556-1.

Özbek, Z.A., and Ergönül, P.G. (2020). Determination of physicochemical properties, fatty acid, tocopherol, sterol, and phenolic profiles of expeller–pressed poppy seed oils from Turkey. JAOCS **97**: 591–602. doi:10.1002/aocs.12337.

Pali, V., and Mehta, N. (2014). Evaluation of oil content and fatty acid compositions of flax (*Linum usitatissimum* L.) varieties of India. J. Ag. Sci. **6**: 198-207. doi:10.5539/jas.v6n9p198.

Paula, da Silva, Brandao, Dai, and Faciola. (2019). Feeding canola, camelina, and carinata meals to ruminants. An. **9**: 704. doi:10.3390/ani9100704.

Peng, B., Kong, H., Li, Y., Wang, L., Zhong, M., Sun, L., Gao, G., Zhang, Q., Luo, L., Wang, G., Xie, W., Chen, J., Yao, W., Peng, Y., Lei, L., Lian, X., Xiao, J., Xu, C., Li, X., and He, Y.

(2014). OsAAP6 functions as an important regulator of grain protein content and nutritional quality in rice. Nat. Comm. **5**: 4847. doi:10.1038/ncomms5847.

Peng, D., Zhang, L., Tan, X., Yuan, D., Liu, X., and Zhou, B. (2016). Increasing seed oil content and altering oil quality of *Brassica napus* L. by over-expression of diacylglycerol acyltransferase 1 (*SsDGAT1*) from *Sapium sebiferum* (L.) Roxb. Mol. Breed. **36**: 136. doi:10.1007/s11032-016-0543-2.

Peng, L., Hao, Q., Men, S., Wang, X., Huang, W., Tong, N., Chen, M., Liu, Z., Ma, X., and Shu, Q. (2021). Ecotopic over-expression of *PoCHS* from *Paeonia ostii* altered the fatty acids composition and content in *Arabidopsis thaliana*. Phys. Plant. **172**: 64–76. doi:10.1111/ppl.13293.

Perchlik, M., and Tegeder, M. (2017). Improving plant nitrogen use efficiency through alteration of amino acid transport processes. Plant Phys. **175**: 235–247. doi:10.1104/pp.17.00608.

Persson, S., Paredez, A., Carroll, A., Palsdottir, H., Doblin, M., Poindexter, P., Khitrov, N., Auer, M., and Somerville, C.R. (2007). Genetic evidence for three unique components in primary cell-wall cellulose synthase complexes in *Arabidopsis*. PNAS **104**: 15566–15571. doi:10.1073/pnas.0706592104.

Polko, J.K., Barnes, W.J., Voiniciuc, C., Doctor, S., Steinwand, B., Hill, J.L., Tien, M., Pauly, M., Anderson, C.T., and Kieber, J.J. (2018). SHOU4 proteins regulate trafficking of cellulose synthase complexes to the plasma membrane. Curr. Biol. **28**: 3174-3182. doi:10.1016/j.cub.2018.07.076.

Premi, M., and Sharma, H.K. (2013). Oil extraction optimization and kinetics from *Moringa Oleifera* (PKM 1) seeds. Intl. J. Ag. Food Sci. Tech. **4**: 371–378.

Pyc, M., Gidda, S.K., Seay, D., Esnay, N., Kretzschmar, F.K., Cai, Y., Doner, N.M., Greer, M.S., Hull, J.J., Coulon, D., Bréhélin, C., Yurchenko, O., de Vries, J., Valerius, O., Braus, G.H., Ischebeck, T., Chapman, K.D., Dyer, J.M., and Mullen, R.T. (2021). LDIP cooperates with SEIPIN and LDAP to facilitate lipid droplet biogenesis in *Arabidopsis*. Plant Cell **33**: 3076–3103. doi:10.1093/plcell/koab179.

Qiao, Z., Qi, W., Wang, Q., Feng, Y., Yang, Q., Zhang, N., Wang, S., Tang, Y., and Song, R. (2016). ZmMADS47 regulates zein gene transcription through interaction with Opaque2. PLOS Genet. **12**: e1005991. doi:10.1371/journal.pgen.1005991.

Rahman, M., and de Jiménez, M.M. (2016). Chapter 15. Designer oil crops. *In* Breeding Oilseed Crops for Sustainable Production. 1st Ed. Elsevier. pp. 361–376. doi:10.1016/B978-0-12-801309-0.00015-X.

Rajavel, A., Klees, S., Schlüter, J.-S., Bertram, H., Lu, K., Schmitt, A.O., and Gültas, M. (2021). Unravelling the complex interplay of transcription factors orchestrating seed oil content in *Brassica napus* L. Intl. J. Mol. Sci. **22**: 1033. doi:10.3390/ijms22031033.

Reidt, W., Wohlfarth, T., Ellerstrom, M., Czihal, andreas, Tewes, A., Ezcurra, I., Rask, L., and Baumlein, H. (2000). Gene regulation during late embryogenesis: the RY motif of maturation-specific gene promoters is a direct target of the FUS3 gene product. Plant J. **21**: 401–408. doi:10.1046/j.1365-313x.2000.00686.x.

Riebeseel, E., Häusler, R.E., Radchuk, R., Meitzel, T., Hajirezaei, M.-R., Emery, R.J.N., Küster, H., Nunes-Nesi, A., Fernie, A.R., Weschke, W., and Weber, H. (2009). The 2-oxoglutarate/malate translocator mediates amino acid and storage protein biosynthesis in pea embryos: OMT controls amino acid biosynthesis in seeds. Plant J. **61**: 350–363. doi:10.1111/j.1365-313X.2009.04058.x.

Roesler, K., Shen, B., Bermudez, E., Li, C., Hunt, J., Damude, H.G., Ripp, K.G., Everard, J.D., Booth, J.R., Castaneda, L., Feng, L., and Meyer, K. (2016). An improved variant of soybean type 1 diacylglycerol acyltransferase increases the oil content and decreases the soluble carbohydrate content of soybeans. Plant Phys. 171: 878-893. doi:10.1104/pp.16.00315.

Rolletschek, H., Schwender, J., König, C., Chapman, K.D., Romsdahl, T., Lorenz, C., Braun, H.-P., Denolf, P., Van Audenhove, K., Munz, E., Heinzel, N., Ortleb, S., Rutten, T., McCorkle, S., Borysyuk, T., Guendel, A., Shi, H., Vander Auwermeulen, M., Bourot, S., and Borisjuk, L. (2020). Cellular plasticity in response to suppression of storage proteins in the *Brassica napus* embryo. Plant Cell **32**: 2383–2401. doi:10.1105/tpc.19.00879.

Rossak, M., Smith, M., and Kunst, L. (2001). Expression of the FAE1 gene and FAE1 promoter activity in developing seeds of *Arabidopsis thaliana*. Plant Mol. Biol. **46**: 717–725.

Sader, A.P.O., Oliveira, S.G., and Berchielli, T.T. (2004). Application of Kjeldahl and Dumas combustion methods for nitrogen analysis. Arch. Vet. Sci. **9**: 73-79. doi:10.5380/avs.v9i2.4068.

Salas, J.J., and Ohlrogge, J.B. (2002). Characterization of substrate specificity of plant FatA and FatB acyl-ACP thioesterases. Arch. Biochem. Biophy. **403**: 25–34. doi:10.1016/S0003-9861(02)00017-6.

Salie, M.J., Zhang, N., Lancikova, V., Xu, D., and Thelen, J.J. (2016). A family of negative regulators targets the committed step of *de novo* fatty acid biosynthesis. Plant Cell **28**: 2312–2325. doi:10.1105/tpc.16.00317.

Sánchez-Rodríguez, C., Ketelaar, K., Schneider, R., Villalobos, J.A., Somerville, C.R., Persson, S., and Wallace, I.S. (2017). BRASSINOSTEROID INSENSITIVE2 negatively regulates cellulose synthesis in *Arabidopsis* by phosphorylating cellulose synthase 1. PNAS **114**: 3533–3538. doi:10.1073/pnas.1615005114.

Sanders, A., Collier, R., Trethewy, A., Gould, G., Sieker, R., and Tegeder, M. (2009). AAP1 regulates import of amino acids into developing *Arabidopsis* embryos. Plant J. **59**: 540–552. doi:10.1111/j.1365-313X.2009.03890.x.

Santiago, J.P., and Tegeder, M. (2016). Connecting source with sink: The Role of *Arabidopsis* AAP8 in phloem loading of amino acids. Plant Phys. **171**: 508–521. doi:10.1104/pp.16.00244.

Savadi, S., Naresh, V., Kumar, V., and Bhat, S.R. (2016). Seed-specific overexpression of *Arabidopsis DGAT1* in Indian mustard (*Brassica juncea*) increases seed oil content and seed weight. Bot. **94**: 177–184. doi:10.1139/cjb-2015-0218.

Schmidt, M.A., Barbazuk, W.B., Sandford, M., May, G., Song, Z., Zhou, W., Nikolau, B.J., and Herman, E.M. (2011). Silencing of soybean seed storage proteins results in a rebalanced protein composition preserving seed protein content without major collateral changes in the metabolome and transcriptome. Plant Phys. **156**: 330–345. doi:10.1104/pp.111.173807.

Schmidt, R., Stransky, H., and Koch, W. (2007). The amino acid permease AAP8 is important for early seed development in *Arabidopsis thaliana*. Planta **226**: 805–813. doi:10.1007/s00425-007-0527-x.

Serrato-Valenti, G., Ferro, M., and Modenesi, P. (1990). Structural and histochemical changes in palisade cells of *Prosopis juliflora* seed coat in relation to its water permeability. Ann. Bot. **65**: 529–532. doi:10.1093/oxfordjournals.aob.a087965.

Shah, F.A., Ni, J., Chen, J., Wang, Q., Liu, W., Chen, X., Tang, C., Fu, S., and Wu, L. (2018). Proanthocyanidins in seed coat tegmen and endospermic cap inhibit seed germination in *Sapium sebiferum*. PeerJ **6**: e4690. doi:10.7717/peerj.4690.

Shanklin, J., and Somerville, C. (1991). Stearoyl-acyl-carrier-protein desaturase from higher plants is structurally unrelated to the animal and fungal homologs. PNAS **88**: 2510–2514. doi:10.1073/pnas.88.6.2510.

Shen, L., Luo, G., Song, Y., Xu, J., Ji, J., Zhang, C., Gregová, E., Yang, W., Li, X., Sun, J., Zhan, K., Cui, D., Liu, D., and Zhang, A. (2020). A novel NAC family transcription factor *SPR* suppresses seed storage protein synthesis in wheat. Plant Biotech. J. **19**: 992–1007. doi:10.1111/pbi.13524.

Shi, L., Katavic, V., Yu, Y., Kunst, L., and Haughn, G. (2012). *Arabidopsis* glabra2 mutant seeds deficient in mucilage biosynthesis produce more oil: Mucilage-deficient gl2 seeds produce more oil. Plant J. **69**(37–46. doi:10.1111/j.1365-313X.2011.04768.x.

Shockey, J.M., Fulda, M.S., and Browse, J.A. (2002). *Arabidopsis* contains nine long-chain acyl-coenzyme A synthetase genes that participate in fatty acid and glycerolipid metabolism. Plant Phys. **129**: 1710–1722. doi:10.1104/pp.003269.

Singer, S.D., Chen, G., Mietkiewska, E., Tomasi, P., Jayawardhane, K., Dyer, J.M., and Weselake, R.J. (2016). *Arabidopsis* GPAT9 contributes to synthesis of intracellular glycerolipids but not surface lipids. J. Exp. Bot. **67**: 4627–4638. doi:10.1093/jxb/erw242.

Singer, S.D., Jayawardhane, K.N., Jiao, C., Weselake, R.J., and Chen, G. (2021). The effect of AINTEGUMENTA-LIKE 7 over-expression on seed fatty acid biosynthesis, storage oil accumulation and the transcriptome in *Arabidopsis thaliana*. Plant Cell Rep. **40**: 1647–1663. doi:10.1007/s00299-021-02715-3.

Slack, C.R., Campbell, L.C., Browse, J.A., and Roughan, P.G. (1983). Some evidence for the reversibility of the cholinephosphotransferasecatalysed reaction in developing linseed cotyledons in vivo. Bioch. Biophys. Acta **754**: 10–20. doi:10.1016/0005-2760(83)90076-0.

Slack, C.R., Roughan, P.G., Browse, J.A., and Gardiner, S.E. (1985). Some properties of cholinephosphotransferase from developing safflower cotyledons. Bioch. Biophys. Acta **833**: 438–448. doi:10.1016/0005-2760(85)90101-8.

Slominski, B.A., and Campbell, L.D. (1990). Non-starch polysaccharides of canola meal: quantification, digestibility in poultry and potential benefit of dietary enzyme supplementation. J. Sci. Food Ag. **53**: 175–184. doi:10.1002/jsfa.2740530205.

Slominski, B.A., Campbell, L.D., and Guenter, W. (1994). Carbohydrates and dietary fiber components of yellow- and brown-seeded canola. J. Ag. Food Chem. **42**: 704–707. doi:10.1021/jf00039a020.

Slominski, B.A. (1997). Developments in the breeding of low fibre rapeseed/canola. J. An. Feed Sci. **6**: 303–318. doi:10.22358/jafs/69527/1997.

Slominski, B.A., Jia, W., Rogiewicz, A., Nyachoti, C.M., and Hickling, D. (2012). Low-fiber canola. Part 1. Chemical and nutritive composition of the meal. J. Ag. Food Chem. **60**: 12225–12230. doi:10.1021/jf302117x.

Smykal, P., Vernoud, V., Blair, M.W., Soukup, A., and Thompson, R.D. (2014). The role of the testa during development and in establishment of dormancy of the legume seed. Front. Plant Sci. **5**: 351. doi:10.3389/fpls.2014.00351.

Speicher, T., Li, P., and Wallace, I. (2018). Phosphoregulation of the plant cellulose synthase complex and cellulose synthase-like proteins. Plants **7**: 52. doi:10.3390/plants7030052.

Somerville, C. (2006). Cellulose synthesis in higher plants. Annu. Rev. Cell Dev. Biol. **22**: 53–78. doi:10.1146/annurev.cellbio.22.022206.160206.

Song, G., Li, X., Munir, R., Khan, A.R., Azhar, W., Yasin, M.U., Jiang, Q., Bancroft, I., and Gan, Y. (2020). The WRKY6 transcription factor affects seed oil accumulation and alters fatty acid compositions in *Arabidopsis thaliana*. Phys. Plant. **169**: 612–624. doi:10.1111/ppl.13082.

Song, Y., He, L., Wang, X.-D., Smith, N., Wheeler, S., Garg, M.L., and Rose, R.J. (2017A). Regulation of carbon partitioning in the seed of the model legume *Medicago truncatula* and *Medicago orbicularis*: a comparative approach. Front. Plant Sci. **8**: 2070. doi:10.3389/fpls.2017.02070.

Song, Y., Wang, X.-D., and Rose, R.J. (2017B). Oil body biogenesis and biotechnology in legume seeds. Plant Cell Rep. **36**: 1519–1532. doi:10.1007/s00299-017-2201-5.

Srigley C.T., and Mossoba M.M. (2016). Current analytical techniques for food lipids. Food Saf. Innov. Anal. Tools Saf. Assess. **29**: 33-64.

Ståhl, U., Carlsson, A.S., Lenman, M., Dahlqvist, A., Huang, B., Banaś, W., Banaś, A., and Stymne, S. (2004). Cloning and functional characterization of a phospholipid:diacylglycerol acyltransferase from *Arabidopsis*. Plant Phys. **135**: 1324–1335. doi:10.1104/pp.104.044354.

Stymne, S., and Stobart, A.K. (1984). Evidence for the reversibility of the acyl-CoA:lysophosphatidylcholine acyltransferase in microsomal preparations from developing safflower (*Carthamus tinctorius* L.) cotyledons and rat liver. Biochem. J. **223**: 305–314. doi:10.1042/bj2230305.

Su, Y., Liang, W., Liu, Z., Wang, Y., Zhao, Y., Ijaz, B., and Hua, J. (2017). Overexpression of GhDof1 improved salt and cold tolerance and seed oil content in *Gossypium hirsutum*. J. Plant Phys. **218**: 222–234. doi:10.1016/j.jplph.2017.07.017.

Subedi, U., Jayawardhane, K.N., Pan, X., Ozga, J., Chen, G., Foroud, N.A., and Singer, S.D. (2020). The potential of genome editing for improving seed oil content and fatty acid composition in oilseed crops. Lipids **55**: 495–512. doi:10.1002/lipd.12249.

Sun, F., Liu, X., Wei, Q., Liu, J., Yang, T., Jia, L., Wang, Y., Yang, G., and He, G. (2017). Functional characterization of TaFUSCA3, a B3- superfamily transcription factor gene in the wheat. Fron. Plant Sci. **8**: 1133. doi:10.3389/fpls.2017.01133.

Sun, J.-Y., Hammerlindl, J., Forseille, L., Zhang, H., and Smith, M.A. (2014). Simultaneous over-expressing of an acyl-ACP thioesterase (FatB) and silencing of acyl-acyl carrier protein desaturase by artificial microRNAs increases saturated fatty acid levels in *Brassica napus* seeds. Plant Biotech. J. **12**: 624–637. doi:10.1111/pbi.12168.

Sun, Q., Xue, J., Lin, L., Liu, D., Wu, J., Jiang, J., and Wang, Y. (2018). Overexpression of soybean transcription factors GmDof4 and GmDof11 significantly increase the oleic acid content in seed of *Brassica napus* L. Agro. **8**: 222. doi:10.3390/agronomy8100222.

Tan, S.H., Mailer, R.J., Blanchard, C.L., and Agboola, S.O. (2011). Extraction and characterization of protein fractions from Australian canola meals. Food Res. Intl. **44**: 1075–1082. doi:10.1016/j.foodres.2011.03.023.

Tang, G., Xu, P., Ma, W., Wang, F., Liu, Z., Wan, S., and Shan, L. (2018). Seed-specific expression of AtLEC1 increased oil content and altered fatty acid composition in seeds of peanut (*Arachis hypogaea* L.). Fron. Plant Sci. **9:** 260. doi:10.3389/fpls.2018.00260.

Taylor, D.C., Zhang, Y., Kumar, A., Francis, T., Giblin, E.M., Barton, D.L., Ferrie, J.R., Laroche, A., Shah, S., Zhu, W., Snyder, C.L., Hall, L., Rakow, G., Harwood, J.L., and Weselake, R.J. (2009). Molecular modification of triacylglycerol accumulation by over-

expression of *DGAT1* to produce canola with increased seed oil content under field conditions. Plant Biotech. Inst. Bot. **87**: 533–543. doi:10.1139/B08-101.

Taylor, N.G., Howells, R.M., Huttly, A.K., Vickers, K., and Turner, S.R. (2003). Interactions among three distinct CesA proteins essential for cellulose synthesis. PNAS **100**: 1450–1455. doi:10.1073/pnas.0337628100.

Thelen, J.J., and Ohlrogge, J.B. (2002). Metabolic engineering of fatty acid biosynthesis in plants. Met. Eng. **4**: 12–21. doi:10.1006/mben.2001.0204.

Thompson, R.D. (2018). Storage protein synthesis. In: eLS. John Wiley & Sons, Ltd: Chichester. DOI: 10.1002/9780470015902.a0023693.

Tian, Y., Lv, X., Xie, G., Zhang, J., Xu, Y., and Chen, F. (2018). Seed-specific overexpression of AtFAX1 increases seed oil content in *Arabidopsis*. Biochem. Biophys. Res. Comm. **500**: 370–375. doi:10.1016/j.bbrc.2018.04.081.

Tian, Y., Lv, X., Xie, G., Wang, L., Dai, T., Qin, X., Chen, F., and Xu, Y. (2019). FAX2 mediates fatty acid export from plastids in developing *Arabidopsis* seeds. Plant Cell Phys. **60**: 2231–2242. doi:10.1093/pcp/pcz117.

Troncoso-Ponce, M.A., Barthole, G., Tremblais, G., To, A., Miquel, M., Lepiniec, L., and Baud, S. (2016). Transcriptional activation of two delta-9 palmitoyl-ACP desaturase genes by MYB115 and MYB118 is critical for biosynthesis of omega-7 monounsaturated fatty acids in the endosperm of *Arabidopsis* seeds. Plant Cell **28**: 2666–2682. doi:10.1105/tpc.16.00612.

Tzen, J.T.C. 2012. Integral proteins in plant oil bodies. ISRN Bot. **2012**: 173954. doi:10.5402/2012/173954.

Updegraff D.M. (1969). Semimicro determination of cellulose in biological materials. An. Biochem. **32**: 420–424.

Vain, T., Crowell, E.F., Timpano, H., Biot, E., Desprez, T., Mansoori, N., Trindade, L.M., Pagant, S., Robert, S., Höfte, H., Gonneau, M., and Vernhettes, S. (2014). The cellulase KORRIGAN is part of the cellulose synthase complex. Plant Phys. **165**: 1521–1532. doi:10.1104/pp.114.241216.

van de Loo, F.J., Broun, P., Turner, S., and Somerville, C. (1995). An oleate 12-hydroxylase from *Ricinus communis* L. is a fatty acyl desaturase homolog. PNAS **92**: 6743–6747. doi:10.1073/pnas.92.15.6743.

van Erp, H., Kelly, A.A., Menard, G., and Eastmond, P.J. (2014). Multigene engineering of triacylglycerol metabolism boosts seed oil content in *Arabidopsis*. Plant Phys. **165**: 30–36. doi:10.1104/pp.114.236430.

van Erp, H., Shockey, J., Zhang, M., Adhikari, N.D., and Browse, J. (2015). Reducing isozyme competition increases target fatty acid accumulation in seed triacylglycerols of transgenic *Arabidopsis*. Plant Phys. **168**: 36–46. doi:10.1104/pp.114.254110.

Van Wychen, S., Ramirez, K., and Laurens, L.M.L. (2016). Determination of total lipids as fatty acid methyl esters (FAME) by in situ transesterification: laboratory analytical procedure (LAP). Nat. Ren. En. Lab. doi:10.2172/1118085.

Vanhercke, T., Wood, C.C., Stymne, S., Singh, S.P., and Green, A.G. (2013). Metabolic engineering of plant oils and waxes for use as industrial feedstocks. Plant Biotech. J. **11**: 197–210. doi:10.1111/pbi.12023.

Vishwanath S.J., Domergue F., and Rowland O. (2014). Seed coat permeability test: tetrazolium penetration assay. Bio-Prot. **4**: e1173. doi: 10.21769/BioProtoc.1173.

Wan, Y., Wang, Y., Shi, Z., Rentsch, D., Ward, J.L., Hassall, K., Sparks, C.A., Huttly, A.K., Buchner, P., Powers, S., Shewry, P.R., and Hawkesford, M.J. (2021). Wheat amino acid

transporters highly expressed in grain cells regulate amino acid accumulation in grain. PLOS ONE **16**: e0246763. doi:10.1371/journal.pone.0246763.

Wanasundara, J.P.D., McIntosh, T.C., Perera, S.P., Withana-Gamage, T.S., and Mitra, P. (2016). Canola/rapeseed protein-functionality and nutrition. OCL **23**: D407. doi:10.1051/ocl/2016028.

Wang, T., Xing, J., Liu, X., Liu, Z., Yao, Y., Hu, Z., Peng, H., Xin, M., Zhou, D.-X., Zhang, Y., and Ni, Z. (2016A). Histone acetyltransferase general control non-repressed protein 5 (GCN5) affects the fatty acid composition of *Arabidopsis thaliana* seeds by acetylating *fatty acid desaturase3* (*FAD3*). Plant J. **88**: 794–808. doi:10.1111/tpj.13300.

Wang, J., Chen, Z., Zhang, Q., Meng, S., and Wei, C. (2020). The NAC transcription factors OsNAC20 and OsNAC26 regulate starch and storage protein synthesis. Plant Phys. **184**: 1775–1791. doi:10.1104/pp.20.00984.

Wang, Y., Peng, D., Zhang, L., Tan, X., Yuan, D., Liu, X., and Zhou, B. (2016B). Overexpression of SsDGAT2 from *Sapium sebiferum* (L.) Roxb increases seed oleic acid level in *Arabidopsis*. Plant Mol. Biol. Rep. **34**: 638–648. doi:10.1007/s11105-015-0954-y.

Wang, Y., Zhao, J., Chen, H., Zhang, Q., Zheng, Y., and Li, D. (2021). Molecular cloning and characterization of long-chain acyl-CoA synthetase 9 from the mesocarp of African oil palm (*Elaeis guineensis* Jacq.). Sci. Hort. **276**: 109751. doi:10.1016/j.scienta.2020.109751.

Wang, Z., Yang, M., Sun, Y., Yang, Q., Wei, L., Shao, Y., Bao, G., and Li, W. (2019). Overexpressing *Sesamum indicum* L.'s DGAT1 increases the seed oil content of transgenic soybean. Mol. Breed. **39**: 101. doi:10.1007/s11032-019-1016-1.

Warsame, A.O., O'Sullivan, D.M., and Tosi, P. (2018). Seed storage proteins of faba bean (*Vicia faba* L): current status and prospects for genetic improvement. J. Agric. Food Chem. **66**: 12617–12626. doi:10.1021/acs.jafc.8b04992.

Watson J, Greenough EB, Leet JE, Ford MJ, Drexler DM, Belcastro JV, Herbst JJ, Chatterjee M, Banks M. (2009). Extraction, identification, and functional characterization of a bioactive substance from automated compound-handling plastic tips. J. Biomol. Screen. **24**: 566-572. doi: 10.1177/1087057109336594

Watson, M.E., and Galliher, T.L. (2001). Comparison of Dumas and Kjeldahl methods with automatic analyzers on agricultural samples under routine rapid analysis conditions. Comm. Soil Sci. Plant An. **32**: 2007–2019. doi:10.1081/CSS-120000265.

Weigelt, K., Küster, H., Radchuk, R., Müller, M., Weichert, H., Fait, A., Fernie, A.R., Saalbach, I., and Weber, H. (2008). Increasing amino acid supply in pea embryos reveals specific interactions of N and C metabolism, and highlights the importance of mitochondrial metabolism. Plant J. **55**: 909–926. doi:10.1111/j.1365-313X.2008.03560.x.

Weiss, S.B., Kennedy, E.P., and Kiyasu, J.Y. (1960). The enzymatic synthesis of triglycerides. J. Biol. Chem. **235**: 40–44. doi:10.1016/S0021-9258(18)69581-X.

Welch, R.W. (1977). A micro-method for the estimation of oil content and composition in seed crops. J. Sci. Food Agric. **28**: 635–638. doi:10.1002/jsfa.2740280710.

Wickramasuriya, S.S., Yi, Y.-J., Yoo, J., Kang, N.K., and Heo, J.M. (2015). A review of canola meal as an alternative feed ingredient for ducks. J. Anim. Sci. Tech. **57**: 29. doi:10.1186/s40781-015-0062-4.

Wijekoon CP, Singer SD, Weselake RJ, Petrie JR, Singh S, Jayawardhane KN, Chen G, Eastmond PJ, Acharya SN. (2020). Enhancement of total lipid production in vegetative tissues

of alfalfa and sainfoin using chemical mutagenesis. Crop Breed. Genet. **60**: 2990-3003. doi: 10.1002/csc2.20027

Williams, M., and Randall, D.D. (1979). Pyruvate dehydrogenase complex from chloroplasts of *Pisum sativum* L. Plant Phys. **64**: 1099–1103. doi:10.1104/pp.64.6.1099.

Wilson, T.H., Kumar, M., and Turner, S.R. (2021). The molecular basis of plant cellulose synthase complex organisation and assembly. Biochem. Soc. Trans. **49**: 379–391. doi:10.1042/BST20200697.

Wood, C.C., Okada, S., Taylor, M.C., Menon, A., Mathew, A., Cullerne, D., Stephen, S.J., Allen, R.S., Zhou, X.-R., Liu, Q., Oakeshott, J.G., Singh, S.P., and Green, A.G. (2018). Seed-specific RNAi in safflower generates a superhigh oleic oil with extended oxidative stability. Plant Biotech. J. **16**: 1788–1796. doi:10.1111/pbi.12915.

Wu, P., Xu, X., Li, J., Zhang, J., Chang, S., Yang, X., and Guo, X. (2021). Seed-specific overexpression of cotton GhDGAT1 gene leads to increased oil accumulation in cottonseed. The Crop J. **9**: 487–490. doi:10.1016/j.cj.2020.10.003.

Xiao, S., and Chye, M.-L. (2011). New roles for acyl-CoA-binding proteins (ACBPs) in plant development, stress responses and lipid metabolism. Prog. Lip. Res. **50**: 141–151. doi:10.1016/j.plipres.2010.11.002.

Xiang, X., Wu, Y., Planta, J., Messing, J., and Leustek, T. (2018). Overexpression of serine acetyltransferase in maize leaves increases seed-specific methionine-rich zeins. Plant Biotech. J. **16**: 1057–1067. doi:10.1111/pbi.12851.

Xiong, Y., Ren, Y., Li, W., Wu, F., Yang, W., Huang, X., and Yao, J. (2019). NF-YC12 is a key multi-functional regulator of accumulation of seed storage substances in rice. J. Exp. Bot. **70**: 3765–3780. doi:10.1093/jxb/erz168.

Xu, Y., Caldo, K.M.P., Pal-Nath, D., Ozga, J., Lemieux, M.J., Weselake, R.J., and Chen, G. (2018A). Properties and biotechnological applications of acyl-CoA:diacylglycerol acyltransferase and phospholipid:diacylglycerol acyltransferase from terrestrial plants and microalgae. Lipids **53**: 663–688. doi:10.1002/lipd.12081.

Xu, Y., Holic, R., Li, D., Pan, X., Mietkiewska, E., Chen, G., Ozga, J., and Weselake, R.J. (2018B). Substrate preferences of long-chain acyl-CoA synthetase and diacylglycerol acyltransferase contribute to enrichment of flax seed oil with α-linolenic acid. Biochem. J. **475**: 1473–1489. doi:10.1042/BCJ20170910.

Xu, Y., Mietkiewska, E., Shah, S., Weselake, R.J., and Chen, G. (2020). Punicic acid production in *Brassica napus*. Met. Eng. **62**: 20–29. doi:10.1016/j.ymben.2020.08.011.

Xu, Z., Li, J., Guo, X., Jin, S., and Zhang, X. (2016). Metabolic engineering of cottonseed oil biosynthesis pathway via RNA interference. Sci. Rep. **6**: 33342. doi:10.1038/srep33342.

Yamamoto, M.P., Onodera, Y., Touno, S.M., and Takaiwa, F. (2006). Synergism between RPBF Dof and RISBZ1 bZIP activators in the regulation of rice seed expression genes. Plant Phys. 141: 1694–1707. doi:10.1104/pp.106.082826.

Yang B, Kallio HP. (2001). Fatty acid composition of lipids in sea buckthorn (*Hippophae rhamnoides* L.) berries of different origins. J. Ag. Food. Chem. **49**: 1939-1947.

Yang, G., Wei, Q., Huang, H., and Xia, J. (2020). Amino acid transporters in plant cells: a brief review. Plants **9**: 967. doi:10.3390/plants9080967.

Yang, J., Ji, C., and Wu, Y. (2016). Divergent transactivation of maize storage protein zein genes by the transcription factors Opaque2 and OHPs. Genet. **204**: 581–591. doi:10.1534/genetics.116.192385.

Yang, T., Guo, L., Ji, C., Wang, H., Wang, J., Zheng, X., Xiao, Q., and Wu, Y. (2021). The B3 domain-containing transcription factor ZmABI19 coordinates expression of key factors required for maize seed development and grain filling. Plant Cell **33**: 104–128. doi:10.1093/plcell/koaa008.

Yang, T., Wu, X., Wang, W., and Wu, Y. (2023). Regulation of seed storage protein synthesis in monocot and dicot plants: A comparative review. Mol. Plant **16**: 145–167. doi:10.1016/j.molp.2022.12.004.

Yatsu, L.Y., and Jacks, T.J. (1972). Spherosome membranes: half unit-membranes. Plant Phys. **49**: 937–943. doi:10.1104/pp.49.6.937.

Ye, J., Wang, C., Sun, Y., Qu, J., Mao, H., and Chua, N.-H. (2018). Overexpression of a transcription factor increases lipid content in a woody perennial *Jatropha curcas*. Fron. Plant Sci. **9**: 1479. doi:10.3389/fpls.2018.01479.

Ye, Y., Nikovics, K., To, A., Lepiniec, L., Fedosejevs, E.T., Van Doren, S.R., Baud, S., and Thelen, J.J. (2020). Docking of acetyl-CoA carboxylase to the plastid envelope membrane attenuates fatty acid production in plants. Nat Comm. **11**: 6191. doi:10.1038/s41467-020-20014-5.

Yeap, W.-C., Lee, F.-C., Shabari Shan, D.K., Musa, H., Appleton, D.R., and Kulaveerasingam, H. (2017). WRI1-1, ABI5, NF-YA3 and NF-YC2 increase oil biosynthesis in coordination with hormonal signaling during fruit development in oil palm. Plant J. **91**: 97–113. doi:10.1111/tpj.13549.

Yuan, N., Balasubramanian, V.K., Chopra, R., and Mendu, V. (2019). The photoperiodic flowering time regulator FKF1 negatively regulates cellulose biosynthesis. Plant Phys. **180**: 2240–2253. doi:10.1104/pp.19.00013.

Yuan, Y., Gao, L., Sun, R., Yu, T., Liang, Y., Li, D., and Zheng, Y. (2017). Seed-specific expression of an acyl-acyl carrier protein thioesterase CnFatB3 from coconut (*Cocos nucifera* L.) increases the accumulation of medium-chain fatty acids in transgenic *Arabidopsis* seeds. Sci. Hort. **223**: 5–9. doi:10.1016/j.scienta.2017.05.029.

Zduńczyk, Z., Jankowski, J., Juśkiewicz, J., Mikulski, D., and Slominski, B.A. (2013). Effect of different dietary levels of low-glucosinolate rapeseed (canola) meal and non-starch polysaccharide-degrading enzymes on growth performance and gut physiology of growing turkeys. Can. J. An. Sci. **93**: 353–362. doi:10.4141/cjas2012-085.

Zhai, Z., Liu, H., and Shanklin, J. (2017). Phosphorylation of WRINKLED1 by KIN10 results in its proteasomal degradation, providing a link between energy homeostasis and lipid biosynthesis. Plant Cell **29**: 871–889. doi:10.1105/tpc.17.00019.

Zhao, H., Kosma, D.K., and Lü, S. (2021). Functional role of long-chain acyl-coa synthetases in plant development and stress responses. Fron. Plant Sci. **12**: 640996. doi:10.3389/fpls.2021.640996.

Zhao, J., Bi, R., Li, S., Zhou, D., Bai, Y., Jing, G., Zhang, K., and Zhang, W. (2019A). Genome-wide analysis and functional characterization of Acyl-CoA:diacylglycerol acyltransferase from soybean identify GmDGAT1A and 1B roles in oil synthesis in *Arabidopsis* seeds. J. Plant Phys. **242**: 153019. doi:10.1016/j.jplph.2019.153019.

Zhao, L., Haslam, T.M., Sonntag, A., Molina, I., and Kunst, L. (2019B). Functional overlap of long-chain acyl-coa synthetases in *Arabidopsis*. Plant Cell Phys. **60**: 1041–1054. doi:10.1093/pcp/pcz019.

Zhao, L., Song, Z., Wang, B., Gao, Y., Shi, J., Sui, X., Chen, X., Zhang, Y., and Li, Y. (2022). R2R3-MYB transcription factor NtMYB330 regulates proanthocyanidin biosynthesis and seed

germination in tobacco (*Nicotiana tabacum* L.). Front. Plant Sci. **12**: 819247. doi:10.3389/fpls.2021.819247.

Zhao, P., Li, X., Jia, J., Yuan, G., Chen, S., Qi, D., Cheng, L., and Liu, G. (2019C). *bHLH92* from sheepgrass acts as a negative regulator of anthocyanin/proanthocyandin accumulation and influences seed dormancy. J. Exp. Bot. **70**: 269–284. doi:10.1093/jxb/ery335.

Zhang, D., Zhang, H., Hu, Z., Chu, S., Yu, K., Lv, L., Yang, Y., Zhang, X., Chen, X., Kan, G., Tang, Y., An, Y.-Q.C., and Yu, D. (2019A). Artificial selection on GmOLEO1 contributes to the increase in seed oil during soybean domestication. PLOS Genet. **15**: e1008267. doi:10.1371/journal.pgen.1008267.

Zhang, L., Garneau, M.G., Majumdar, R., Grant, J., and Tegeder, M. (2015). Improvement of pea biomass and seed productivity by simultaneous increase of phloem and embryo loading with amino acids. Plant J. **81**: 134–146. doi:10.1111/tpj.12716.

Zhang, M., Cao, X., Jia, Q., and Ohlrogge, J. (2016A). *FUSCA3* activates triacylglycerol accumulation in *Arabidopsis* seedlings and tobacco BY2 cells. Plant J. **88**: 95–107. doi:10.1111/tpj.13233.

Zhang, M., Fan, J., Taylor, D.C., and Ohlrogge, J.B. (2009). DGAT1 and PDAT1 acyltransferases have overlapping functions in *Arabidopsis* triacylglycerol biosynthesis and are essential for normal pollen and seed development. Plant Cell **21**: 3885–3901. doi:10.1105/tpc.109.071795.

Zhang, S., Sheng, H., Ma, Y., Wei, Y., Liu, D., Dou, Y., Cui, H., Liang, B., Liesche, J., Li, J., and Chen, S. (2022). Mutation of CESA1 phosphorylation site influences pectin synthesis and methylesterification with a role in seed development. J. Plant Phys. **270**: 153631. doi:10.1016/j.jplph.2022.153631.

Zhang, T.-T., He, H., Xu, C.-J., Fu, Q., Tao, Y.-B., Xu, R., and Xu, Z.-F. (2021). Overexpression of type 1 and 2 diacylglycerol acyltransferase genes (*JcDGAT1* and *JcDGAT2*) enhances oil production in the woody perennial biofuel plant *Jatropha curcas*. Plants **10**: 699. doi:10.3390/plants10040699.

Zhang, Y., Nikolovski, N., Sorieul, M., Vellosillo, T., McFarlane, H.E., Dupree, R., Kesten, C., Schneider, R., Driemeier, C., Lathe, R., Lampugnani, E., Yu, X., Ivakov, A., Doblin, M.S., Mortimer, J.C., Brown, S.P., Persson, S., and Dupree, P. (2016B). Golgi-localized STELLO proteins regulate the assembly and trafficking of cellulose synthase complexes in *Arabidopsis*. Nat. Comm. **7**: 11656. doi:10.1038/ncomms11656.

Zhang, Y.-Q., Lu, X., Zhao, F.-Y., Li, Q.-T., Niu, S.-L., Wei, W., Zhang, W.-K., Ma, B., Chen, S.-Y., and Zhang, J.-S. (2016C). Soybean GmDREBL increases lipid content in seeds of transgenic *Arabidopsis*. Sci. Rep. **6**: 34307. doi:10.1038/srep34307.

Zhang, Z., Yang, J., and Wu, Y. (2015). Transcriptional regulation of zein gene expression in maize through the additive and synergistic action of Opaque2, prolamine-box binding factor, and O2 heterodimerizing proteins. Plant Cell **27**: 1162–1172. doi:10.1105/tpc.15.00035.

Zhang, Z., Dong, J., Ji, C., Wu, Y., and Messing, J. (2019B). NAC-type transcription factors regulate accumulation of starch and protein in maize seeds. PNAS **116**: 11223–11228. doi:10.1073/pnas.1904995116.

Zheng, X., Li, Q., Li, C., An, D., Xiao, Q., Wang, W., and Wu, Y. (2019). Intra- kernel reallocation of proteins in maize depends on VP1-mediated scutellum development and nutrient assimilation. Plant Cell **31**: 2613–2635. doi:10.1105/tpc.19.00444R1.

Zheng, Y.-S., Chen, H., Yuan, Y., Wang, Y., Chen, L., Liu, X., and Li, D.-D. (2018). Cloning and functional characterization of long-chain acyl-CoA synthetase 1 from the mesocarp of African

oil palm (*Elaeis guineensis* Jacq.). Ind. Crops Prod. **122**: 252–260. doi:10.1016/j.indcrop.2018.06.003.

Zhong C., Xu H., Zhang S., and Wang X. (2016). *Arabidopsis* seed germination sssay with gibberellic acid. Bio-Prot. **6**: e2005. doi: 10.21769/BioProtoc.2005.

Zhou, W., Wang, X., Zhou, D., Ouyang, Y., and Yao, J. (2017). Overexpression of the 16-kDa α-amylase/trypsin inhibitor RAG2 improves grain yield and quality of rice. Plant Biotech. J. **15**: 568–580. doi:10.1111/pbi.12654.

Zhou, Y., Cai, H., Xiao, J., Li, X., Zhang, Q., and Lian, X. (2009). Over-expression of aspartate aminotransferase genes in rice resulted in altered nitrogen metabolism and increased amino acid content in seeds. Theo. App. Genet. **118**: 1381–1390. doi:10.1007/s00122-009-0988-3.

Zhu, Y., Xie, L., Chen, G.Q., Lee, M.Y., Loque, D., and Scheller, H.V. (2018). A transgene design for enhancing oil content in *Arabidopsis* and *Camelina* seeds. Biotech. Biof. **11**: 46. doi:10.1186/s13068-018-1049-4.

Appendix

Table S1. Fatty acid percent mass of *Arabidopsis* seeds transmethylated at 80°C in 3M methanolic HCl at different incubation lengths

FA\Mins	60	90	120	180	240	ON (1hx)	ON (2hx)
16:0	1.75 ± 0.02	2.14 ± 0.02	2.21 ± 0.00	2.61 ± 0.00	2.77 ± 0.02	2.66 ± 0.02	2.72 ± 0.01
16:1	0.55 ± 0.07	0.34 ± 0.05	0.24 ± 0.01	0.16 ± 0.02	0.15 ± 0.01	0.10 ± 0.01	0.09 ± 0.00
18:0	0.49 ± 0.02	0.71 ± 0.01	0.81 ± 0.00	1.00 ± 0.01	1.09 ± 0.01	1.17 ± 0.02	1.14 ± 0.00
18:1	2.97 ± 0.08	4.22 ± 0.08	4.59 ± 0.01	5.56 ± 0.05	6.00 ± 0.07	5.99 ± 0.05	5.99 ± 0.04
18:2	7.21 ± 0.04	8.70 ± 0.04	8.64 ± 0.03	10.12 ± 0.10	10.79 ± 0.15	10.45 ± 0.05	10.48 ± 0.10
18:3	5.65 ± 0.04	6.33 ± 0.10	5.78 ± 0.08	6.70 ± 0.12	7.10 ± 0.12	6.46 ± 0.09	6.62 ± 0.05
20:0	0.27 ± 0.02	0.41 ± 0.01	0.51 ± 0.00	0.62 ± 0.03	0.67 ± 0.01	0.79 ± 0.00	0.74 ± 0.02
20:1	2.68 ± 0.01	3.89 ± 0.06	4.41 ± 0.09	6.11 ± 0.32	6.59 ± 0.42	6.34 ± 0.04	7.04 ± 0.28
20:2	0.29 ± 0.01	0.42 ± 0.01	0.47 ± 0.00	0.54 ± 0.01	0.62 ± 0.01	0.59 ± 0.01	0.58 ± 0.03
22:1	0.19 ± 0.01	0.29 ± 0.02	0.39 ± 0.00	0.51 ± 0.02	0.58 ± 0.03	0.62 ± 0.03	0.54 ± 0.03

Table S2. Fatty acid percent mass of *Arabidopsis* seeds transmethylated at 95°C in 3M methanolic HCl

FA\Mins	60	90	120	180	240
16:0	2.27 ± 0.00	2.64 ± 0.00	2.60 ± 0.00	2.76 ± 0.01	2.83 ± 0.00
16:1	0.25 ± 0.00	0.21 ± 0.00	0.17 ± 0.00	0.15 ± 0.00	0.30 ± 0.01
18:0	0.89 ± 0.00	1.01 ± 0.00	1.09 ± 0.00	1.13 ± 0.00	1.05 ± 0.00
18:1	4.51 ± 0.01	5.42 ± 0.02	5.65 ± 0.01	5.90 ± 0.03	5.54 ± 0.01
18:2	8.89 ± 0.00	10.37 ± 0.01	10.33 ± 0.00	10.94 ± 0.01	11.20 ± 0.01
18:3	5.85 ± 0.01	6.78 ± 0.01	6.49 ± 0.03	7.10 ± 0.00	7.50 ± 0.01
20:0	0.52 ± 0.00	0.64 ± 0.00	0.73 ± 0.00	0.74 ± 0.00	0.73 ± 0.00
20:1	4.78 ± 0.00	5.87 ± 0.00	6.28 ± 0.02	6.37 ± 0.01	6.29 ± 0.01
20:2	0.47 ± 0.00	0.56 ± 0.00	0.57 ± 0.00	0.60 ± 0.00	0.57 ± 0.00
22:1	0.40 ± 0.00	0.47 ± 0.00	0.53 ± 0.00	0.57 ± 0.00	0.52 ± 0.00

Table S3. Fatty acid percent mass of *Arabidopsis* seeds transmethylated at 95°C in 2% methanolic H_2SO_4

FA\Mins	60	75	90	120	240
16:0	1.62 ± 0.01	1.96 ± 0.01	2.38 ± 0.05	2.86 ± 0.00	2.92 ± 0.01
16:1	0.18 ± 0.01	0.17 ± 0.00	0.16 ± 0.01	0.15 ± 0.00	0.11 ± 0.00
18:0	0.53 ± 0.01	0.69 ± 0.01	0.89 ± 0.02	1.16 ± 0.02	1.27 ± 0.01
18:1	2.65 ± 0.01	3.38 ± 0.02	4.25 ± 0.06	5.38 ± 0.05	5.54 ± 0.08
18:2	6.24 ± 0.07	7.42 ± 0.02	9.07 ± 0.15	11.09 ± 0.03	11.11 ± 0.10
18:3	4.35 ± 0.06	5.06 ± 0.01	5.88 ± 0.08	7.22 ± 0.09	6.98 ± 0.11
20:0	0.52 ± 0.00	0.64 ± 0.00	0.73 ± 0.00	0.74 ± 0.00	0.73 ± 0.00
20:1	4.78 ± 0.00	5.87 ± 0.00	6.28 ± 0.02	6.37 ± 0.01	6.29 ± 0.01
20:2	0.47 ± 0.00	0.56 ± 0.00	0.57 ± 0.00	0.60 ± 0.00	0.57 ± 0.00
22:1	0.40 ± 0.00	0.47 ± 0.00	0.53 ± 0.00	0.57 ± 0.00	0.52 ± 0.00

Table S4. Fatty acid percent mass of *Arabidopsis* seeds transmethylated at 95°C in 5% methanolic H_2SO_4

FA\Mins	60	75	90	120	180	240
16:0	1.87 ± 0.01	2.08 ± 0.01	2.35 ± 0.02	2.91 ± 0.02	2.78 ± 0.01	2.84 ± 0.01
16:1	0.14 ± 0.00	0.11 ± 0.00	0.12 ± 0.01	0.11 ± 0.00	0.10 ± 0.00	0.10 ± 0.00
18:0	0.66 ± 0.00	0.78 ± 0.01	0.89 ± 0.01	1.22 ± 0.02	1.18 ± 0.02	1.25 ± 0.00
18:1	3.23 ± 0.01	3.71 ± 0.00	4.21 ± 0.02	5.48 ± 0.01	5.27 ± 0.01	5.29 ± 0.01
18:2	7.11 ± 0.02	7.87 ± 0.02	8.85 ± 0.05	11.07 ± 0.02	10.42 ± 0.01	10.57 ± 0.02
18:3	4.70 ± 0.01	5.16 ± 0.03	5.80 ± 0.04	7.11 ± 0.02	6.56 ± 0.01	6.61 ± 0.00
20:0	0.35 ± 0.01	0.44 ± 0.01	0.52 ± 0.02	0.74 ± 0.00	0.76 ± 0.01	0.75 ± 0.00
20:1	3.67 ± 0.01	4.44 ± 0.02	5.09 ± 0.06	6.86 ± 0.03	6.73 ± 0.03	6.70 ± 0.03
20:2	0.33 ± 0.00	0.38 ± 0.00	0.44 ± 0.00	0.58 ± 0.00	0.61 ± 0.02	0.70 ± 0.00
22:1	0.23 ± 0.01	0.31 ± 0.01	0.36 ± 0.01	0.53 ± 0.01	0.55 ± 0.00	0.54 ± 0.00

Table S5. Fatty acid percent mass of *Arabidopsis* seeds transmethylated at 110°C in 2% methanolic H_2SO_4

FA\Mins	40	50	60	70	80	120
16:0	2.19 ± 0.02	2.77 ± 0.02	2.64 ± 0.02	2.78 ± 0.01	2.79 ± 0.00	2.74 ± 0.01
16:1	0.14 ± 0.00	0.16 ± 0.01	0.15 ± 0.01	0.15 ± 0.00	0.16 ± 0.01	0.11 ± 0.00
18:0	0.81 ± 0.01	1.07 ± 0.02	1.06 ± 0.00	1.16 ± 0.01	1.17 ± 0.01	1.18 ± 0.01
18:1	4.45 ± 0.05	5.77 ± 0.04	5.61 ± 0.02	6.08 ± 0.03	6.13 ± 0.05	5.97 ± 0.01
18:2	8.35 ± 0.07	10.66 ± 0.05	9.98 ± 0.02	10.73 ± 0.03	10.76 ± 0.03	10.22 ± 0.01
18:3	5.59 ± 0.14	7.25 ± 0.14	6.54 ± 0.04	6.96 ± 0.08	7.06 ± 0.08	6.41 ± 0.02
20:0	0.47 ± 0.01	0.66 ± 0.01	0.67 ± 0.01	0.76 ± 0.01	0.76 ± 0.01	0.82 ± 0.01
20:1	5.02 ± 0.17	7.08 ± 0.08	6.94 ± 0.05	7.63 ± 0.06	7.66 ± 0.05	7.65 ± 0.02
20:2	0.39 ± 0.01	0.54 ± 0.01	0.53 ± 0.00	0.59 ± 0.00	0.57 ± 0.00	0.62 ± 0.03
22:1	0.32 ± 0.01	0.47 ± 0.01	0.49 ± 0.01	0.56 ± 0.01	0.56 ± 0.00	0.61 ± 0.00

Table S6. Fatty acid percent mass of Alfalfa leaves transmethylated at 95°C in 2% methanolic H_2SO_4

FA\Mins	45	60	120
16:0	0.73 ± 0.01	0.72 ± 0.01	0.71 ± 0.00
18:0	0.09 ± 0.00	0.10 ± 0.01	0.09 ± 0.00
18:1	0.08 ± 0.00	0.08 ± 0.00	0.08 ± 0.00
18:2	0.10 ± 0.00	0.11 ± 0.01	0.09 ± 0.00
18:3	0.74 ± 0.03	0.69 ± 0.00	0.67 ± 0.00

Table S7. Fatty acid percent mass of Canola (*Brassica napus*) seeds transmethylated at 95°C in 2% methanolic H_2SO_4

FA\Mins	45	60	70	120
16:0	1.50 ± 0.03	1.71 ± 0.07	1.95 ± 0.01	1.99 ± 0.05
18:0	0.58 ± 0.01	0.68 ± 0.00	0.83 ± 0.02	0.87 ± 0.02
18:1	21.96 ± 0.11	25.30 ± 0.23	29.99 ± 0.09	29.74 ± 0.15
18:2	6.88 ± 0.08	7.89 ± 0.16	9.22 ± 0.09	8.96 ± 0.11
18:3	4.06 ± 0.05	4.55 ± 0.02	5.45 ± 0.02	5.12 ± 0.04

Table S8. Fatty acid percent mass of *Caragana arborescens* seeds transmethylated at 95°C in 2% methanolic H_2SO_4

FA/Mins	90	120	180
16:0	0.57 ± 0.00	0.56 ± 0.01	0.64 ± 0.07
18:0	0.36 ± 0.00	0.37 ± 0.00	0.29 ± 0.03
18:1	4.50 ± 0.03	4.51 ± 0.02	3.19 ± 0.05
18:2	8.73 ± 0.02	8.73 ± 0.03	10.07 ± 0.11
18:3	0.18 ± 0.00	0.18 ± 0.00	0.22 ± 0.02

Table S9. Fatty acid percent mass of Flax (*Linum usitatissimum*) seeds transmethylated at 95°C in 2% methanolic H_2SO_4

FA/Mins	60	90	120	150
16:0	2.43 ± 0.03	2.32 ± 0.03	2.24 ± 0.01	2.22 ± 0.02
18:0	1.69 ± 0.03	1.55 ± 0.05	1.48 ± 0.03	1.51 ± 0.03
18:1	7.70 ± 0.06	7.57 ± 0.04	7.39 ± 0.05	7.22 ± 0.06
18:2	5.21 ± 0.03	5.40 ± 0.03	5.27 ± 0.02	5.06 ± 0.03
18:3	16.63 ± 0.08	17.17 ± 0.11	16.75 ± 0.07	15.91 ± 0.09

Table S10. Fatty acid percent mass of Proso Millet (*Panicum miliaceum*) seeds transmethylated at 95°C in 2% methanolic H_2SO_4

FA/Mins	45	75	120	180
16:0	0.53 ± 0.02	0.46 ± 0.02	0.45 ± 0.03	0.46 ± 0.01
18:0	0.06 ± 0.00	0.06 ± 0.00	0.07 ± 0.01	0.05 ± 0.00
18:1	1.03 ± 0.01	0.90 ± 0.01	0.83 ± 0.03	0.99 ± 0.02
18:2	3.53 ± 0.03	2.94 ± 0.02	2.96 ± 0.04	3.07 ± 0.02
18:3	0.06 ± 0.00	0.05 ± 0.00	0.07 ± 0.01	0.06 ± 0.01

Table S11. Fatty acid percent mass of Apple of Peru (*Nicandra physalodes*) seeds transmethylated at 95°C in 2% methanolic H_2SO_4

FA/Mins	90	180	240
16:0	2.16 ± 0.01	2.39 ± 0.01	2.28 ± 0.01
18:0	0.79 ± 0.01	0.94 ± 0.01	0.87 ± 0.01
18:1	3.28 ± 0.02	3.62 ± 0.07	3.32 ± 0.10
18:2	16.85 ± 0.04	18.80 ± 0.08	17.70 ± 0.10

Table S12. Fatty acid percent mass of Poppy (*Papaver somniferum*) seeds transmethylated at 95°C in 2% methanolic H_2SO_4

FA/Mins	45	75	120	180
16:0	3.90 ± 0.01	4.48 ± 0.01	4.52 ± 0.01	4.61 ± 0.01
18:0	0.73 ± 0.00	0.86 ± 0.00	0.87 ± 0.00	0.90 ± 0.01
18:1	5.01 ± 0.04	5.78 ± 0.03	5.83 ± 0.03	5.95 ± 0.04
18:2	27.92 ± 0.04	32.12 ± 0.04	32.40 ± 0.03	32.76 ± 0.05

Table S13. Fatty acid percent mass of Sea Buckthorn (*Hippophae rhamnoides*) seeds transmethylated at 95°C in 2% methanolic H_2SO_4

FA/Mins	90	180	240
16:0	1.10 ± 0.01	1.11 ± 0.02	1.18 ± 0.03
16:1	0.35 ± 0.01	0.36 ± 0.01	0.38 ± 0.02
18:0	0.33 ± 0.00	0.33 ± 0.00	0.35 ± 0.00
18:1	1.58 ± 0.00	1.52 ± 0.00	1.60 ± 0.01
18:2	3.71 ± 0.01	3.55 ± 0.01	3.77 ± 0.02
18:3	3.58 ± 0.01	3.41 ± 0.02	3.62 ± 0.03
20:0	0.05 ± 0.00	0.05 ± 0.00	0.05 ± 0.00

Table S14. Fatty acid percent mass of Canola, *Arabidopsis*, Flax, Apple of Peru, and Proso millet seeds analyzed by both the optimized Direct Methylation (DM) method and the Hara-Radin (HR) methods

FA\Species	Canola-HR	Canola-DM	*Arabidopsis* -HR	*Arabidopsis* -DM	Flax-HR
16:0	2.08 ± 0.02	1.94 ± 0.04	2.80 ± 0.05	2.84 ± 0.01	2.00 ± 0.08
16:1	0.02 ± 0.02	0.13 ± 0.01	0.00 ± 0.00	0.00 ± 0.00	0.00 ± 0.07
18:0	0.91 ± 0.06	0.85 ± 0.01	1.25 ± 0.05	1.19 ± 0.03	1.35 ± 0.11
18:1	30.41 ± 0.25	29.15 ± 0.12	5.93 ± 0.15	5.37 ± 0.05	7.41 ± 0.09
18:2	8.73 ± 0.06	8.85 ± 0.10	10.04 ± 0.13	10.94 ± 0.02	5.66 ± 0.25
18:3	4.44 ± 0.07	5.08 ± 0.05	6.11 ± 0.10	7.02 ± 0.09	16.91 ± 0.01
20:0	0.21 ± 0.11	0.27 ± 0.01	0.80 ± 0.05	0.72 ± 0.02	0.10 ± 0.00
20:1	0.56 ± 0.10	0.54 ± 0.04	7.10 ± 0.18	6.67 ± 0.09	0.03 ± 0.00
20:2	0.00 ± 0.00	0.00 ± 0.00	0.63 ± 0.03	0.59 ± 0.01	0.00 ± 0.00
22:1	0.00 ± 0.00	0.00 ± 0.00	0.70 ± 0.02	0.52 ± 0.01	0.00 ± 0.00
FA\Species	Flax-DM	Nicandra-HR	Nicandra-DM	Millet-HR	Millet-DM
16:0	2.38 ± 0.03	2.17 ± 0.00	2.24 ± 0.01	0.32 ± 0.01	0.47 ± 0.02
16:1	0.00 ± 0.03	0.07 ± 0.00	0.05 ± 0.00	0.00 ± 0.00	0.00 ± 0.00
18:0	1.65 ± 0.08	0.78 ± 0.02	0.86 ± 0.00	0.05 ± 0.01	0.06 ± 0.01
18:1	7.51 ± 0.04	3.14 ± 0.01	3.40 ± 0.03	0.94 ± 0.01	0.91 ± 0.03
18:2	5.08 ± 0.10	17.00 ± 0.07	17.42 ± 0.04	3.20 ± 0.01	3.11 ± 0.00
18:3	16.21 ± 0.02	0.09 ± 0.00	0.08 ± 0.00	0.06 ± 0.00	0.06 ± 0.00
20:0	0.29 ± 0.00	0.09 ± 0.00	0.09 ± 0.00	0.00 ± 0.00	0.00 ± 0.00
20:1	0.05 ± 0.00	0.00 ± 0.00	0.00 ± 0.00	0.00 ± 0.00	0.00 ± 0.00
20:2	0.00 ± 0.00	0.00 ± 0.00	0.00 ± 0.00	0.00 ± 0.00	0.00 ± 0.00
22:1	0.00 ± 0.00	0.00 ± 0.00	0.00 ± 0.00	0.00 ± 0.00	0.00 ± 0.00

Table S15. Promoter, dsRed, and Kanamycin Nucleotide Sequences for pBin Vectors

Name	Sequence (5' → 3')
Glycinin promoter	gatccgtacgtaagtacgtactcaaaatgccaacaaataaaaaaaaagttgctttaataatgccaaaacaaattaata aaacacttacaacaccggatttttttttaattaaaatgtgccatttaggataaatagttaatatttttaataattatttaaaaa gccgtatctactaaaatgatttttatttggttgaaaatattaatatgtttaaatcaacacaatctatcaaaattaaactaaa aaaaaaataagtgtacgtggttaacattagtacagtaatataagaggaaaatgagaaattaagaaattgaaagcga gtctaatttttaaattatgaacctgcatatataaaaggaaagaaagaatccaggaagaaaagaaatgaaaccatgca tggtcccctcgtcatcacgagtttctgccatttgcaatagaaacactgaaacacctttctctttgtcacttaattgagat gccgaagccacctcacaccatgaacttcatgaggtgtagcacccaaggcttccatagccatgcatactgaagaat gtctcaagctcagcaccctacttctgtgacgtgtccctcattcaccttcctctcttccctataaataaccacgcctcag gttctccgcttcacaactcaaacattctctccattggtccttaaacactcatcagtcatcaccgcggccgcg
CaMV 35S Promoter	gatcctcgacgaattaattccaatcccacaaaaatctgagcttaacagcacagttgctcctctcagagcagaatcgg gtattcaacaccctcatatcaactactacgttgtgtataacggtccacatgccggtatatacgatgactggggttgtac aaaggcggcaacaaacggcgttcccggagttgcacacaagaaatttgccactattacagaggcaagagcagca gctgacgcgtacacaacaagtcagcaaacagacaggttgaacttcatccccaaaggagaagctcaactcaagcc caagagctttgctaaggccctaacaagcccaccaaagcaaaaagcccactggctcacgctaggaaccaaaagg cccagcagtgatccagccccaaaagagatctcctttgccccggagattacaatggacgatttcctctatctttacgat ctaggaaggaagttcgaaggtgaaggtgacgacactatgttcaccactgataatgagaaggttagcctcttcaattt cagaaagaatgctgacccacagatggttagaggcctacgcagcaggtctcatcaagacgatctacccgagta acaatctccaggagatcaaataccttcccaagaaggttaaagatgcagtcaaaagattcaggactaattgcatcaa gaacacagagaaagacatatttctcaagatcagaagtactattccagtatggacgattcaaggcttgcttcataaac caaggcaagtaatagagattggagtctctaaaaaggtagttcctactgaatctaaggccatgcatggagtctaagat tcaaatcgaggatctaacagaactcgccgtgaagactggcgaacagttcatacagagtcttttacgactcaatgac aagaagaaaatcttcgtcaacatggtggagcacgacactctggtctactccaaaaatgtcaaagatacagtctcag aagaccaaagggctattgagacttttcaacaaaggataatttcgggaaacctcctcggattccattgcccagctatct gtcacttcatcgaaaggacagtagaaaaggaaggtggctcctacaaatgccatcattgcgataaaggaaaggcta tcattcaagatctctctgccgacagtggtcccaaagatggacccccacccacgaggagcatcgtggaaaaagaa gacgttccaaccacgtcttcaaagcaagtggattgatgtgacatctccactgacgtaagggatgacgcacaatccc actatccttcgcaagacccttcctctatataaggaagttcatttcatttggagaggacacg
CMV promoter	ctagtagaaggtaattatccaagatgtagcatcaagaatccaatgtttacgggaaaaactatggaagtattatgtgag ctcagcaagaagcagatcaatatgcggcacatatgcaacctatgttcaaaaatgaagaatgtacagatacaagatc ctatactgccagaatacgaagaagaatacgtagaaattgaaaaagaagaaccaggcgaagaaaagaatcttgaa gacgtaagcactgacgacaacaatgaaaagaagaagataaggtcggtgattgtgaaagagacatagaggacac atgtaaggtggaaaatgtaagggcggaaagtaaccttatcacaaaggaatcttatcccccactacttatccttttatat ttttccgtgtcatttttgcccttgagtttcctatataaggaaccaagttcggcatttgtgaaaacaagaaaaaattggtg taagctattttctttgaagtactgaggatacaacttcagagaaatttgtaagaaagtggatcgaaac
dsRed	atggcctcctccgagaacgtcatcaccgagttcatgcgcttcaaggtgcgcatggagggcaccgtgaacggcca cgagttcgagatcgagggcgagggcgagggccgcccctacgagggccacaacaccgtgaagctgaaggtga ccaagggcggccccctgcccttcgcctgggacatcctgtccccccagttccagtacggctccaaggtgtacgtga agcaccccgccgacatccccgactacaagaagctgtccttccccgagggcttcaagtgggagcgcgtgatgaac ttcgaggacggcggcgtggcgaccgtgacccaggactcctccctgcaggacggctgcttcatctacaaggtgaa gttcatcggcgtgaacttcccctccgacggccccgtgatgcagaagaagaccatgggctgggaggcctccaccg

	agcgcctgtacccccgcgacggcgtgctgaagggcgagacccacaaggccctgaagctgaaggacggcggc cactacctggtggagttcaagtccatctacatggccaagaagcccgtgcagctgcccggctactactacgtggac gccaagctggacatcacctcccacaacgaggactacaccatcgtggagcagtacgagcgcaccgagggccgc caccacctgttcctggtaccaatga
Aminoglycoside phosphotransferase (kanamycin resistance gene)	atggctaaaatgagaatatcaccggaattgaaaaaactgatcgaaaaataccgctgcgtaaaagatacggaagga atgtctcctgctaaggtatataagctggtgggagaaaatgaaaacctatatttaaaaatgacggacagccggtataa agggaccacctatgatgtggaacgggaaaaggacatgatgctatggctggaaggaaagctgcctgttccaaagg tcctgcactttgaacggcatgatggctggagcaatctgctcatgagtgaggccgatggcgtcctttgctcggaaga gtatgaagatgaacaaagccctgaaaagattatcgagctgtatgcggagtgcatcaggctctttcactccatcgac atatcggattgtccctatacgaatagcttagacagccgcttagccgaattggattacttactgaataacgatctggcc gatgtggattgcgaaaactgggaagaagacactccatttaaagatccgcgcgagctgtatgatttttttaaagacgg aaaagcccgaagaggaacttgtcttttcccacggcgacctgggagacagcaacatctttgtgaaagatggcaaag taagtggctttattgatcttgggagaagcggcagggcggacaagtggtatgacattgccttctgcgtccggtcgatc agggaggatatcggggaagaacagtatgtcgagctatttttgacttactggggatcaagcctgattgggagaaaa taaaatattatattttactggatgaattgttttag

Table S16. Primers for PCR Amplification of *AtAAP1*, *AtALAAT1*, *AtASN1* & *AtUmamiT18* with vector-overlaps for homology-directed recombination

Vector	Primer Name	Sequence 5' → 3'
pBinGlyRed3 + 35S	UT18_35S_FRAG_FOR	cctctatataaggaagttcatttcatttggagaggacacgATGAAAGGTGGAAGCATGGAGAAAAT
pBinGlyRed3 + 35S	UT18/35S/FRAG_REV	caaaagtggggtagcacatacaaaaagggctgcggccgccTCAGGTACTGGTAACCACACCGT
pBinGlyRed3 + 35S	UT18_35S_INT_FOR	TGAGACGGTGAACTTTAGAAAGGTCC
pBinGlyRed3 + 35S	UT18_35S_INT_REV	TGCCGATTTTCCATGCACTCG
pBinGlyRed3 + Glycinin	AAP1_GLY_FRAG_FOR	attggtccttaaacactcatcagtcatcaccgcggccgcgATGAAGAGTTTCAACACAGAAGGACACA
pBinGlyRed3 + Glycinin	AAP1_GLY_FRAG_REV	caaaagtggggtagcacatacaaaaagggctgcggccgccTCACTCATGCATAGTCCGGAAGG
pBinGlyRed3 + Glycinin	AAP1_GLY_INT_FOR	TTCCACGATAAAGGGCACACTGC
pBinGlyRed3 + Glycinin	AAP1_GLY_INT_REV	TTGCAAAGTCAATGAGCCAAAAGGG
pBinGlyRed3 + Glycinin	AlaAT1_GLY_FRAG.FOR	attggtccttaaacactcatcagtcatcaccgcggccgcgATGCGGAGATTCGTGATTGGC
pBinGlyRed3 + Glycinin	AlaAT1_GLY_FRAG.REV	caaaagtggggtagcacatacaaaaagggctgcggccgccTTAGTCGCGGAACTCGTCCATG
pBinGlyRed3 + Glycinin	AlaAT1_GLY_INT_FOR	AATTGCTGATGGAATCGAAGCCC

pBinGlyRed3 + Glycinin	AlaAT1_GLY_INT_REV	TCTTTTCCCACACTCTCCATAGTACCC
pBinGlyRed3 + Glycinin	ANS1_GLY_FRAG_FOR	attggtccttaaacactcatcagtcatcaccgcggccgcgATGTGTGGAATACTTGCCGTGT
pBinGlyRed3 + Glycinin	ANS1_GLY_FRAG_REV	caaaagtggggtagcacatacaaaaagggctgcggccgccTTATGACTGAATCACAACTCCTTGACCCA
pBinGlyRed3 + Glycinin	ANS1_GLY_INT_FOR	TTCAATGAATCTGTTCCTTCAACGCC
pBinGlyRed3 + Glycinin	ANS1_GLY_INT_REV	TTTGTCAAGGAAAGGAACACGTGCC
pBinGlyRed3 + Glycinin	UT18_GLY_FRAG_FOR	attggtccttaaacactcatcagtcatcaccgcggccgcgATGAAAGGTGGAAGCATGGAG
pBinGlyRed3 + Glycinin	UT18_GLY_FRAG_REV	caaaagtggggtagcacatacaaaaagggctgcggccgccTCAGGTACTGGTAACCACACCGT
pBinGlyRed3 + Glycinin	UT18_GLY_INT_FOR	TCATTCTCGCCCTCATTTTCAGGC
pBinGlyRed3 + Glycinin	UT18_GLY_INT_REV	ACAAACCACTCCAGAGTAAACCGC

Lowercase letters indicate nucleotides that are complementary with the vectors (pBinGlyRed or pBin35SRed) while uppercase letters are complementary to the insert.

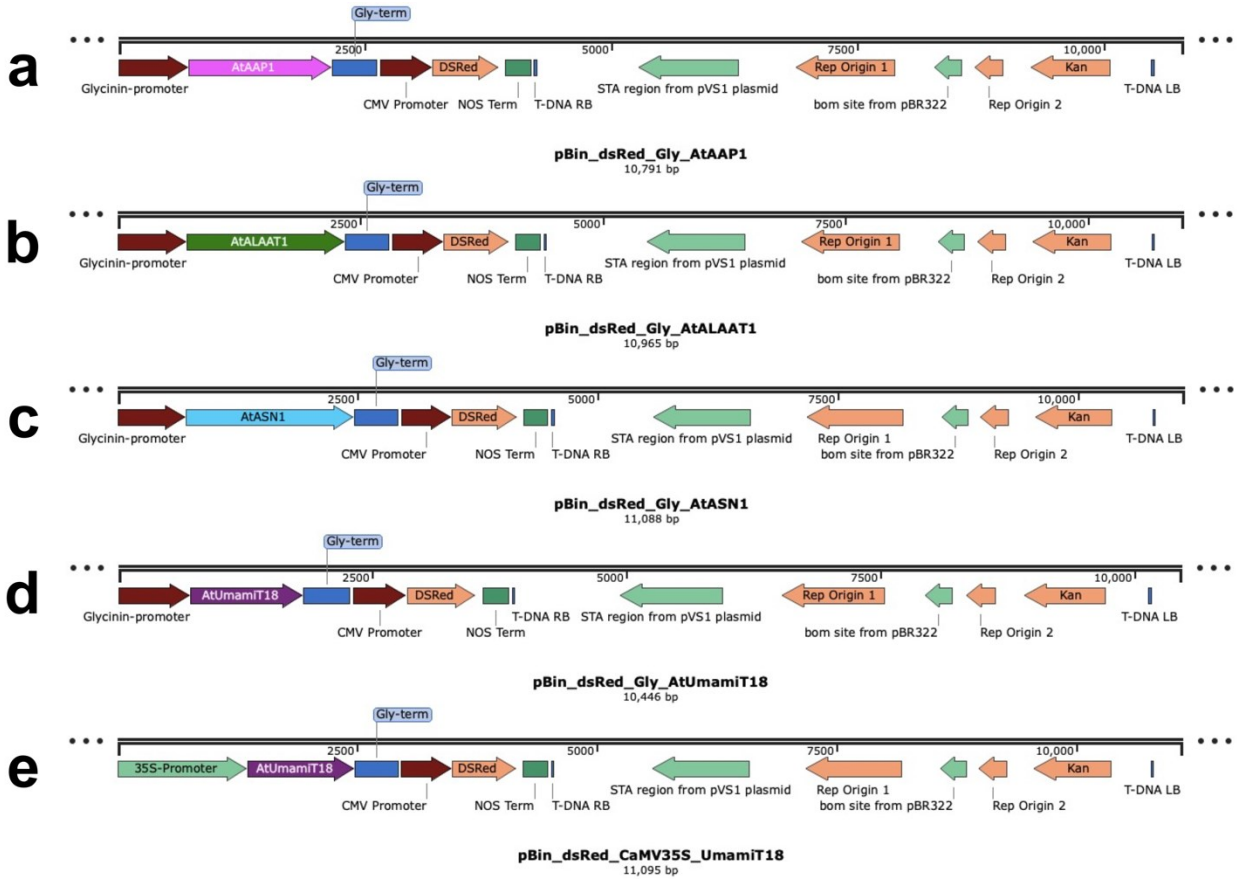

Figure S1. Schematic vector maps of *AtAAP1*, *AtALAAT1*, *AtASN1*, & *AtUmamiT18* overexpression constructs in pBinGlyRed and pBinGly35S plasmids
All constructs employed the constitutive expression of dsRed as a fluorescent selection marker. Overexpression construct of *AtAAP1* driven by the glycinin seed specific promoter (a), overexpression construct of *AtALALAAT1* driven by the glycinin seed specific promoter (b), overexpression construct of *AtASN1* driven by the glycinin seed specific promoter (c), overexpression construct of *AtUmamiT18* driven by the glycinin seed specific promoter (d), overexpression construct of *AtUmamiT18* driven by the constitutive Cauliflower Mosaic Virus 35S promoter (e). Arrows indicate the direction of transcription. LB, left border; RB, right border; CMV promoter, Cassava vein mosaic virus promoter; NOS term, Nopaline synthase transcriptional terminator; DSRed, *Discosoma sp*. red fluorescent protein; Kan, kanamycin resistance marker gene (*neomycin phosphotransferase II, NPTII*).